

**AN A.C. BRIDGE FOR THE MEASUREMENT  
OF MAGNETIC SUSCEPTIBILITY  
OF ROCKS IN LOW FIELDS**

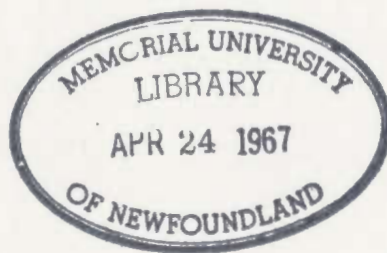
**CENTRE FOR NEWFOUNDLAND STUDIES**

**TOTAL OF 10 PAGES ONLY  
MAY BE XEROXED**

**(Without Author's Permission)**

**BHASKAR IQBAL PANDIT**









AN A.C. BRIDGE FOR THE MEASUREMENT  
OF MAGNETIC SUSCEPTIBILITY  
OF ROCKS IN LOW FIELDS.

By



BHASKAR IQBAL PANDIT, M.TECH.

Submitted in partial fulfilment of the requirements  
for the degree of Master of Science,

Memorial University of Newfoundland

October 11, 1966.

## ABSTRACT

An a.c bridge for the measurement of the magnetic susceptibility of rocks in low fields has been constructed. The sensing unit is a double coil similar to the design by Bruckshaw and Robertson (1948), where two co-axial windings are connected in series opposition so that the net output emf is zero in the absence of a specimen. Following a treatment by Hall (1963) aimed at maximizing the sensitivity; the coil was designed for almost optimum proportions for the case when the specimen is placed on the coil axis at a bounding plane. The coil is 7.9 cms. thick, has an outer radius of 16.0 cms., and the inner radius of the inner winding is 4.0cms. The inner and outer windings have 33,090 and 12,550  $\pm 10$  turns respectively. Use of relatively thick wire (AWG No. 26) resulted in a low Johnson noise level of  $7.0 \times 10^{-9}$  volts rms. The signal due to a specimen of volume susceptibility  $\kappa = 1.0 \times 10^{-5}$  cgs units placed 4.0 cms. beyond a bounding plane is  $0.67 \mu\text{v}$  rms, giving a signal-to-noise ratio of 95.

Because of its large distributed capacitance the coil could be balanced adequately only at frequencies below 250 cps. The present frequency was 33.0 cps, and at this value the phase difference between the output emf's in the two windings could be made almost exactly  $180^\circ$  with the aid of  $0.079 \mu\text{F}$  capacitor placed across the outer winding. The output

signal was amplified by a pre-amplifier and two narrow-band amplifiers connected in cascade, the total gain being 2700. To measure  $\kappa \sim 1 \times 10^{-7}$  cgs units would require a gain of about  $10^5$  but so far an increase in gain has been precluded by the presence in the bridge output of second and higher harmonics; moreover, the output signal at 'balance' has a serious instability with the time constant of the order of  $10^{-1}$  sec. The cause of instability has been traced to the oscillator and power amplifier in the input and the selective amplifiers in the output.

The bridge was calibrated with rock specimens whose absolute volume susceptibility had been determined with an astatic magnetometer. With a calibration value of  $(7.3 \pm 0.2) \times 10^{-5}$  cgs units/cm potentiometer reading for a specimen at the coil center, the susceptibility of a fairly wide range of igneous rocks and the more strongly magnetic sedimentary rocks could be measured. For  $\kappa \sim 1 \times 10^{-3}$  the error in a single measurement is 6%, increasing to 25% for  $\kappa \sim 8 \times 10^{-5}$ , the actual error being reducible through repeat measurements.

Volume susceptibilities of 80 cylindrical specimens cut from 21 basalt samples from Southern Labrador were measured with the calibrated bridge. The mean value of  $\kappa$  at two basalt exposures was  $(3.27 \pm 1.02) \times 10^{-3}$  and  $(9.74 \pm 0.19) \times 10^{-3}$  cgs units respectively where the quoted standard deviations are based on

sample averages and, apart from error in the method are a measure of the inhomogeneous distribution of the chief ferromagnetic constituents in the rocks.

The bridge was used to determine  $\kappa$  in fields as low as 0.005 oe. rms. A significant decrease in  $\kappa$  was observed in the case of three specimens when the magnetizing field was lowered from 0.02 to 0.005 oe. rms.

The experimental variation of sensitivity with specimen positioning relative to the coil was compared in two cases with the theoretical variation and found to agree to less than 10% at the coil center.

## TABLE OF CONTENTS.

	Page No.
ABSTRACT	
LIST OF TABLES	(i)
LIST OF FIGURES	(ii)
CONTENTS	1 - 168

### CHAPTER ONE. INTRODUCTION

1. 1. Ferromagnetism	1
1. 2. Magnetic Susceptibility	6
1. 3. Measurement of Magnetic Susceptibility of Rocks.	18
1. 4. Aim of the Present Investigation	28

### CHAPTER TWO. THEORY AND DESIGN OF THE DOUBLE COIL.

2. 1. Principle of the Double Coil	30
2. 2. Expression for the emf induced in a Double Coil by an Alternating Magnetic Dipole	30
2.3. Maximization of the Sensitivity of the Double Coil	40
2. 4. Present Design of the Double Coil	49

## TABLE OF CONTENTS. (Contd.)

Page No.

### CHAPTER THREE. DESCRIPTION OF AUXILARY APPARATUS

3. 1. Oscillator	59
3. 2. Power Amplifier	59
3. 3. Helmholtz Coils	66
3. 4. Pre-Amplifier	66
3. 5. Tuned Amplifiers	69

### CHAPTER FOUR. 'BALANCING' THE DOUBLE COIL.

4. 1. Distributed Capacitance of Coils	79
4. 2. Calculation of the Induced emf in the inner and the outer coil	80
4. 3. Induced voltages of the inner and outer windings as a function of frequency.	85
4. 4. Procedures in Balancing the Double Coil.	93
4. 5. Discussion of the 'Balance'.	105
4. 6. Probable reasons for instability of the Balance.	116

### CHAPTER FIVE. CALIBRATION AND SUSCEPTIBILITY MEASUREMENTS WITH ROCK SPECIMENS FROM LABRADOR.

5. 1. Method of Measurement.	120
------------------------------	-----



## TABLE OF CONTENTS. (Contd.)

Page No.

### CHAPTER FIVE (Contd.)

5. 2. Calibration	120
5. 3 Discussion of Errors	133
5. 4. Determination of the susceptibility of rocks from Henley Harbour and Table Head, Labrador	143
5. 5. Measurement of susceptibility in low magnetizing fields.	148

<u>CHAPTER SIX.</u> SUMMARY AND CONCLUSIONS	157
---	-----

APPENDIX I	165
------------	-----

REFERENCES	168
------------	-----

ACKNOWLEDGEMENTS	
------------------	--

## LIST OF TABLES.

	Page No.
1. 1. Susceptibility of Common Rocks.	20
2. 1. Dimensions of the Double Coil.	52
2. 2. Wire and Resistance Data for Double Coil.	54
2. 3. Output and Sensitivity of Double Coil.	55
3. 1. Data on Helmholtz Coils.	64
3. 2. Magnetic field at various points in the Helmholtz Coil region.	65
3. 3. Data on Amplifiers in the Bridge Output	76
5. 1. Calibration of the Susceptibility Bridge.	129
5. 2a. Volume Susceptibility of Specimens from "Typical" Basalt Samples from Henley Harbour and Table Head, Labrador.	144
5. 2b. Mean Susceptibility of the Samples.	145
5. 3. Volume Susceptibility of Samples from Henley Harbour and Table Head, Labrador	146

## LIST OF FIGURES.

	Page No.
1. 1. Magnetization Curve of ferromagnetics.	9
1. 2. Initial Specific susceptibility as dependent on particle size.	16
1. 3. Schematic view of the principal parts of the apparatus for measuring the magnetic susceptibility of rocks by means of alternating magnetic field.	25
2. 1.	32
2. 2.	32
2. 3.	37
2. 4. Contours of the function $z_0$ in a plane representing coil proportions a, and b, applicable to positioning of specimen at center of coil or at a bounding plane.	46
2. 5. Pick-Up Coil Cross section showing various coil dimensions	57
3. 1. Block Diagram of the Experimental Set Up.	60
3. 2. Circuit Diagram, Type 122 Low-Level Pre-Amplifier	67
3. 3. Schematic Diagram Selective Amplifier.	70
3. 4. Circuit Diagram of Tuned Amplifier.	72

## LIST OF FIGURES (Contd.)

	Page No.
3. 4. Circuit Diagram of Tuned Amplifier.	72
3. 5. Frequency Response of Stacey Type Tuned Amplifiers.	75
4. 1. Voltage induced in the double coil windings by an alternating field $H = 0.56$ oe. (peak-to-peak) as a function of frequency.	86
4. 2. Phase difference between the voltages induced in the double coil windings by an alternating field, as a function of frequency.	88
4. 3. Resultant output voltage of double coil as a function of the square of frequency for different numbers of layers in the outer winding.	89
4. 3a. Resultant output voltage of double coil as a function of frequency at 3 stages of removal of layers from outer winding.	96
4.3b. Resultant output voltage of double coil as a function of number of excess layers removed from outer winding for a frequency of 100.0 cps.	100

LIST OF FIGURES (Contd.)

Page No.

4. 4. Resultant output emf of the double coil  
as a function of no. of turns on the  
outer winding, after phase adjustment  
with a capacitor C across outer winding. 101
4. 5. Potentiometric arrangement for balancing  
of double coil. 103
5. 1a. Calibration of the susceptibility Bridge.  
Specimen at 0.63 cm. beyond the  
bounding plane of the double coil. 131
5. 1b. Calibration of the Susceptibility Bridge.  
Specimen at center of the double coil. 132
5. 2. Variation of theoretical output signal  
of the double coil with distance of  
an alternating point dipole from its  
center when the dipole is in the coil  
axis. 140
5. 3. Variation of output signal of the  
double coil with distance between  
the coil center, and the center of  
the specimen on its axis. 141

LIST OF FIGURES (Contd.)

Page No.

- |   |      |
|---|------|
| 5. 4. Variation of output signal of the<br>double coil with distance between<br>the coil center, and the center of<br>the specimen on its axis. | 142  |
| 5. 5. Variation of volume susceptibility<br>with a.c magnetizing field.   | 150. |



## CHAPTER ONE

### INTRODUCTION

#### 1. 1. Ferromagnetism.

Any material placed in a magnetic field acquires a moment in a direction opposing the field. This is the phenomenon of diamagnetism and is due to the Larmor precession of electron orbits. The moment acquired is very small and the full effect is observed only if the magnetic moment of the atoms is zero in the absence of an external field. If this condition is not met the diamagnetism is generally masked by either of two stronger phenomena; these are paramagnetism and ferromagnetism. While the former effect tends to be much weaker than the latter, paramagnetism and ferromagnetism both have their origin in the intrinsic magnetic moments of the individual atoms of the material which acquire a resultant moment in the direction of the magnetizing field. Paramagnetism appears in materials composed of atoms with magnetic moments due to their electron spins, but because of very weak interactions between the atoms the distribution of their spin orientations is random in the absence of an external field, resulting in a zero net moment. A finite field causes the average spin orientations to change slightly, so that a weak magnetization parallel to the applied field is induced. Increased thermal agitation arising from a temperature increase will tend to randomize the spin orientations, so that the paramagnetic susceptibility, a measure of the ease with which such a magnetization is acquired in a given field,

is temperature-dependent; the susceptibility in this case is inversely proportional to the absolute temperature (Curie's Law).

Ferromagnetism is a kind of cooperative phenomenon exhibited by a few metals, alloys and compounds. The positive interaction of spins among the neighbouring atoms is here so strong that all atomic magnetic moments tend to be parallel against the disturbing forces of thermal agitation. Contrary to the paramagnetic case, there will be a net magnetization, called the spontaneous magnetization, in the absence of an external field. With increasing temperature, the spins tend to be increasingly deflected from their close alignment, so that the spontaneous magnetization decreases, falling to zero at the Curie Temperature above which the material behaves as a paramagnetic substance.

An important characteristic of all ferromagnetic materials is a crystalline structure. However, it is known that, despite the existence of spontaneous magnetization, ferromagnetic materials, and generally even single crystals, exhibit no magnetization after being cooled from above the Curie temperature in a zero field. This can be explained by the Domain Theory of ferromagnetism due to Weiss (1907). It has been verified experimentally (first by Bitter, 1931) that even a single ferromagnetic crystal usually consists of a large number of so-called magnetic domains separated by discontinuous boundaries (the Bloch Walls). Earlier, indirect verification of domain structure had been obtained by Barkhausen (1919),

who observed experimentally that the magnetization process of a ferromagnetic material proceeds in small discontinuous steps called Barkhausen Jumps.

While each domain has the parallel spin alignment and hence the magnetization predicted by theory, the vector sum of the moments of a large number of domains is zero in a demagnetized state. The reason for the presence of domains lies in the fact that the total free energy of a crystal must be a minimum. Therefore the arrangement of the magnetic moment of the atoms in a ferromagnetic crystal is controlled not only by the spin orientations, tending to produce uniform alignment of all atomic magnetic moments in the crystal, but also by forces which resist the formation of large domains, and so the condition of minimum resultant energy in the crystal will be met when the domains have a certain size and shape.

The magnetization of ferromagnetic crystals is concerned with four different forms of energy, the (1) exchange energy, (2) magnetocrystalline or anisotropy energy, (3) magnetostatic energy and (4) magnetoelastic energy. In ferromagnetism, the predominant form is the exchange energy, which according to the quantum mechanical interpretation due to Heisenberg (1928), will be a minimum when the spins of neighbouring atoms become parallel or anti-parallel, depending upon the sign of the exchange integral. Due to the magnetocrystalline energy, however, the parallel spins tend to align themselves with the direction of easy magnetization of the

crystal. If the entire volume of the ferromagnetic specimen were thus composed of a single domain, the magnetostatic energy should become significant due to the appearance of free magnetic poles. The division of the crystal into domains minimizes the appearance of free poles and thereby reduces the magnetostatic energy. The internal stress might also be effective in causing the small strain known as magnetostriction. In positive magnetostriction, the domains tend to expand parallel to, and contract perpendicular to the direction of domain magnetization, so that a considerable amount of magneto-elastic energy may be stored in the material to maintain contact between neighbouring domains.

Within the Bloch walls the direction of spin varies continuously from that of one domain to that of the adjacent one. The thickness and energy of the wall depend on the relative contributions of the exchange and magnetocrystalline energies, the former tending to increase the thickness and the latter tending to decrease it, since, in the walls, the spins would be mostly directed away from the axes of easy magnetization. Thus the minimum wall energy is determined by competition between the exchange and magnetocrystalline energies.

Three phenomena closely related to ferromagnetism are important in rock magnetism; these are antiferromagnetism, parasitic ferromagnetism and ferrimagnetism. In crystals exhibiting the former phenomenon the spins of neighbouring ions are also aligned,

as in ferromagnetism, but in an antiparallel sense because the exchange interaction is negative. Below a certain temperature, called the Néel (or  $\lambda$  - point), the plus and minus spins completely cancel one another, so that application of an external field will produce a net alignment of atomic magnetic moments with a small positive susceptibility similar in magnitude to that of a paramagnetic material. However, the tendency to be magnetized by the external field is opposed by the strong negative exchange interaction, so that below the Néel temperature the susceptibility increases with increasing temperature, contrary to paramagnetic behaviour. At the Néel point the susceptibility reaches its maximum, while beyond it the spin arrangement becomes random and the susceptibility decreases with increasing temperature.

Associated with antiferromagnetism one sometimes finds parasitic ferromagnetism, e.g. in the case of  $\alpha$  -  $\text{Fe}_2\text{O}_3$  (hematite) which is of major importance in rock magnetism. Above the Néel temperature such substances exhibit a feeble ferromagnetism which disappears when they are heated further towards the Curie temperature. Parasitic ferromagnetism may be due to the presence of minor ferromagnetic impurities, though it has also been proposed that an imbalance in the opposing spins of an otherwise antiferromagnetic material may be responsible; this could be caused by crystal imperfections or by the presence of antiferromagnetic domain boundaries.

Ferrimagnetism is the phenomenon exhibited by some of the

ferrites, which are metallic oxides with a crystal structure of the spinel type. In these substances the magnetic ions occupy sites in two sublattices, A and B, where the spins in A point in the opposite direction to those in B because of strong negative interaction between the two spin systems. The result is an antiparallel spin arrangement as in antiferromagnetism, but with a net magnetic moment in one or the other direction, because the number of ions as well as the magnitude of their individual moments differs in the two sub-lattices. Thus ferrimagnetic substances possess spontaneous magnetization and a Curie point above which the material becomes paramagnetic, and hence their properties resemble those of ferromagnetics. An example of primary importance in rock magnetism is magnetite ( $\text{Fe}_3\text{O}_4$ ), an inverse spinel in which 8 sites in sub-lattice A of the unit cell are occupied by  $\text{Fe}^{3+}$  ions having spins in one sense, compared with 16 sites in sub-lattice B which are occupied by  $8\text{Fe}^{3+}$  ions and  $8\text{Fe}^{2+}$  ions having spins in the opposite sense to those in A.

## 1. 2. Magnetic Susceptibility.

### Definition.

In a material placed in a uniform magnetic field,  $H$ , the magnetic moment per unit volume acquired in  $H$  is termed the intensity of magnetization,  $J$ . This is related to the magnetic induction or flux density,  $B$ , by the equation (in c.g.s. units)

$$\vec{B} = \vec{H} + 4\pi\vec{J} \quad (1.1)$$

where  $\vec{B}$ ,  $\vec{H}$ ,  $\vec{J}$  are vector quantities in the general case. We then



define the volume susceptibility,  $K$ , of the material by

$$K = J/H \quad (1.2)$$

When the magnetization  $J$  has been produced by the field  $H$ .

If  $\rho$  is the density of the material then  $I = J/\rho$  is the specific intensity of magnetization, and  $\chi$  the specific susceptibility, with

$$\chi = I/H = K/\rho \quad (1.3)$$

For the three principal types of magnetic behaviour, the volume susceptibility  $K$  has the typical magnitudes shown below:

Magnetic Behaviour	Sign of $K$	Order of magnitude of $K$ (e.m.u/cm <sup>3</sup> )
Diamagnetic	-	$10^{-6}$
Paramagnetic	+	$10^{-6}$ - $10^{-4}$
Ferromagnetic	+	$10$ - $10^5$

Thus diamagnetic behaviour is characterized by a negative susceptibility, because the magnetization is acquired in opposition to the external field. On the other hand, there are two important aspects in which ferromagnetic materials differ from those

exhibiting the other two kinds of behaviour : (1) their susceptibilities are much larger; (2) their magnetization reaches a saturated value in a finite magnetizing field but does not return to its original value when the field is reversed; such an irreversible process is called "hysteresis" and constitutes an important characteristic of ferromagnetic materials.

One aspect of hysteresis is that the ferromagnetic susceptibility is, in general, a function of the external field, so that  $J$  does not increase linearly with  $H$ ; this appears from inspection of the typical magnetization curve (or hysteresis loop) in Fig. 1.1. It follows that equations (1.2) and (1.3) generally do not apply to ferromagnetic susceptibility and must be replaced by expression of the form

$$K(H) = \left( \frac{\partial J}{\partial H} \right)_H \quad (1.4).$$

#### Types of susceptibilities.

Fig. 1.1 illustrates the relation between the intensity of magnetization  $J$  of a ferromagnetic material and the magnetizing field  $H$ .

O represents the demagnetized state of a ferromagnetic material. The intensity of magnetization  $J$  increases along OABCD with increase of  $H$ , reaching a saturation value  $J_s$  at C corresponding to the magnetizing field  $H_s$ .  $J_s$  is termed the saturation

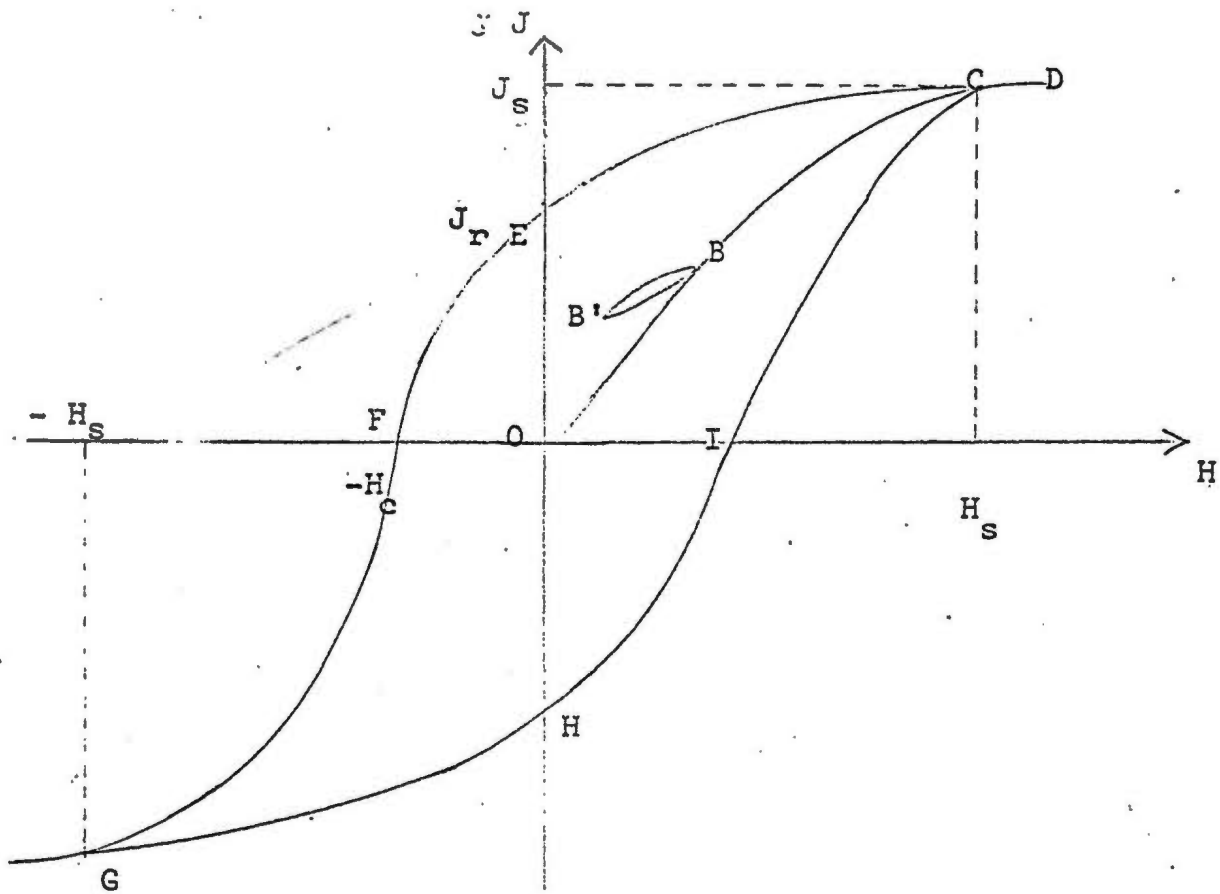


Fig. 1.1. Magnetization Curve of ferromagnetics.

magnetization, and the curve OABCD is called the virgin curve.

The initial slope of the virgin curve is given by

$$\left(\frac{dJ}{dH}\right)_{H=0} = K_0 \quad (1.5)$$

where  $K_0$  is termed the initial susceptibility and  $J$  changes reversibly with  $H$  in the initial part of the curve OA. A slight change in  $H$  at B produces a minor loop BB' with a slope which differs from that of the magnetization curve at B; the slope of BB' is termed the reversible susceptibility,  $K_{rev}$ , while the slope of the magnetization curve at any point is the differential susceptibility,  $K_{dif}$ .

$$\text{Then, } K_{dif} - K_{rev} = K_{irrev} \quad (1.6)$$

where  $K_{irrev}$  is defined as the irreversible susceptibility.

When the field  $H$  is decreased from its value required to produce saturation in the ferromagnetic material,  $J$  will decrease along the path DCE, which differs from the virgin curve. When  $H = 0$ ,  $J = J_r$ , where  $J_r$  is defined as the remanent or residual magnetization. Application of a field  $H$  increasing from zero in opposition to its previous direction will further reduce  $J$ , so that it becomes zero at  $H = -H_c$ , where  $H_c$  is called the coercive force. A further increase in the reverse magnetic field  $H$  results in a saturation value at G. On increasing  $H$  from  $-H_s$  to  $+H_s$ , the magnetization curve follows GHIC.

A typical hysteresis loop (e.g. Fig. 1.1) exhibits symmetry in the sense that the lower half, FGHI, if rotated  $180^\circ$  about the J axis, would be symmetrical with the upper half, FECI, about the H axis. This means that, in the typical case,

$$OE = OH = /J_r/ \text{ and } OF = OI = /H_c/ \quad (1.7)$$

It must be mentioned that H represents the effective magnetizing field  $H_{\text{eff}}$ , which differs in general from the applied external field  $H_{\text{ex}}$ . owing to the appearance of free magnetic poles within the ferromagnetic material. The resulting demagnetizing field,  $H_d$ , is not uniform in the general case and depends upon the distribution of the magnetization and the shape of the ferromagnetic body. Thus we can write

$$\vec{H}_{\text{eff.}} = \vec{H}_{\text{ex.}} - \vec{H}_d = \vec{H}_{\text{ex.}} - N\vec{J} \quad (1.8)$$

where N is called the demagnetization factor. Then, as long as J is uniform,  $H_d$  is proportional and opposite to it.

#### Magnetic Susceptibility of Rocks.

The ferromagnetism of rocks is principally due to the presence of more or less pure oxides of iron, or the sulphide pyrrhotite. These minerals usually constitute a very small proportion of a rock, the groundmass consisting mainly of paramagnetic or diamagnetic silicate minerals.

Magnetite ( $\text{Fe}_3\text{O}_4$ ) and Ulvöspinel ( $\text{Fe}_2\text{TiO}_4$ ) are the end members of the continuous solid solution series, Titanomagnetite. While both members have the inverse spinel structure, only magnetite is ferrimagnetic (see Section 1.1), with a Curie temperature of  $578^\circ\text{C}$ , whereas ulvöspinel is paramagnetic at atmospheric temperature and possibly antiferromagnetic at lower temperatures. However, the solid solution is also ferrimagnetic, with a continuous increase in the ( $\text{Fe}_2\text{TiO}_4$ ) content corresponding almost linearly to an increase in the unit cell dimensions and a decrease in the Curie temperature from  $578^\circ\text{C}$ . Pure ulvöspinel has never been isolated and the extrapolated "Curie" temperature of pure ulvöspinel is  $-153^\circ\text{C}$ .

Ilmenite ( $\text{FeTiO}_3$ ) is antiferromagnetic with a Néel temperature of  $-205^\circ\text{C}$  to  $-218^\circ\text{C}$  (Nagata, 1961). Hematite ( $\alpha\text{-Fe}_2\text{O}_3$ ) exhibits parasitic ferromagnetism (Section 1.1) and has a Curie temperature of  $675^\circ\text{C}$ . Hematite and Ilmenite form another solid solution series,  $x\text{FeTiO}_3 \cdot (1-x)\text{Fe}_2\text{O}_3$ , with magnetic properties that vary according to composition: (i) antiferromagnetism, for  $x = 1$  (pure Ilmenite); (ii) ferrimagnetism, for the range  $0.45 < x < 0.5$ ; (iii) antiferromagnetism with superimposed parasitic ferromagnetism, for  $0.5 > x > 0$ . At atmospheric temperature, ferrimagnetism, which is the property of chief interest in rock magnetism, is shown in the range  $0.8 > x > 0.5$ .

Maghemite ( $\gamma\text{-Fe}_2\text{O}_3$ ) is ferrimagnetic and has an inverse spinel structure like magnetite, but with a lattice defect



equivalent to one vacancy for every nine iron positions in the magnetite cell. The Curie temperature of maghemite has not been measured, as it inverts irreversibly to  $\alpha$ -Fe<sub>2</sub>O<sub>3</sub> at temperatures which different authors quote as 275°C and 400 ~ 800°C, respectively (Nagata, 1961). It is likely that the complete solid solution series of titanomaghemite, (Fe<sub>3</sub>O<sub>4</sub>)<sub>1-x</sub> and  $\gamma$ -Fe<sub>2</sub>O<sub>3</sub> can be formed.

Pyrrhotite has the composition Fe S<sub>1+x</sub>, where x is in the range 0 < x < 0.14. At room temperature, the mineral is antiferromagnetic in the range 0 < x < 0.10 and ferrimagnetic in the range 0.10 < x < 0.14 with a Curie temperature of 300-325°C.

The ferromagnetic\* susceptibility of a rock is primarily controlled by the proportion of ferromagnetic\* minerals - typically magnetite - it contains. Qualitatively, it can be said that, to a rough approximation the susceptibility measured in a weak field varies linearly with the proportion of magnetite in a rock. Several empirical formulae are quoted in the literature: Mooney and Bleifuss (1953) measured the susceptibilities of a suite of Pre-Cambrian rocks in Minnesota in the field, and found

$$K = 2.89 \times 10^{-3} V^{1.01},$$

where V is the volume percentage of magnetite. Balsley and Buddington (1958) related the susceptibility of a suite of Adirondack rocks to the fractional volume of all minerals visually identified as 'magnetite' and obtained the relation

\* where "ferromagnetic" is here used in the wider sense that includes ferrimagnetic, parasitic ferromagnetic and anti-ferromagnetic behaviour. \*

$$K = 2.6 \times 10^{-3} V^{1.33}$$

Factors other than magnetite content affecting the susceptibility of rocks at a given temperature are:

1. Magnetising Field.

The magnetic susceptibility,  $K(H)$ , as given by equation (1.4) in general increase with increase of the magnetising field  $H$  when  $H$  is small, say in the range from 0 to a little beyond  $A$  in Fig. 1.1

2. Particle Size.

As long as the particles of the minerals remains relatively large - say, with diameters in excess of  $10^2$  microns - the initial susceptibility  $K$  does not show any marked dependence on grain size. When the diameter is reduced and approaches a certain critical value determined by the transition from multi-domain to single-domain structure,  $K_0$  approaches a minimum; with a further reduction in particle size, it rises again, reaches a sharp peak and then drops abruptly. In the latter region, the material exhibits the phenomenon of superparamagnetism, a state resembling paramagnetism in which the magnetization of an assembly of particles is largely controlled by thermal agitation. The dependence of the initial specific susceptibility upon particle size

is shown schematically in Fig. 1.2. For sizes exceeding the superparamagnetic range, changes in the coercive force  $H_c$  due to changes in particle size tend to be opposite to susceptibility changes; i.e.  $H_c$  increases when the particles become smaller. This was first verified experimentally by Gottschalk (1935) with natural and artificial magnetite powders; he found that a decrease of particle diameters within the range below  $200\mu$  caused  $K_o$  to decrease and  $H_c$  to increase, gradually at first, but very sharply below about  $20\mu$ .

### 3. Previous Magnetic History of the Rock.

This depends largely upon the age and mode of formation of the rock, and hence its thermal history and upon the origin and subsequent modifications of its remanent magnetism.

### 4. Mineralogical Composition.

The presence of ferromagnetic minerals other than magnetite, and hence with different susceptibility will, of course, affect a susceptibility estimate based upon magnetite content alone. Another mineralogical factor is crystalline anisotropy, which can give rise to susceptibility anisotropy. This is generally negligible in cubic minerals such as titanomagnetite, but can be important when the susceptibility of rocks containing predominantly pyrrhotite or minerals in the ilmenite-hematite series is to be measured, as these minerals exhibit strong crystalline anisotropy.

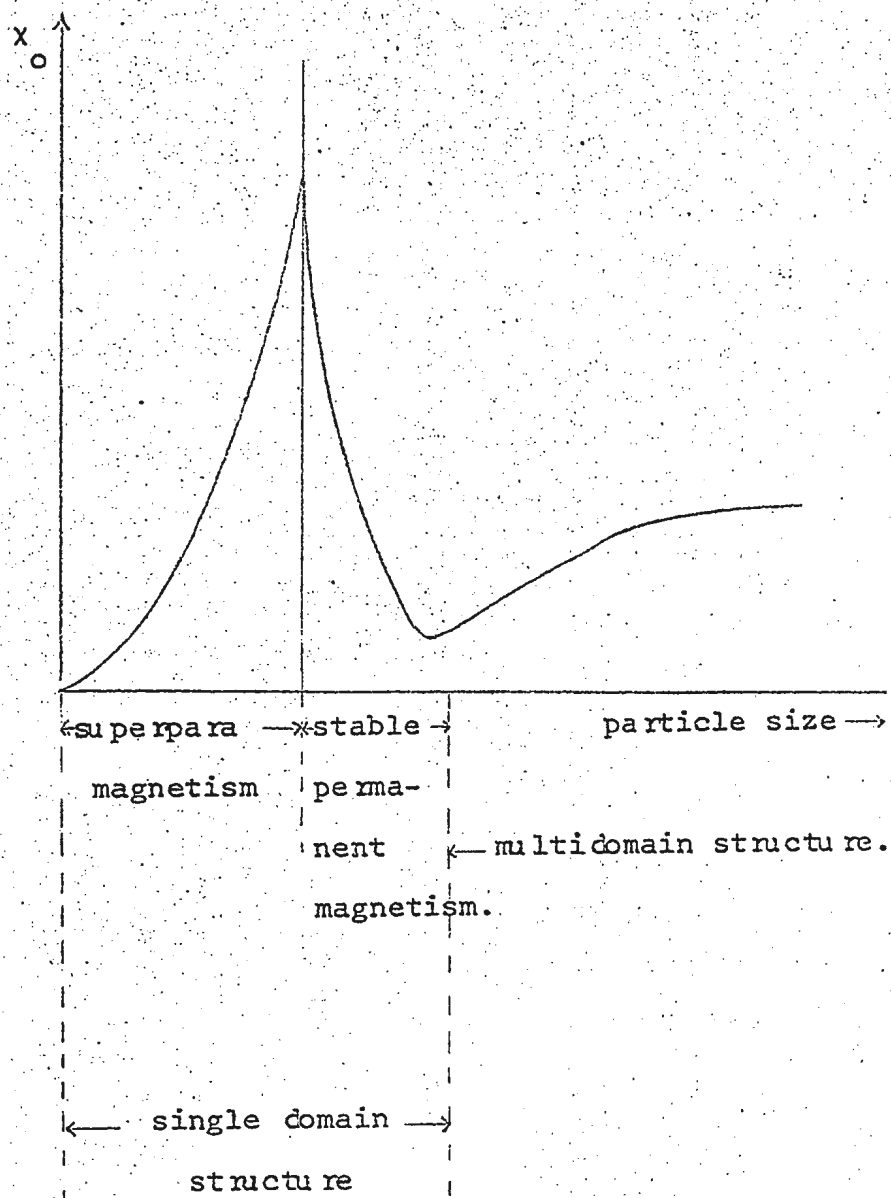


Fig. 1.2. Initial specific susceptibility as dependent on particle size. (Schematic).

with the minimum susceptibility being directed perpendicular to the basal plane of the crystal. In an assemblage of particles the directions of the axes of the susceptibility ellipsoid (which corresponds to the property of anisotropic susceptibility as a second-rank tensor) are not necessarily randomized, so that crystal anisotropy may have caused the remanent magnetization direction in rocks containing the above minerals to be deflected from that of the original magnetizing field; this is of importance in palaeomagnetism.

#### 5. Petrological Characteristics.

Factors such as homogeneity in rock composition, the presence of fractures, or the degree of metamorphism, may have varying influence on the value of bulk susceptibility. Again an important factor can be susceptibility anisotropy, as this may be caused not only by crystalline anisotropy, but also by anisotropy of shape; i.e., elongated ferromagnetic grains can have a shape-controlled direction of remanence even when crystalline anisotropy is negligible. Hence anisotropy in the bulk rock susceptibility may be caused by non-random packing of the grains. While igneous rocks are usually magnetically isotropic, the susceptibility of some sedimentary rocks as measured parallel to the bedding planes can be appreciably different from that measured perpendicular to it: discrepancies amounting to as much as 20% have been reported.

The relative importance of shape and crystalline anisotropy in rock magnetism has been studied by Uyeda et.al. (1963), and measurements of the susceptibility anisotropy of minerals and rocks have been carried out by an increasing number of investigators in recent years.

### 1.3. Measurement of Magnetic Susceptibility of Rocks.

#### Geophysical Importance.

Susceptibility is a fundamental property of a magnetic material and hence a knowledge of the susceptibility of rocks and its dependence on the above factors form a part of the subject of rock magnetism. In magnetic prospecting for iron and other ores, however, susceptibility is a vital consideration in the interpretation of the magnetic anomalies. Because of its dependence on the magnetizing field, it is necessary, therefore, that for prospecting purposes the susceptibility of rocks be measured in magnetic fields of the same magnitude as that of the earth. Since the magnitude of the earth's field is about 0.5 oersted, the susceptibility measured is the initial susceptibility,  $K_0$ .

The range of susceptibility of rocks in weak magnetic fields is typically as follows: (Nagata, 1961)

<u>Rock Type</u>	<u>Volume susceptibility</u> <u>K (e.m.u/cc).</u>
Volcanic	$10^{-4} - 10^{-2}$
Plutonic	$10^{-4} - 5 \times 10^{-3}$
Metamorphic	$10^{-5}$ to $3 \times 10^{-4}$
Sedimentary	$< 10^{-5}$

Table 1.1 gives a more detailed estimate of the susceptibility of common rocks.

#### Previous Work Done.

The magnetic susceptibility of a material can be measured by a number of methods, as summarized below.

##### 1. Balance Method

The Balance Method, used by the earliest workers such as Gouy (1889) Kelvin (1890) and Curie and Chenevesu (1903), measures the susceptibility of dia-, para- and ferromagnetic materials in high fields ( $\sim 10^3$  oe.), and has been adapted for temperatures ranging from that of liquid helium to greater than  $1000^\circ\text{C}$ .

TABLE 1. 1.

Susceptibility of Common Rocks.

(From Slichter, 1942)

Rock Type	No. of Samples	Percent having volume susceptibility, K (e.m.u./cc)				
		$K < 10^{-4}$	$10^{-4} < K < 10^{-3}$	$10^{-3} < K < 4 \times 10^{-3}$	$K > 4 \times 10^{-3}$	
Basic effusive	97	5	29	47	19	
Basic plutonic	53	24	27	28	21	
Granite and allied rocks	74	60	23	16	1	
Gneiss schist and slate	45	71	22	7	0	
Sedimentary rocks	48	73	19	4	4	



A consequence of the respective properties of paramagnetic and diamagnetic materials in a homogeneous magnetic field is their behaviour in the presence of a field gradient. Since induction in a magnetic field increases the flux density in a paramagnetic body it will tend to move into the strongest part of a non-uniform field. Therefore if a paramagnetic specimen is kept in an inhomogeneous field and allowed to move only at right angles to the direction of lines of force, it will be attracted in the direction of the increasing field. With the same arrangement a diamagnetic body would be repelled in the diminishing field direction. This attractive or repulsive force  $F$ , is a function of the susceptibility  $K$  of the material and hence can be determined from a measurement of  $F$  (in terms of a mechanical force). Such methods can be applied to ferromagnetic bodies as well.

In the Curie method the mechanical force is measured by a torsion balance, while in the Gouy method the test material is suspended from one of the pans of a chemical balance and magnetized by a non-uniform field varying from a large value to essentially zero over the length of the rod, \* the magnetic force on the specimen placed in the field gradient is then measured in terms of its apparent gain or loss of mass.

## 2. Ballistic Method

The method (Chevallier, 1925, Stchodro, 1927; and Nagata, 1940) is based on the principle that the magnetic flux

threading a search coil will change as a result of the movement of the magnetic moment vector of a specimen relative to the coil. This in turn induces an electric charge which can be measured with a ballistic galvanometer and is a function of susceptibility. The magnetizing field is provided by a field coil-generally a solenoid if high fields are used - and the flux through the search coil is changed either by altering its geometrical relationship with the coil and specimen or by reversing the polarity of the current through the field coils. To avoid the effects of the geomagnetic field, the axes of the field and search coils are usually set perpendicular to the geomagnetic meridian.

### 3. Induction Balance.

In the Hughes Induction Balance, first developed by Hughes, (1879) and used by Grenet (1930), the magnetizing field is produced by feeding the output of an oscillator to the primary of a double solenoid system. The induced e.m.f. in the secondary circuit is nullified before and after introducing the specimen by a compensating coil system in conjunction with a small trimming inductance M. The net e.m.f. due to the specimen is then a measure of its susceptibility.

### 4. Mooney's Susceptibility Bridge.

Mooney's (1952) instrument consists basically of three coils, two of these (A and B) being energized by a 1000 cps alternating current, and the third (C) being positioned between A and B. Coils A and B are so wound that their magnetic fields

cancel at the position of coil C. Mutual induction between C and the system A, B then reduce to a minimum. If a magnetic material is introduced between C and one of the other coils, the additional coupling produces a net magnetic field, which is a measure of the susceptibility. The extent of the imbalance is measured by an alternating current bridge as an imbalanced resistance, the bridge being calibrated in units of magnetic susceptibility.

The next two methods are primarily employed for the measurement of anisotropy of magnetic susceptibility of rocks.

#### 6. Torque Meter.

In the torque meter method (Stacey, 1960; King and Rees, 1962; and Stone, 1962) the specimen is suspended in a uniform magnetic field by means of a fine fibre. If the specimen is anisotropic, the axis of greatest susceptibility will tend to align itself parallel to the field. The deflection is proportional to the small susceptibility difference itself. King and Rees designed for a maximum sensitivity of  $8 \times 10^{-11}$  e.m.u./cm<sup>3</sup> at a field of 200e., so that anisotropy of  $10^{-8}$  emu/cm<sup>3</sup> could be accurately measured.

#### 7. A.C. Transformer Bridge Method.

Although the Torque Meter method achieves adequate sensitivity, the specimen has to be subjected to high fields. This is not so in the a.c. bridge method where magnetizing fields of the

order of 1 oe. are used. In this method the sample functions as an element in a balanced a.c. bridge circuit which is connected to a detector having sensitivity adequate for measuring the variations of the small error signals that appear as the sample is placed within the test coil in various orientations. Graham (1964) reports a sensitivity such that susceptibilities of the order of  $10^{-8}$  emu/cm<sup>3</sup> could be adequately measured in a magnetizing field of 1 oe. Sensitivities of the same order have also been reported by Girdler (1961) and Fuller (1964) using the a.c. transformer bridge method primarily to measure bulk susceptibility.

#### 8. Inductance Bridge Method.

Bruckshaw and Robertson (1948) developed an inductive apparatus for measuring magnetic susceptibility in a low field of about 0.5 oe. A uniform alternating field is produced by a pair of Helmholtz coils HH (Fig. 1.3) carrying an alternating current. A pick-up coil consisting of an inner and outer winding, W<sub>1</sub> and W<sub>2</sub>, wound in series opposition is placed at the centre of the Helmholtz Coils. The turns on the windings are adjusted for a minimum (ideally zero) output e.m.f. in a uniform time-varying field. A rock specimen placed at the centre of such a coil causes a differential output because of its closer coupling with the inner coil. By means of a potentiometric arrangement, the differential voltage is measured in terms of that set up in a third coil, W<sub>3</sub>, of very few turns, which is wound on the outside of the double coil and excited by the Helmholtz coil. A tuned Campbell vibration galvanometer preceded by a 3 stage low-noise, high-gain amplifier was used as a null detector.

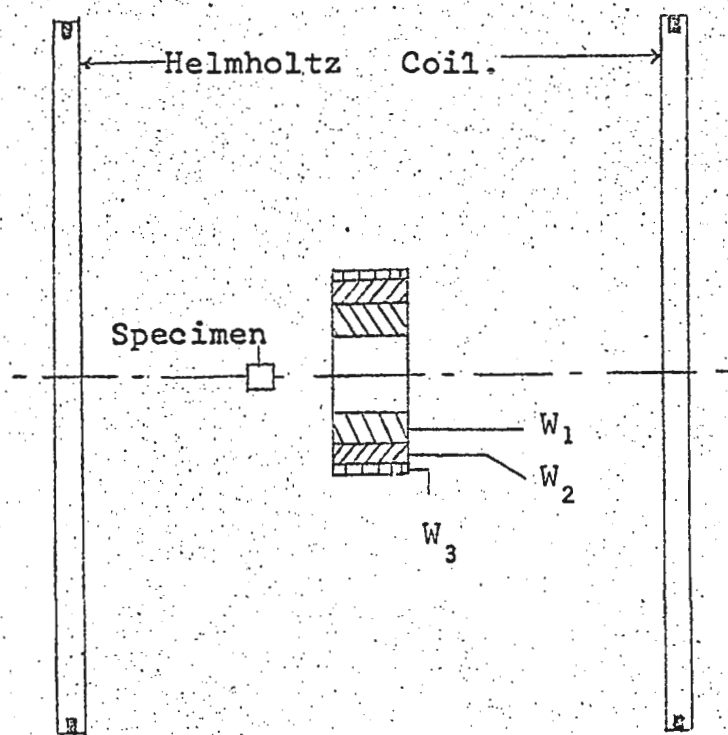


Fig. 1.3. Schematic view of the principal parts of the apparatus for measuring the magnetic susceptibility of rocks by means of alternating magnetic field. (after Bruckshaw and Robertson, 1948).

The lowest value of susceptibility that could be measured was  $1 \times 10^{-5}$  emu/cm<sup>3</sup>. at a frequency of 50 cps. The chief limitations of Bruckshaw and Robertson's apparatus were:

- (1) loss of sensitivity because of non-optimum dimensions of the double coil;
- (2) large noise level of the first stage of the amplifier;
- (3) relatively large Johnson noise level of the double coil because of its large resistance.

Likhite and Radhakrishnamurthy (1965) designed a double coil smaller in size than that of Bruckshaw and Robertson and also of non-optimum dimensions. They used it at frequencies greater than 200 cps for measuring the susceptibility of sedimentary rocks in weak fields. The smallest measurable susceptibility was  $5 \times 10^{-7}$  cgs units which represents a considerable improvement over Bruckshaw and Robertson's apparatus.

#### 9. D.C. Method

Blackett (1952) used the astatic magnetometer to determine the susceptibility of rocks. A known field is applied by means of secondary windings on one pair of the 3-component Helmholtz coil system used to obtain a zero field at the magnetometer. The magnetization then measured will be the sum of the permanent and induced magnetizations. The effect of the former

can be eliminated through a suitable measuring procedure following which the reversible susceptibility is deduced.

The a.c. method of measuring the susceptibility has the following advantages over the d.c. method:

(1) The output signal due to a specimen varies directly with the frequency of a sinusoidally varying magnetizing field, and hence the sensitivity can be increased by using higher frequencies. Further sufficient amplification permits the measurement of very weak specimens.

(2) The a.c. method can be used in the presence of time-varying magnetic fields and mechanical vibration such as exist in the average laboratory. This is an important practical advantage over the d.c. method.

(3) The time required to make a measurement is not more than 30 seconds - much less than that required by the d.c. method.

Disadvantages of the a.c. method are:

1. The balance condition drifts due to changes in the inductance and resistance of the double coil as a result of temperature variation. This problem is reported to have been successfully solved by use of automatic servo loops which maintain the bridge in approximate balance for long periods. (Graham 1964).

It should be noted here that the above methods measure

only the apparent susceptibility because of the self-demagnetizing effect of the ferromagnetic minerals contained in the rocks.

#### 1.4. Aim of the Present Investigation.

The aims of the present investigations were as follows:

1. To design and construct a double coil of optimum dimensions, for maximum sensitivity, based on the calculations of Hall (1963), together with a bridge circuit for the measurement of the bulk susceptibility of rocks in weak fields;
2. To balance the double coil;
3. To calibrate the bridge and measure the susceptibility of some rock samples from Newfoundland and Labrador;
4. To investigate the possibility of adapting the bridge circuit to the measurement of the postulated variation of susceptibility with frequency, as suggested by Vincenz (1965) on the basis of Neel's theory of the fluctuating viscosity field in ferromagnetic substances (Neel, 1950). Likhite and Radhakrishnamurthy (1965) attempted to measure this effect in igneous rocks, but without success, either because of still insufficient instrumental sensitivity or because the effect was not present. No experimental confirmation is available from



any other source. As will be discussed in Chapter Four, it proved difficult to adapt the bridge to measurements over a wide frequency range, and frequency dependence tests were not carried out. Other, more promising possibilities (e.g. the low-frequency measurement of susceptibility in very low fields or at high temperatures) are discussed in Chapters Five and Six.

## CHAPTER TWO

### THEORY AND DESIGN OF THE DOUBLE COIL

#### 2. 1. Principle of the Double Coil.

A double coil consists of two windings - inner and outer - wound in opposite directions, and the number of turns in each winding so adjusted that when the coil is placed in a uniform time-varying magnetic field, its differential output is a minimum (ideally zero). If a rock specimen is placed at any position along the axis - generally at the centre or the bounding plane - a net differential output is observed because the specimen produces a non-uniform time-varying field due to its closer proximity to the inner coil. Implicit in the above statement is the assumption that the specimen acts as an alternating magnetic dipole. Bruckshaw and Robertson (1948) estimated the error in the above assumption for their coil and found it to be less than 0.5%.

#### 2. 2. Expression for the e.m.f. Induced in a Double Coil by an Alternating Magnetic Dipole.

In designing a double coil of optimum proportions, it is required first to calculate the electrical output of such a coil under ideal conditions. The main assumption is that a test sample

placed on the axis of the coil and magnetized by induction in an alternating field, may be represented by an alternating dipole at a point on the coil axis. For simplicity, it is further assumed that the dipole moment is aligned with the coil axis, while its magnitude changes sinusoidally with time; such a model, in fact, closely approximates to the actual experimental model. The expression for the output of the double coil is conveniently derived in three stages:

(1) E.m.f. in a single circular turn due to alternating point dipole along the axis.

The arrangement for a single circular turn is shown in Fig. 2.1, where a horizontal dipole with a moment of amplitude  $M$  has been placed at the origin of the co-ordinate system  $x, y, z$ . The moment is aligned with the  $x$ -axis, which is also the axis of the single turn. Then if the field due to the dipole has a component  $H_x$  parallel to the coil axis at a point  $P (r, \theta)$  in its plane, the magnetic flux element  $d\phi$  through the areal element  $rdrd\theta$  at  $P$  is:

$$d\phi = H_x r dr d\theta \quad (2.1)$$

Therefore the total flux through the circular turn is

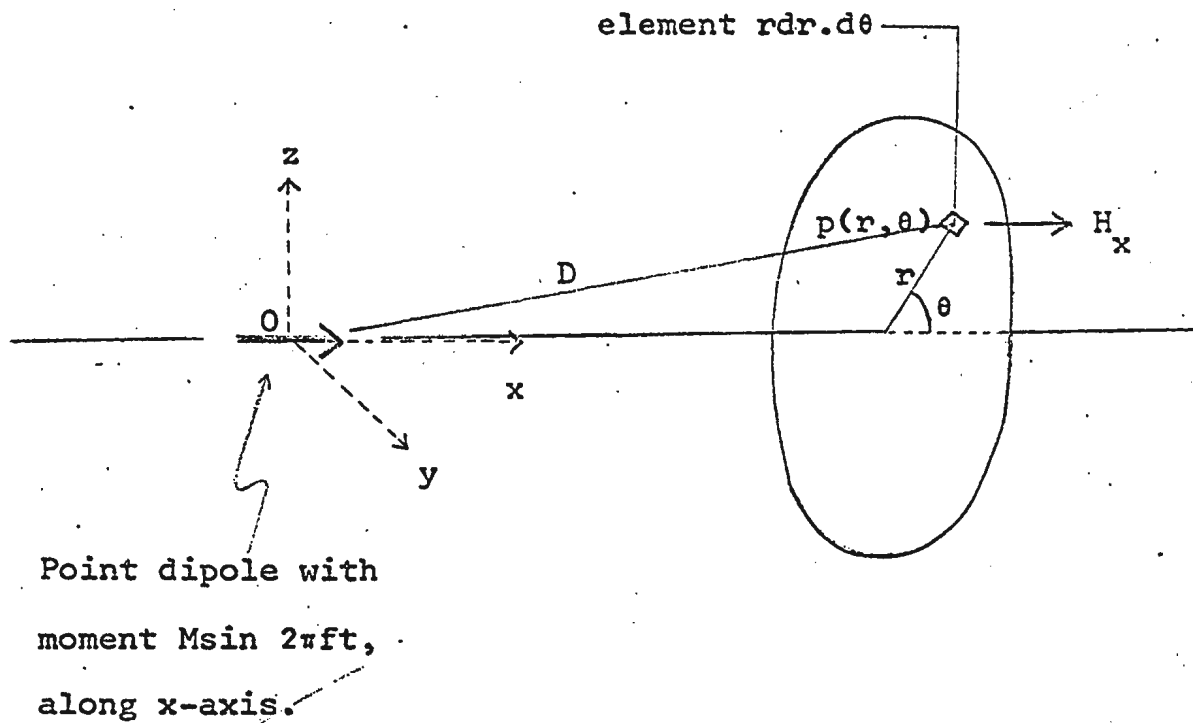


Figure 2.1

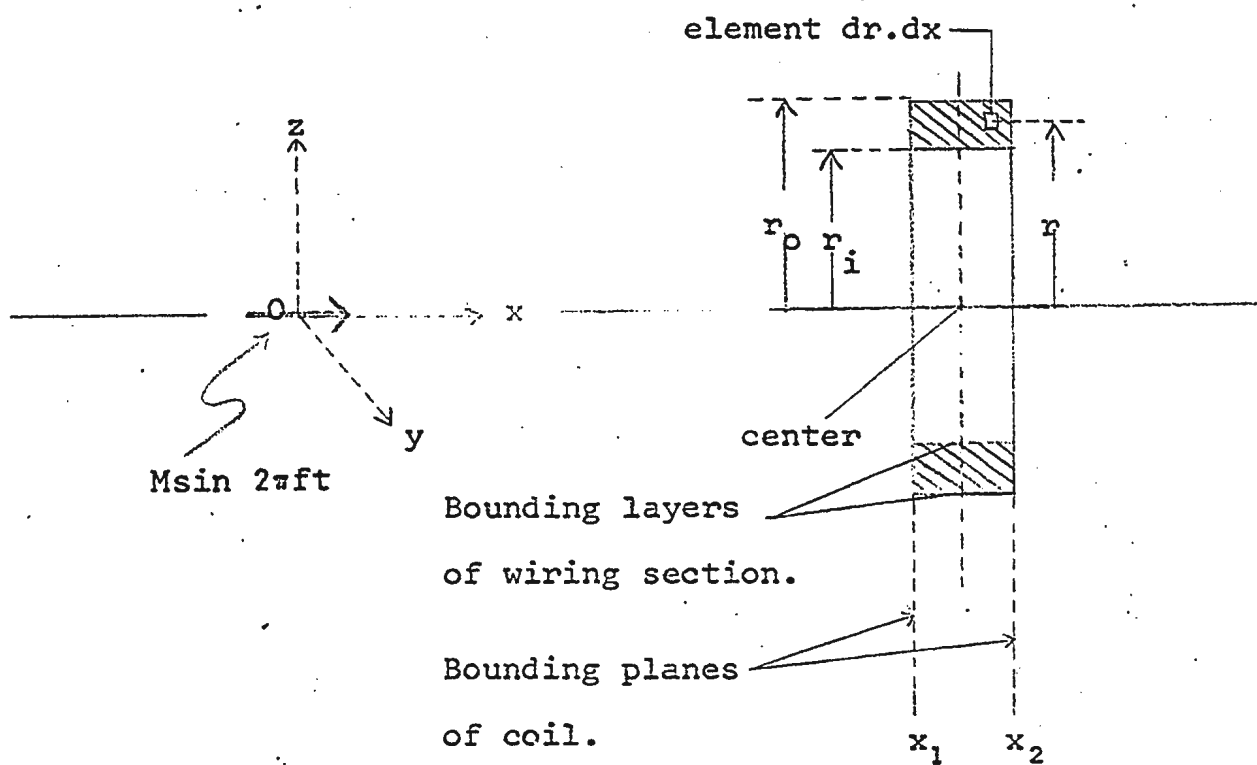


Figure 2.2

$$\phi = \int_0^r \int_{\theta=0}^{2\pi} H_x \, r \, dr \, d\theta \quad (2.2)$$

$$\text{with } H_x = - \frac{\partial V}{\partial x} \quad (2.3)$$

$$\text{and } V = M \sin 2\pi f t \frac{x}{D^3} \quad (2.4)$$

where  $V$  is the potential due to the dipole at  $P$  at time  $t$ ;

$f$  is the frequency of the dipole; and  $D$  is the distance from the origin  $O$  to  $P$ .

Then, since  $D^2 = x^2 + r^2$

$$H_x = M \sin 2\pi f t \frac{2x^2 - r^2}{(x^2 + r^2)^{5/2}} \quad (2.5)$$

Substituting  $H_x$  in (2.2) and performing the integration, we have,

$$\phi = 2\pi M \sin (2\pi f t) \frac{r}{(x^2 + r^2)^{3/2}} \quad (2.6)$$

$$e^1 = - \frac{\partial \phi}{\partial t} \times 10^{-8} = -4\pi^2 M f \cos (2\pi f t) \frac{r^2}{(x^2 + r^2)^{3/2}} \times 10^{-8} \quad (2.7)$$

Where  $M$  is in c.g.s. units, and  $e^1$  is the e.m.f. in volts induced in a single turn.

$$\frac{e^1}{\text{rms}} = \sqrt{8} \pi^2 M f \frac{r^2}{(x^2 + r^2)^{3/2}} x^{10-8} \text{volts} \quad (2.8)$$

Which is the desired expression.

(2) E.m.f. in circular coil of square cross-section due to alternating point dipole along axis.

Following Hall (1963), let the coil have  $n$  turns per unit cross-sectional area, so that the elemental area  $dr \cdot dx$  at  $(x, r)$  contains  $n dr \cdot dx$  turns (Fig. 2.2) Therefore the e.m.f. induced in the whole coil of cross-section  $(r_0 - r_i)$   $(x_2 - x_1)$  is given by:

$$e'' = \sqrt{8} \pi^2 f M n \int_{x_1}^{x_2} \int_{r_i}^{r_0} \frac{r^2}{(x^2 + r^2)^{3/2}} dr dx x^{10-8} \text{volts rms} \quad (2.9)$$

where  $r_0$  and  $r_i$  are the outer and inner radii of the coil, and  $x_1, x_2$  are the intercepts of the bounding planes on the coil axis (all in c.g.s. units)

If  $d$  is the diameter of the wire, then, neglecting spaces occupied by insulating material:

$$n = \frac{1}{d^2} \quad (2.10)$$

and the solution of (2.9) is

$$e'' = \frac{\sqrt{8\pi^2 f M x_1} 10^{-8}}{d^2} \quad F \text{ volts r.m.s.} \quad (2.11)$$

$$\begin{aligned} \text{Where } F &= \int_{x_1}^{x_2} \int_{r_i}^{r_0} \frac{r^2}{(x^2 + r^2)^{3/2}} dr dx \\ &= x_2 \left[ \sinh^{-1} \frac{r_0}{x_2} - \sinh^{-1} \frac{r_i}{x_2} \right] - x_1 \times \\ &\quad \times \left[ \sinh^{-1} \frac{r_0}{x_1} - \sinh^{-1} \frac{r_i}{x_1} \right] \quad (2.12) \end{aligned}$$

(3) Net e.m.f. in double coil due to alternating point dipole along axis.

If  $e_1$ ,  $e_2$  are the e.m.f.'s generated in the inner and outer coil, respectively (Fig. 2.3) then the net e.m.f.,  $e$ , is given by an expression analogous to (2.11):

$$e = e_1 - e_2 = \frac{\sqrt{8\pi^2 M f}}{d^2} \times 10^{-8} (F_1^1 - F_2^1) \text{ volts r.m.s.} \quad (2.13)$$

where  $F_1^1$  and  $F_2^1$  are functions corresponding to expression (2.12), and relating to the inner and outer coil, respectively.

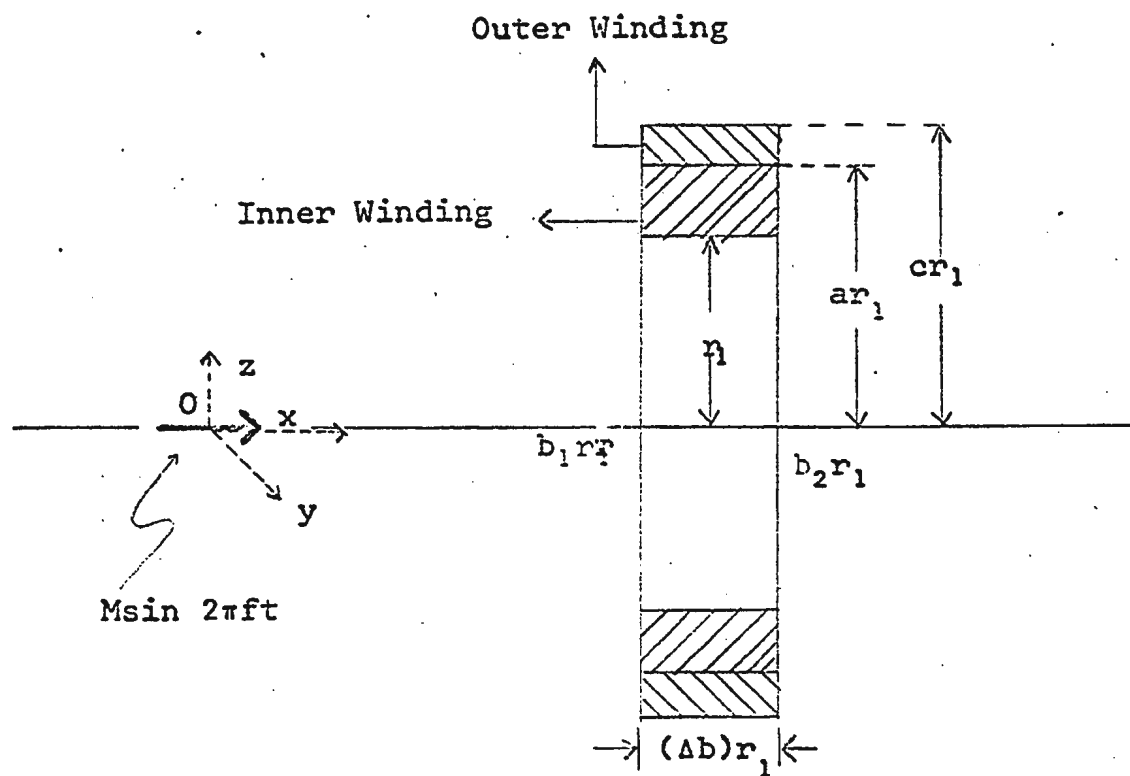
To determine  $F_1^1 - F_2^1$ , one substitutes the dimensions of the double coil windings (Fig. 2.3) for those of the single coil (Fig. 2.2), i.e.,  $r_i$ ,  $r_o$ ,  $x_1$  and  $x_2$  in Fig. (2.2) are replaced by  $r_1$ ,  $ar_1$ ,  $b_1r_1$  and  $b_2r_1$ , respectively, in the case of the inner winding, and by  $ar_1$ ,  $cr_1$ ,  $b_1r_1$  and  $b_2r_2$ , respectively, in the outer winding, so that the thickness of the double coil is given by:


$$(\Delta b) r_1 = (b_2 - b_1) r_1 \quad (2.14)$$

Substituting the new symbols in (2.12) for each winding, and subtracting, one obtains:

$$\text{therefore, } F_1 - F_2 = \frac{r_1}{b_2} (F_1^1 - F_2^1) = b_2 \left[ 2 \sinh^{-1} \frac{a}{b_2} - \sinh^{-1} \frac{1}{b_2} - \sinh^{-1} \frac{c}{b_2} \right] - \frac{b_1}{1} \left[ 2 \sinh^{-1} \frac{a}{b_1} - \sinh^{-1} \frac{1}{b_1} - \sinh^{-1} \frac{c}{b_1} \right] \quad (2.15)$$





 Inner Winding:  $N_1$  turns; resistance  $R_1$  (ohms)


 Outer Winding:  $N_2$  turns, resistance  $R_2$  (ohms)

Figure 2.3

If the expressions within brackets are replaced by a function  $y$ , given by:

$$y = 2\sinh^{-1} \frac{a}{b} - \sinh^{-1} \frac{c}{b} - \sinh^{-1} \frac{1}{b} \quad (2.16)$$

$$\text{then, } F_1 - F_2 = b_2 y_2 - b_1 y_1 \quad (2.17)$$

where  $y$  is defined for negative as well as positive values of  $b$ ;

$$\text{i.e., } y(-b) = -y(b) \quad (2.18)$$

$$\text{Then } e = e_1 - e_2 = \frac{\sqrt{g^2} \text{ Mfr}_1}{d^2} \times 10^{-8} (F_1 - F_2) \text{ volts r.m.s.} \quad (2.19)$$

We further define

$$u^2 = c^2 - 1$$

and if  $c^2 \gg 1$ , we can substitute  $u \approx c$  in equation (2.16), in which case the expression for  $y$  may be simplified with the aid of certain expansions of  $\sinh^{-1} u$ .

Finally, the condition that  $e$  be zero in a uniform field is given by Nagata (1953) as

$$c = \sqrt[3]{2a^3 - 1} \quad (2.20a)$$

$$\text{and hence } c \approx 1.26 a \quad (2.20b)$$

where for  $a > 2$ , the approximation (2.20b) holds with less than 2% error. :

The main advantage of using expression 2.13 for the output of the double coil lies in the separation of the factors dependent upon the linear proportions and coil-specimen arrangement. Factor (ii) is represented by  $F_1 - F_2$ . Factor (i) is the remainder of equation (2.19) and expresses the proportionality of  $e$  to the amplitude of the alternating dipole moment, to the frequency, to the number of turns per unit area in the coil, and to the inner radius of the inner winding of the coil. The latter parameter ( $r_1$ ) is the only one dependent upon the size of the double coil, the remaining dimensions of the coil being expressed as products of  $r_1$  and dimensionless parameters contained in the factor  $F_1 - F_2$ , which therefore is a shape factor.

Hall has plotted the function  $y$  against  $a$  for different values of  $b$  from which the factor  $F_1 - F_2$  can be readily determined. When  $M$ ,  $f$ ,  $r$ , and  $d$  are known, the output  $e$  can then be calculated.

### 2. 3. Maximization of the Sensitivity of the Double Coil.

The expression 2.19 for the output was utilized by Hall to make a detailed analysis of the dependence of the signal-to-noise ratio, and hence the sensitivity, on the linear dimensions of the coil.

The e.m.f.  $e_n$ , due to thermal noise is given by Johnson (1938):

$$e_n = 1.27 \times 10^{-10} (R \Delta f)^{\frac{1}{2}} \text{ volts r.m.s.} \quad (2.21)$$

where  $R$  is the resistance of the coil in ohms and  $\Delta f$  is the observed bandwidth in cycles/sec. .

The total resistance  $R_t$  of a double coil is equal to that of a square-sectional coil with inner radius  $r_1$  and outer radius  $cr_1$ . Substituting these values into another expression given by Johnson (1938), one obtains:

$$R_t = \frac{4 \rho r_1^3 (\Delta b) u^2}{d^4} \quad (2.22)$$

where  $\rho$  is the resistivity in ohm-cm,  $r_1$  and  $d$  are in cms, and other parameters are as previously defined.

Substituting  $R_t$  in (2.22) for  $R$  in 2.21 we have

$$e_n = \frac{2.54 \times 10^{-10} r_1^{3/2} \rho^{\frac{1}{2}} (\Delta f)^{\frac{1}{2}} u \Delta b^{\frac{1}{2}}}{d^2} \text{ volts r.m.s.} \quad (2.23)$$

Division of (2.19) by (2.23) gives the signal to noise ratio:

$$\frac{e}{e_n} = \frac{1.10 \times 10^3 M f}{(r_1 \xi_{\Delta} f)^{\frac{1}{2}}} \frac{F_1 - F_2}{u \Delta b^{\frac{1}{2}}} \quad (2.24)$$

Thus the signal-to-noise ratio also has been separated into two factors: one dependent on the magnitudes involved and the other on the proportion of coil dimensions and the coil-specimen arrangement.

It should be mentioned here that formulae (2.22) - (2.24) hold only for uninsulated wire. If the insulation thickness is not negligible, let  $d_1$  and  $d$  be the diameters of the insulated and the bare wire, respectively, then the total resistance  $R_t^1$  of such a double coil is given by

$$R_t^1 = \frac{4 \xi r_1^3 (\Delta b) u^2}{d_1^2 d^2} \quad \left[ \begin{array}{l} \text{see equation (viii)} \\ \text{Appendix I} \end{array} \right]$$

Then the signal output may be written:

$$(e)_1 = \frac{\sqrt{8} \pi^2 M f r_1 \times 10^{-8} (F_1 - F_2)}{d_1^2} \text{ volts r.m.s.} \quad (2.25)$$

and the corrected noise voltage is:

$$(e_n)_1 = \frac{2.54 \times 10^{-10} r_1^{3/2} \xi^{\frac{1}{2}} \Delta f^{\frac{1}{2}} u \Delta b^{\frac{1}{2}}}{d_1 d} \text{ volts r.m.s.} \quad (2.26)$$

Hence the corrected signal-to-noise ratio is:

$$\left[ \frac{e}{e_n} \right] = \frac{d}{d_1} \frac{e}{e_n} \quad (2.27),$$

and it follows that the error in the signal-to-noise ratio obtained from the uncorrected equation (2.24) is proportional to the thickness of the insulation layer relative to the total wire diameter, the true ratio given by (2.27) being smaller than the uncorrected ratio.

An error that is more difficult to estimate results from the insertion of insulation material (e.g. oil-impregnated paper) between adjoining layers of wire, usually several layers apart. This, together with certain departures from uniformity that are generally unavoidable in the winding of coils, will cause the parameter  $n$  to vary within the coils, and the coil to become larger than estimated from the given value of  $n$  (for tight wiring) and the chosen dimensions only. The use of relatively thick wire, as in the present design, tends to reduce the error from these sources, both because the windings in such a coil can be made tighter and more uniform than in thin-wire coils, and because the insulation material will have a practical minimum thickness; hence it will occupy a smaller proportion of the winding section in the thick-wire coil.

Again following Hall (1963), to determine the importance of the signal-to-noise ratio on the proportions of the coil dimensions, the second factor in (2.24), which he calls  $z$ , has to be considered, i.e.,

$$z = \frac{F_1 - F_2}{(u\Delta b)^{\frac{1}{2}}} \quad (2.28)$$

Hall then defines another function,  $z_o$ , such that

$$z_o = \frac{b^{\frac{1}{2}}y}{u} \quad (2.29)$$

and considers once more two standard specimen locations on the coil axis: (1) at the center of the coil, and (2) at one of its bounding planes. Then we have:

$$\text{for case (1): } b_1 = b_2 = \frac{\Delta b}{2}; \quad \text{for case (2): } b_1 = 0, b_2 = \Delta b \quad (2.30)$$

Inserting these values into equation (2.17) and using (2.18), one obtains  $F_1 - F_2$ ;  $z$  and  $z_o$  may then be evaluated from equations (2.28) and (2.29), with the result:

$$\text{For case 1, } Z = \sqrt{2} Z_o \quad (2.31)$$

$$\text{and for case 2, } Z = Z_o \quad (2.32)$$

Fig. (2.4) shows the contours of  $Z_0$  in the  $a$ - $b$  plane enclosing a maximum around  $a=5$ ,  $b=2$ . These are also the contours of signal-to-noise ratio. When  $a \approx 5$ ,  $u^2 = c^2 - 1$  can be written approximately as  $u^2 = c^2$ . Hall then used the expansion

$$\text{Sinh}^{-1}u = \log 2u + \frac{1}{4} \frac{1}{u^2} - \frac{3}{32} \frac{1}{u^4} \quad (2.33)$$

(where only the first term on the right is important),

for the first two terms in (2.16), obtaining an approximation for  $y$ . Substituting this into (2.29) putting  $u = c$ , and using equation (2.20a) or (2.20b), one finds

$$Z_0 = \frac{0.794}{a} b^{\frac{1}{2}} \left[ 0.462 + \log a - \log b - \text{Sinh}^{-1} \frac{1}{b} \right] \quad (2.34)$$

For a maximum, the condition is

$$\frac{\partial Z}{\partial a} = \frac{\partial Z}{\partial b} = 0, \text{ simultaneously} \quad (2.35)$$

Differentiating and equating to zero gives

$$\left. \begin{aligned} y &= 0.462 + \log a - \log b - \text{Sinh}^{-1} \frac{1}{b} \\ \text{and } y - 2 + \frac{2}{\sqrt{1+b^2}} &= 0 \end{aligned} \right] \quad (2.36)$$



Simultaneous solution of the above equations gives the desired optimum values of the parameters:

$$a = 5.1, \text{ and } b = \sqrt{3}$$

Examination of the contours in Fig. (2.4) shows a broad maximum around  $a = 5.1$ ,  $b = \sqrt{3}$  bordered by relatively narrow zones where  $z$  falls off rapidly. Then by using the conditions in (2.30), one obtains the following values for the optimum coil proportions as a function of positioning of the specimen:

Specimen position along coil axis.	Optimum proportions.	
	$a$	$\Delta b$
Coil center ( $b = \Delta b/2$ )	5.1	$2\sqrt{3}$
One of the bounding planes. ( $b = \Delta b$ )	5.1	$\sqrt{3}$

Thus the optimum proportions of the coil vary with the chosen positions of the specimen relative to the coil. It can be shown that for all positions of the specimen on the axis, the value of  $z$  for optimum proportions is given by

$$Z_{\text{max.}} = \frac{\Delta b^{\frac{1}{2}}}{u} \quad (2.37)$$

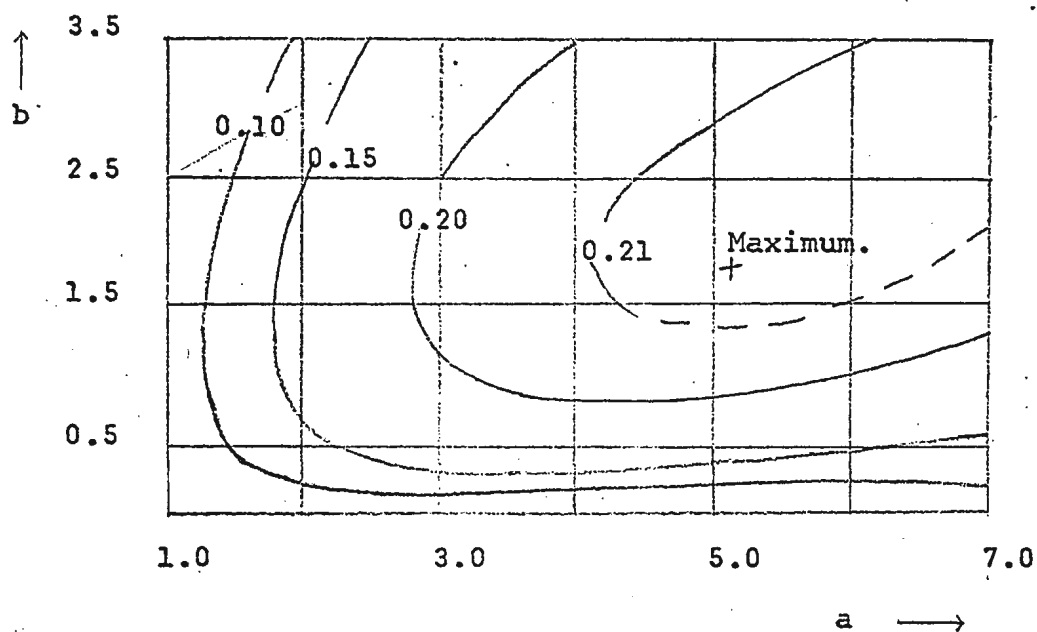


Fig. 2.4

Contours of the function  $Z_0$  in a plane representing coil proportions  $a$  and  $b$ , applicable to positioning of specimen at center of coil or at a bounding plane. (after Hall, 1963).

Further, the optimum value of  $\Delta b$  is a maximum for the specimen at the center of the coil (i.e. the coil is then thickest), and drops off as the specimen is moved away from the center along the axis. The signal-to-noise ratio is largest for a specimen placed at the center of a coil of optimum proportions; in that case substitution of the optimum  $\Delta b$  value and that of  $u$  corresponding to optimum  $a$  into equation (2.37) yields  $Z_{\max} = 0.29$ . The variation of 'a' with the positioning of the specimen is less than that of  $\Delta b$ .

Hall points out further that a coil of optimum proportions for the specimen at the center has very similar values of  $z$  at all points along the axis as one designed for a specimen at the bounding plane. Moreover, optimum proportions are nearly the same for a specimen on the coil axis beyond a bounding plane (but with  $|b_1| < 1$  or  $|b_2| < 1$ ) than in the case of the specimen at the bounding plane. The sensitivity is appreciably reduced, however, when a specimen is used at the center of a coil designed for optimum conditions at a bounding plane rather than at the center (i.e. a coil which is too thin).

From (2.24), it is seen that the signal-to-noise ratio also increases with the frequency employed and decreases in proportion to the square root of the bandwidth and inner radius  $r$ , respectively.

With respect to  $r_1$  it is also useful to consider the intensity of magnetization  $J_m$  of a specimen giving the minimum detectable signal with a particular coil. Since the signal-to-noise ratio varies inversely as the square root of the inner radius, the coil should fit as tightly as possible around the specimen when the latter is placed at the coil center. If the specimen is a cube with edges just touching the inner circumference and  $V$  is the specimen volume, then ideally

$$V = \sqrt{8} r_1^3 \quad (2.38)$$

(though in practice  $V$  is generally smaller because of the finite thickness of the coil former, whose inner radius is  $< r_1$ ).

Then, since by definition of the intensity of

$$J = \frac{M}{V} \quad (2.39)$$

one can substitute  $J_m V$  for  $M$  in equation (2.24) with  $V$  given by (2.38). This yields

$$J_m = 4.16 \times 10^{-7} n \frac{\Delta f^{\frac{1}{2}}}{f} \frac{Z}{r_1^{5/2}} \quad (2.40)$$

where  $Z$  is defined by (2.28), and  $\rho$  is taken as  $1.67 \times 10^{-6}$  ohm-cm. (for copper). Using a large specimen therefore gives a higher sensitivity with a given coil. Alternatively, the sensitivity increases markedly with increasing inner radius,

provided the specimen size increases accordingly.

Hall (1963) concludes that using a coil of optimum proportions, positioning the specimen at its center and employing a larger specimen by enlarging the inner radius of the coil (and still maintaining the optimum proportions) "can lead to a gain of 30 to 45 times over the sensitivity that can easily result from a failure to utilize the optimum conditions".

#### 2. 4. Present Design of the Double Coil.

The double coil constructed for the present investigations was designed for almost optimum proportions for the case when the specimen is kept at the bounding plane (see Table 2.1). This was done with the ultimate aim of adapting the double coil for high-temperature studies of the magnetic susceptibility of rocks; in this case the total thickness of the oven and thermal insulation surrounding the specimen will amount to a few centimeters, making it practical to locate the specimen an equivalent distance beyond the bounding plane.

While the proportions of the double coil were maintained at near-optimum, it was designed for low resistance, which required the use of relatively thick wire; for  $N_1 + N_2 = 45,640^{+10}$  turns this resulted in a massive coil (Tables 2.1 and 2.2). A coil of low resistance has certain advantages: apart from the fact that it is easier to produce uniform windings with the thicker

wire, the value of the minimum detectable signal is also reduced, as is the noise voltage (equation (2.21)). It should be noted, however, that the use of thicker wire in itself does not imply an increase in the signal-to-noise ratio, in the absence of other criteria [as apparent from the fact that equation (2.24) is independent of  $d$  or  $n$ ].

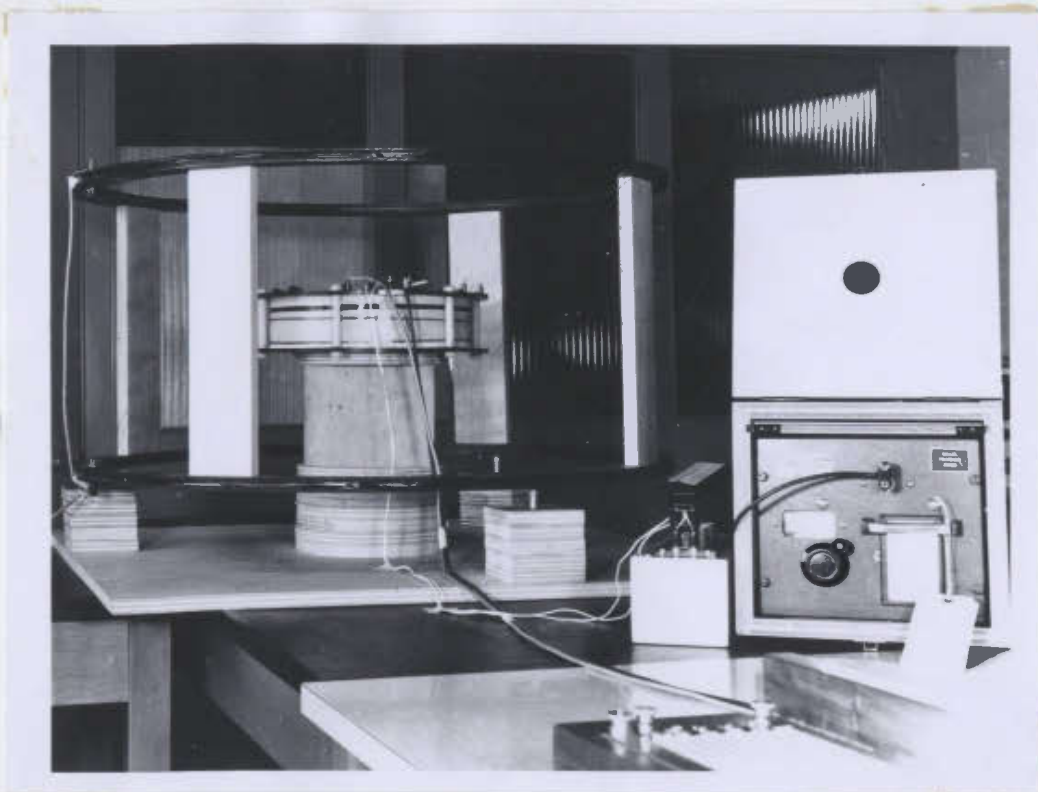
A number of cases using different values of ' $a$ ' and ' $\Delta b$ ' were tried and the final values selected were

$$a = 3.25 \quad \Delta b = 1.97$$

Although these values are not the optimum ones, the departure from the optimum is very small since the signal-to-noise contours have a very broad maximum (Fig. 2.4). For the specimen at the bounding plane, the signal-to-noise ratio corresponding to  $Z$  is 0.21; while for the case chosen ( $a = 3.25$ ,  $\Delta b = 1.97$ )  $Z = 0.20$ , i.e. a decrease by 5% or so from optimum.

Final design data and dimensions of the double coil are given in Tables (2.1) - (2.3) and in Fig. 2.5.

The coil former was made of "tufnol" plastic and its two bounding plates were clamped together rigidly by means of six plastic bolts. This was done to ensure that the coil would suffer minimum distortion due to mechanical stresses or variations in temperature. The last turn of the inner winding is



Photograph showing the double coil placed at the center of the Helmholtz Coil A.

(Tuning capacitors are shown on the right).

TABLE 2.1

DIMENSIONS OF THE DOUBLE COIL.

Preferred location of specimen :	on coil axis beyond one of bounding planes.
Inner radius of Winding $W_1$ :	$r_1 = 4.0\text{cms.}$
Outer radius of Winding $W_1$ :	$r_2 = ar_1 = 13.0\text{cms.}$
Thickness Factor (dimensionless) :	$a = 3.25$
Width Factor (dimensionless) :	$\Delta b = 1.97$
Width of either Winding :	$(\Delta b)r_1 = 7.86 \text{ cms.}$
Distance Factor from specimen to near side of coil (dimensionless) :	$b_1 = 1.00$
Distance Factor to far side of coil :	$b_2 = 3.47$
Distance from specimen to near side of coil :	$b_1r_1 = 4.00 \text{ cms}$
Distance from specimen to far side of coil :	$b_2r_1 = 11.86 \text{ cms}$



TABLE 2.1 (Contd.)

DIMENSIONS OF THE DOUBLE COIL.

Inner radius of Winding $W_2$ :	$r_2 = ar_1 = 13.0 \text{ cms}$
Outer radius of Winding $W_2$ :	$cr_1 = 16.0 \text{ cms.}$
Winding Section Coil $W_1$ : (no units)	$(a - 1) \Delta b = 4.4$
Winding Section Coil $W_2$ (no units) :	$(c - a) \Delta b = 1.5$
Winding Section Coil $W_1$ :	$(a - 1) \Delta b r_1^2 = 71.0 \text{ cm.}^2$
Winding Section Coil $W_2$ :	$(c - a) \Delta b r_1^2 = 23.7 \text{ cm}^2$
Thickness of each bounding plate (tufnol) :	$0.63 \text{ cm.}$
Inner radius of plastic core of coil :	$2.00 \text{ cm.}$
Outer radius of plastic core of coil :	$r_1 = 4.00 \text{ cm.}$

TABLE 2.2.

WIRE AND RESISTANCE DATA FOR DOUBLE COIL.

Size of wire (copper annealed at 20°C) :	A.W.G. No. 26
Diameter of the uninsulated wire at 20°C. :	$d = 4.049 \times 10^{-2} \text{ cm.}$
Insulation (double thickness) :	0.005 cm.
No. of turns on inner Winding $W_1$ :	$N_1 = 33,090$
No. of turns on outer Winding $W_2$ :	$N_2 = 12,550 \pm 10$
Total No. of turns :	$N_1 + N_2 = 45,640 \pm 10$
Resistance of $W_1 + W_2$ :	$R_T = 3.8 \times 10^3 \text{ ohms.}$
Length of Wire at 20°C :	$N_1 + N_2 = 2.8 \times 10^6 \text{ cms.}$
Mass of Wire at 20°C :	$N_1 + N_2 = 3.2 \times 10^4 \text{ gms.}$
No. of Layers in Winding $W_1$ :	192 or 193
No of turns per layer in either winding :	172 or 173
No. of Layers in Winding $W_2$	73.1

TABLE 2.3.

OUTPUT AND SENSITIVITY OF DOUBLE COIL.

A.C. Magnetizing field :  $H = 0.5 \text{ oe. r.m.s.}$

Frequency :  $f = 60 \text{ cps.}$

Volume of the specimen  $V = 8.00 \text{ cm}^3$

Susceptibility of the specimen :  $K = 1.0 \times 10^{-5} \text{ e.m.u/cc.}$

Thermal Noise :  $e_n = 7.0 \times 10^{-9} \text{ volts r.m.s.}$

Position of the specimen along coil axis $b_1 \quad r_1$	Shape Factor $F_1 - F_2$	Signal Output $e(\mu\text{v})$ r.m.s.	Signal-to- Noise Ratio $\frac{e}{e_n}$
--	--------------------------------	--	--

(a) Above the bounding  
plane.

8.75 cms.	0.21	0.28	40
6.00 cms.	0.33	0.44	63
4.30 cms.	0.48	0.63	90

(b) At the bounding  
plane.

1.06	1.55	220
------	------	-----

TABLE 2.3. (Contd.)

OUTPUT AND SENSITIVITY OF DOUBLE COIL.

Position of the specimen along coil axis $b_1 \ r_1$	Shape Factor $F_1 - F_2$	Signal Output $e(\mu v)$ r.m.s.	Signal-to- Noise Ratio $\frac{e}{en}$
(c) 2 cms. from the center	1.48	1.95	280
(d) At the center	1.60	2.12	300

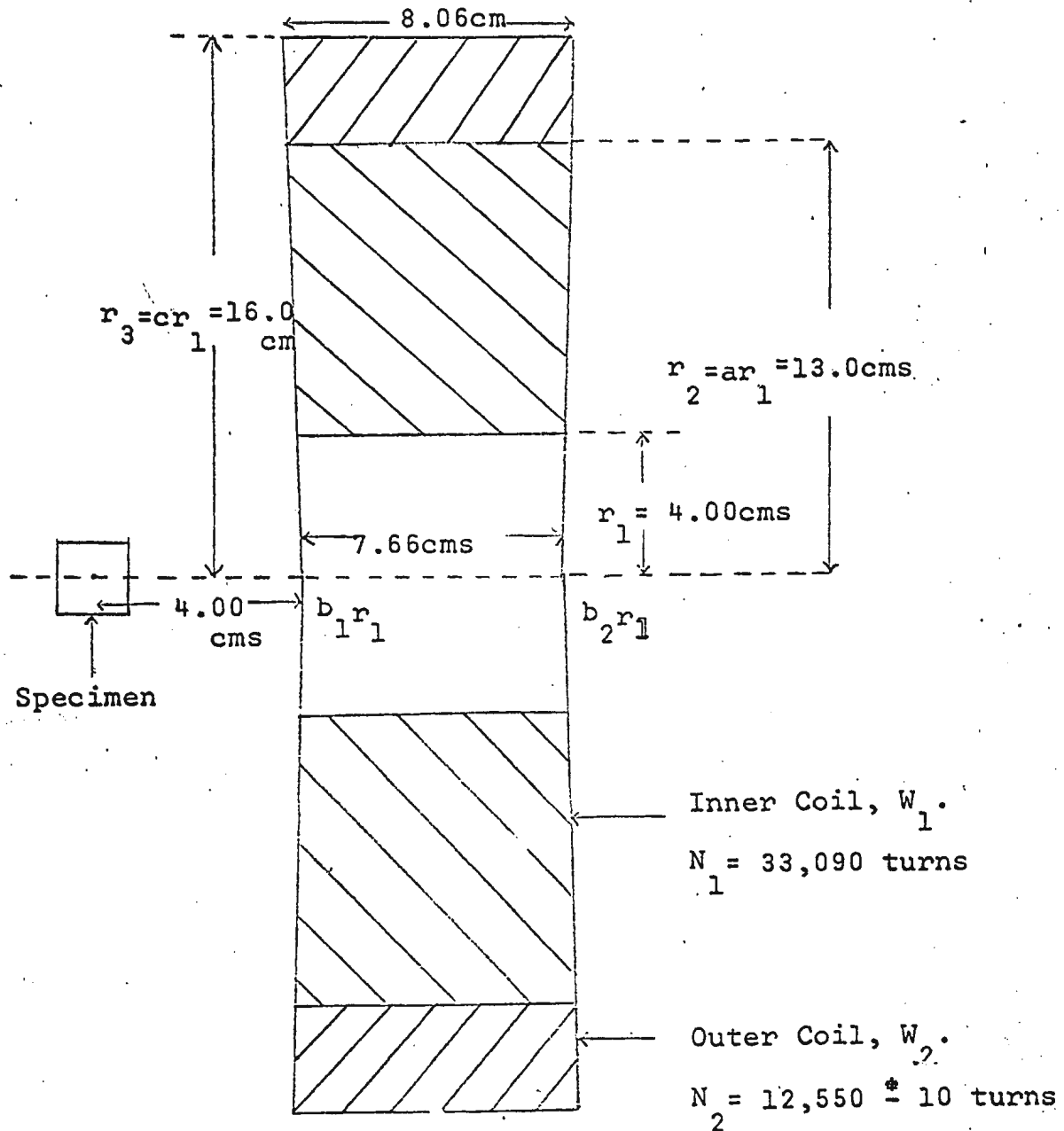


Fig. 2.5 Pick-Up Coil Cross-Section Showing Various Coil Dimension  
(Non-rectangular cross-section of double coil is due to slight bending of coil former during the winding process)

tapped at ten points. This was done to achieve a balance equivalent to  $1/300,000$  of the total e.m.f. induced in the inner coil.

### CHAPTER THREE

#### DESCRIPTION OF AUXILARY APPARATUS.

The a.c. bridge method of measuring susceptibility has been outlined in Chapter One, and the theory of the double coil in Chapter Two. A description of the other components of the bridge network (Fig. 3.1) and their performance is given in this chapter.

##### 3. 1. Oscillator.

A Hewlett-Packard Model 202-C low-frequency oscillator was used in conjunction with a power amplifier and a pair of Helmholtz coils to provide the magnetizing field of the desired frequency. The rated output of the oscillator has  $\pm 2\%$  accuracy under normal ambient temperature conditions and a distortion of less than 0.5% above 5 cps; the distortion being independent of the load impedance. The hum voltage is less than 0.1% of rated output, decreasing as the output is attenuated. The warm-up period for maximum stability is thirty minutes.

##### 3. 2. Power Amplifier.

The output from the oscillator is fed to the input of an audio-frequency power amplifier of the Williamson type (Heathkit Model AA - 23). Its frequency response is  $\pm 1$ db. from 30 to 15,000 cps. at 25 watts, using auxilary input.

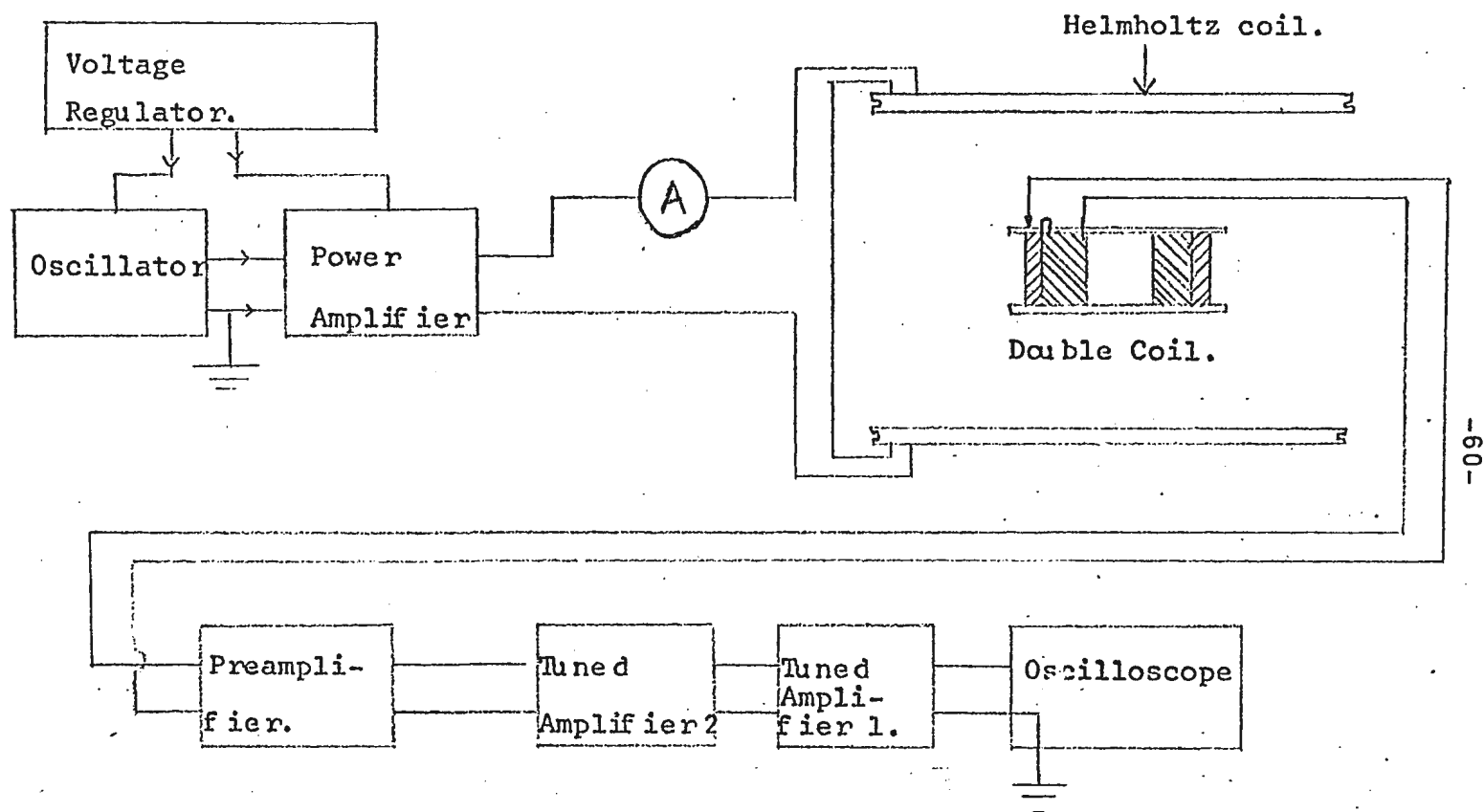


(Fig. 3.1. Block Diagram of the Experimental Set-up.  
(Potentiometer Arrangement not shown).



A modification consisted of placing a  $2\mu\text{F}$ , 1000V W D.C capacitor in parallel with the primary of the output transformer, to resonate the output at about 32cps, close to the frequency at which the double coil operates at present. This was done to attenuate the 60cps. and 120 cps. components in the output of the amplifier. The bass control was kept at the flat position -- a compromise between low distortion and attenuation of the fundamental. The distortion in the output used in the present investigations was about 1.5% when the current output was 0.5 amperes (r.m.s.) and the corresponding voltage output about 5.8 volts (r.m.s.); the distortion was less for lower outputs. At balance of the fundamental mode in the double coil, the magnitude of the above distortion was sufficient to place a serious limitation upon the sensitivity of the susceptibility bridge. This will be discussed further in Chapter Four.

### 3. 3. Helmholtz Coils.

A pair of Helmholtz coils is used to produce the uniform time-varying magnetic field in a central region in which the double coil is placed. The output of the power amplifier is fed to the Helmholtz Coils, their impedance ( $11\text{-}\Omega$ ) being approximately matched to the output impedance ( $15\text{-}\Omega$ ) of the amplifier, so that a current could be sent through the coils with little distortion.

The strength of the magnetic field at a point  $x$  cms along the axis of the pair of Helmholtz coils and  $y$  cms. in any

direction perpendicular to the axis from the center is given by (e.g. Nagata, 1961; p.72):

$$H_x = \frac{32\pi ni}{50\sqrt{5}a} \left[ \frac{1-18}{125a^4} (8x^4 - 24x^2y^2 + 3y^4) + \dots \right] oe \quad (3.1a)$$

and

$$H_y = H_x \left[ 0.576 \frac{xy (4x^2 - 3y^2)}{a^4} + \dots \right] oe \quad (3.1b)$$

At the center of the Helmholtz pair,

$$H_x = \frac{0.899ni}{a} oe \quad (3.1c)$$

$$H_y = 0, \text{ where} \quad (3.1d)$$

$x = 0$  at the center of the coil pair;

$y = 0$  along the coil axis:

$H_x$  is the component of the magnetic field along the axis;

$H_y$  is the component perpendicular to  $H_x$ ;

$a$  is the radius of each coil, and equals the distance between the coils;

$n$  is the number of turns per coil; and  $i$  is the current through the coils.

Two alternative pairs of Helmholtz coils (A and B) were used in the course of the present investigation, with B having larger inductance and smaller resistance than A. (Table 3.1) Coil B was substituted for A, as it gave the same field at its center with approximately one-half of the output of the power amplifier. This in turn reduced the 2nd harmonic content in the output almost proportionally, thus permitting a better balance of the double coil. These improvements will be further discussed in Chapter Four.

The departure from uniformity in the magnetic field near the center of the pair of Helmholtz coils (either A or B), and at two other points, has been calculated on the basis of equations (3.1, a-d) and is expressed in Table 3.2 as the ratio of the field component ( $H_x$  or  $H_y$ ) at point P and that of the x-component at the coil center.

Case 1 is for a specimen cut as a cube of side length 2.0 cms., so that its furthest extension is at  $x = \pm 1.0$  cm.,  $y = \sqrt{2}x = \pm 1.4$  cm.: the greatest difference between the field at any point in the region occupied by the cube, and that at the cube center is then  $< 0.05\%$ . Similarly, Case 2 corresponds to the greatest displacement of the specimen from the coil center likely to be required in actual experiments (cube center 7.5 cm. from the coil center along the axis), here the field is reduced by a maximum of 0.1% compared to its value at the center of the Helmholtz coils.

M. J. N. LIBRARY

TABLE 3.1

DATA ON HELMHOLTZ COILS.

	Pair A.	Pair B.
Diameter to center of wiring section (2a)	90cms.	90cms.
No. of turns per coil (n)	50	98
Wire Gauge (A.W.G.).	20	14
D.C. Resistance per coil	4.8 $\Omega$	2.4 $\Omega$
Field at center of pair, $\frac{H_0}{i}$	0.999 $\frac{oe.}{amp.}$	0.999 $\frac{oe.}{amp.}$

M. J. N. LIBRARY

TABLE 3.2

MAGNETIC FIELD AT VARIOUS POINTS IN THE  
HELMHOLTZ COIL REGION.

(Co-ordinates of Coil Center:  $x=0, y=0$ ; at coil axis  $y=0$ )

Case No.	Co-ordinates of Point P.		Relative Field Component at point P. ( $H_{x0}=1$ )	
	$\pm x$	$\pm y$	$H_x/H_{x0}$	$H_y/H_{x0}$
-	0	0	1.000	0
1.	1.0cm.	1.4 cm	1.000	$4 \times 10^{-7}$
2.	7.5cm.	0	0.999	0
3.	7.5cm.	7.5cm.	1.001	$4.409 \times 10^{-4}$
4.	0	8.5cm.	0.999	0
5.	0	14.5cm.	0.995	0

Because of its relatively large dimensions, the double coil experiences much greater deviations from field uniformity than a specimen placed upon the Helmholtz coil axis. In Cases 4 and 5, for example the central plane of the double coil is assumed to be at the Helmholtz coil center (i.e. at  $x=0$ ), and  $H_x/H_{x0}$  is given for  $y = \pm 8.5$  cms and  $\pm 14.5$  cms., respectively, corresponding to the centers of the inner and outer windings. However, as the geometry of the field over the volume of the double coil remains essentially unchanged before and after the specimen is inserted, the error due to non-uniformity of the field in the region of the double coil is nearly constant and can be accounted for during the calibration. A small non-uniformity of the field over the double coil region has actually some practical advantage in allowing convenient fine balancing of the fundamental output of the double coil: the method is to re-position the latter over a short distance along the Helmholtz coil axis, thus changing the total flux linkage of the outer winding very slightly with respect to that of the inner winding (see e.g. Bruckshaw and Robertson, 1948).

### 3. 4. Pre-Amplifier.

The differential voltage of the double-coil is fed to a Tektronix low-level pre-amplifier, Type 122. (Fig. 3.2)

The input stage is a push-pull common-cathode amplifier

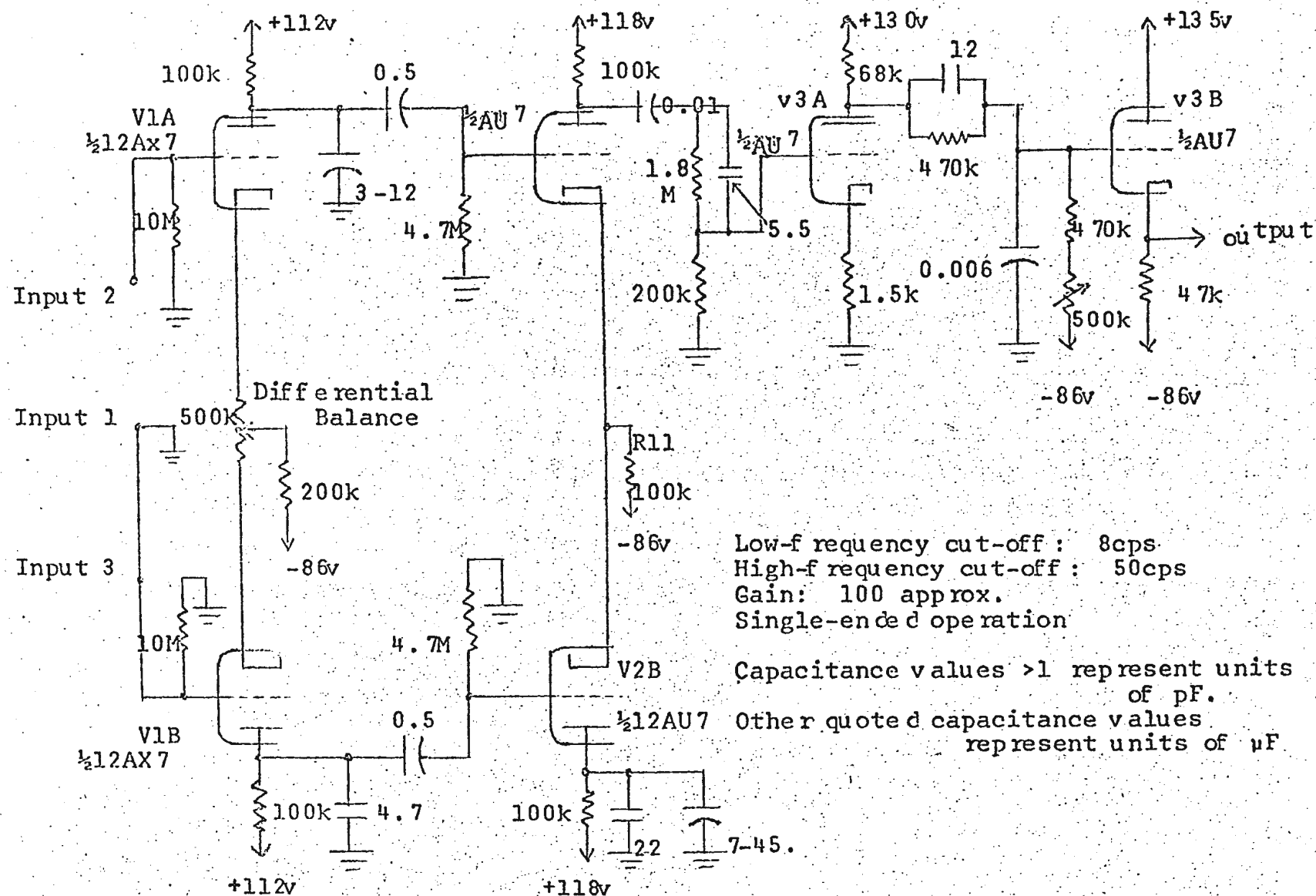


Fig. 3.2 Circuit Diagram, Type 122 Low-Level Preamplifier.

arranged to provide for signal connection to either or both grids. For single-ended input the unused grid must be grounded. For example, one might consider the case when input terminal no. 3 is grounded and the signal applied between input terminal no. 2 and ground. With this connection, V1A applies its signal to V2A through two paths, the first leading directly from the plate of V1A through the 0.5uF capacitor to the grid of V2A. The second path leads from the V1A cathode through a 500 ohm resistance to the cathode of V1B, then from the plate of V1B again through a 0.5uF capacitor to the grid of V2B, and from the cathode of V2B to that of V2A. The resulting phases are such that the current in resistor R11 is kept nearly constant, and current degeneration, which would otherwise occur, is practically eliminated. The remainder of the amplifier circuit is single-ended, starting from the plate of V2A through the coupling capacitor 0.01uF. The plate output from V3A is applied to the grid of V3B through a low-pass network consisting of a 470K resistor as the series arm and a 12pf capacitor as the shunt arm. The output from V3B is taken from the cathode and is available at the front panel through a UHF coaxial connector.

The noise level for the gain position 100 is about 1uv (peak-to-peak), expressed as an equivalent input signal with both grids shorted at input, the lower and upper 3-db. points being 8 and 50 cps. respectively. The actual gain was found to be 107 upon measurement.

M. U. N. LIBRARY



### 3. 5. Tuned Amplifiers.

To achieve the required degree of sensitivity of the bridge, the differential output voltage of the fundamental frequency from the double coil has to be reduced to a value of the order of  $1\mu\text{V}$ , which means that the fundamental frequency has to be balanced approximately to 1 part in  $10^6$  or more. In a laboratory, however, the line frequency noise signals tend to be of the order of a few millivolts and besides, the second and higher harmonics of the balance output become relatively more pronounced as the fundamental is progressively reduced in amplitude. Thus the output from the pre-amplifier consists of a small fundamental component upon which is superposed a large harmonic component. The purpose of the tuned amplifier is ideally to select and amplify only the fundamental component, while rejecting the harmonics. The requirement of sharp selectivity on the part of such amplifiers becomes more stringent when the fundamental frequency is below 100cps, and the design of such low-frequency selective amplifiers is usually difficult.

During preliminary investigations a selective amplifier designed by Crocker (1966) was used (Fig. 3.3). It consists of an input cathode-follower stage, followed by two stages of amplification, with a selective-frequency network forming the feedback path from the output of the second stage to its input. The amount of feedback at frequencies other than the null frequency is actually controlled by the resistance  $R_{13}$ , provided



L and C are kept constant.  $R_{13}$  thus acts as a bandwidth control. The reason for using an L-C combination for the frequency-selective network was that the amplifier was designed for a large frequency range and, consequently, large variations of resistance in an R-C selective network to cover the desired frequency range would have caused impedance mismatching.

Although the gain and selectivity of the Crocker amplifier were found satisfactory, it was not used ultimately, for the reason that the selective network, being a resonant L-C circuit, had its natural frequency nearly at the fundamental frequency. Thus the network constituted an oscillator of very low output amplitude. At high gain the output signal, therefore, becomes unsteady in its amplitude. The variation in signal is rapid, of the order of 1 sec. for a change of 3-4 mv. in a total amplifier output emf of the same order of magnitude and this feature proved detrimental to the performance of the bridge: in practice, it was equivalent to a loss in sensitivity. Hence it was decided to substitute an amplifier with resistance-capacitance components in the selective network.

For this purpose a tuned amplifier based on a design by Stacey (1959) was modified with regard to some of the components he used, and his twin-tee network was redesigned for 33 cps. The circuit diagram of the amplifier is shown in Fig. 3.4 and that of the twin-tee network in Fig. 3.4a.

W. D. N. LIDKANI

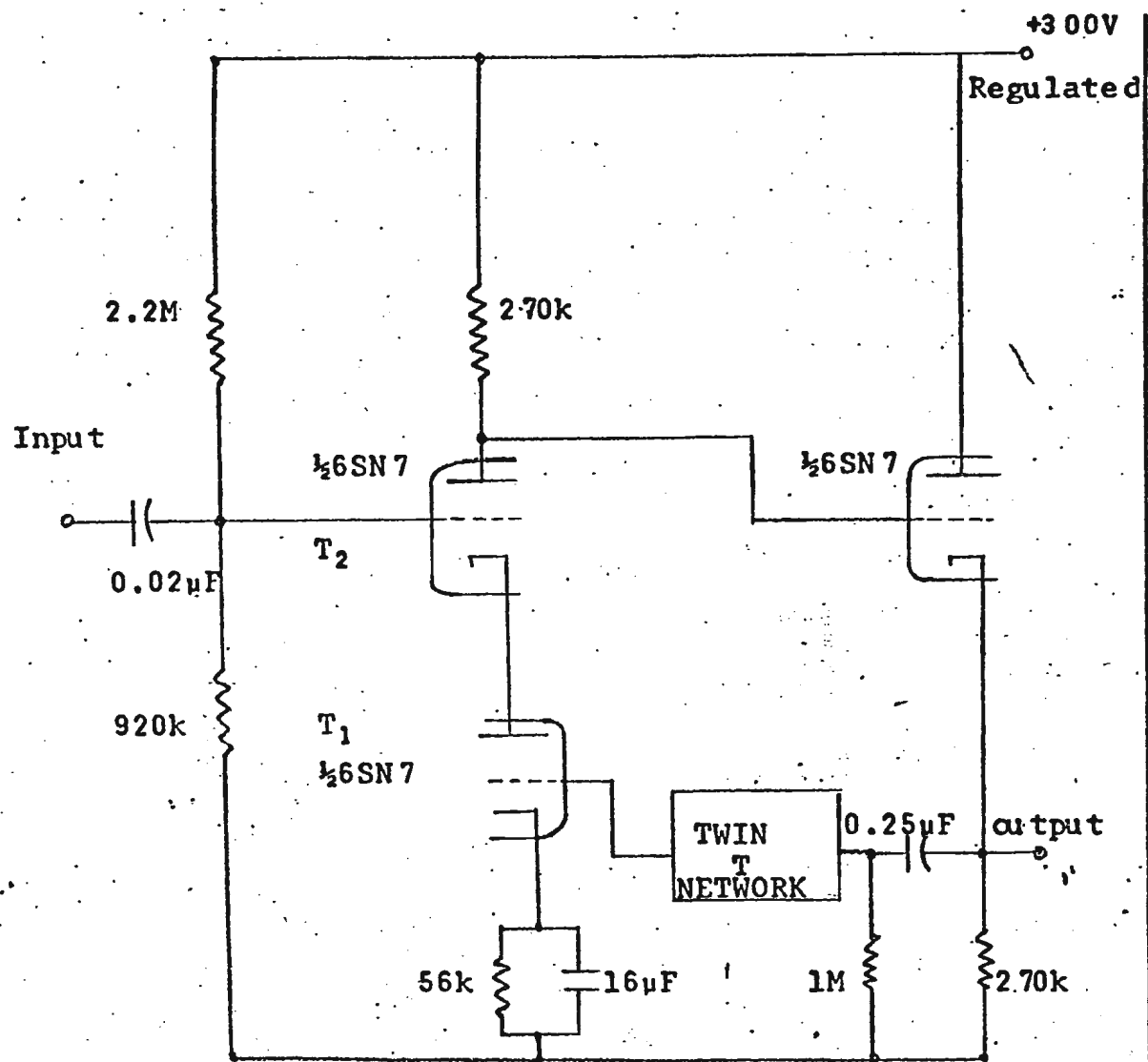
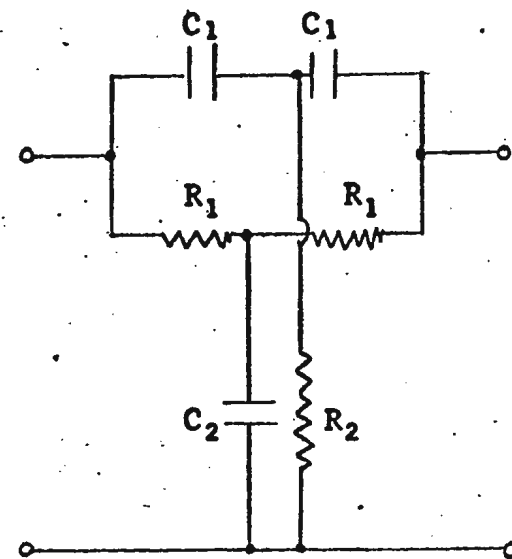


Fig. 3.4 Circuit Diagram of Tuned Amplifier.

(Adapted from Stacey, 1959)



For 1.	For 2
$C_1 = 0.04\mu\text{F}$	$C_1 = 0.04\mu\text{F}$
$R_1 = 115\text{k}\Omega$	$R_1 = 115\text{k}\Omega$
$C_2 = 0.1\mu\text{F}$	$C_2 = 0.099\mu\text{F}$
$R_2 = 53.1\text{k}\Omega$	$R_2 = 59.9\text{k}\Omega$

Fig. 3.4a

Twin-T Network of the Tuned Amplifier.



Photograph showing Stacey-Type Tuned Amplifiers  
Nos. 1 and 2

The main feature of this amplifier is that it employs two triodes in series, in a "cascode" arrangement. It can be shown that in this way a pentode is simulated, but with the low-noise characteristics of a triode. The cascode circuit is used as a feedback amplifier through application of the external signal to the grid of  $T_2$  and the feedback voltage to the grid of  $T_1$ . The output is taken from a cathode-follower stage.

When it was found that one such amplifier was insufficient in rejecting the harmonics to the desired degree, another identical amplifier was constructed and used in cascade arrangement with the first amplifier. Upon actual construction of the second amplifier it was found that the twin-tee network components had to be slightly altered, and thus the frequency response of the two amplifiers is different, as shown in the graph (Fig. 3.5). It was initially intended to adjust the components of the second amplifier to give a response identical to that of the first. This was found to be difficult, however, as the values of the R and C components in the selective network are extremely critical, slight departures from the critical values either throwing the amplifier into oscillation or making the bandwidth  $\Delta f$  undesirably large. With  $\Delta f = 2.88$  cps at the resonant frequency in amplifier 2, no further adjustments were made to reduce  $\Delta f$ , although in this way its gain was only one-third of that of amplifier 1 (see Table 3.3).

Fig.3.5. Frequency Response of Stacey Type Tuned Amplifiers  
Nos. 1 and 2.

(Input signal : 130mv (peak-to-peak)).

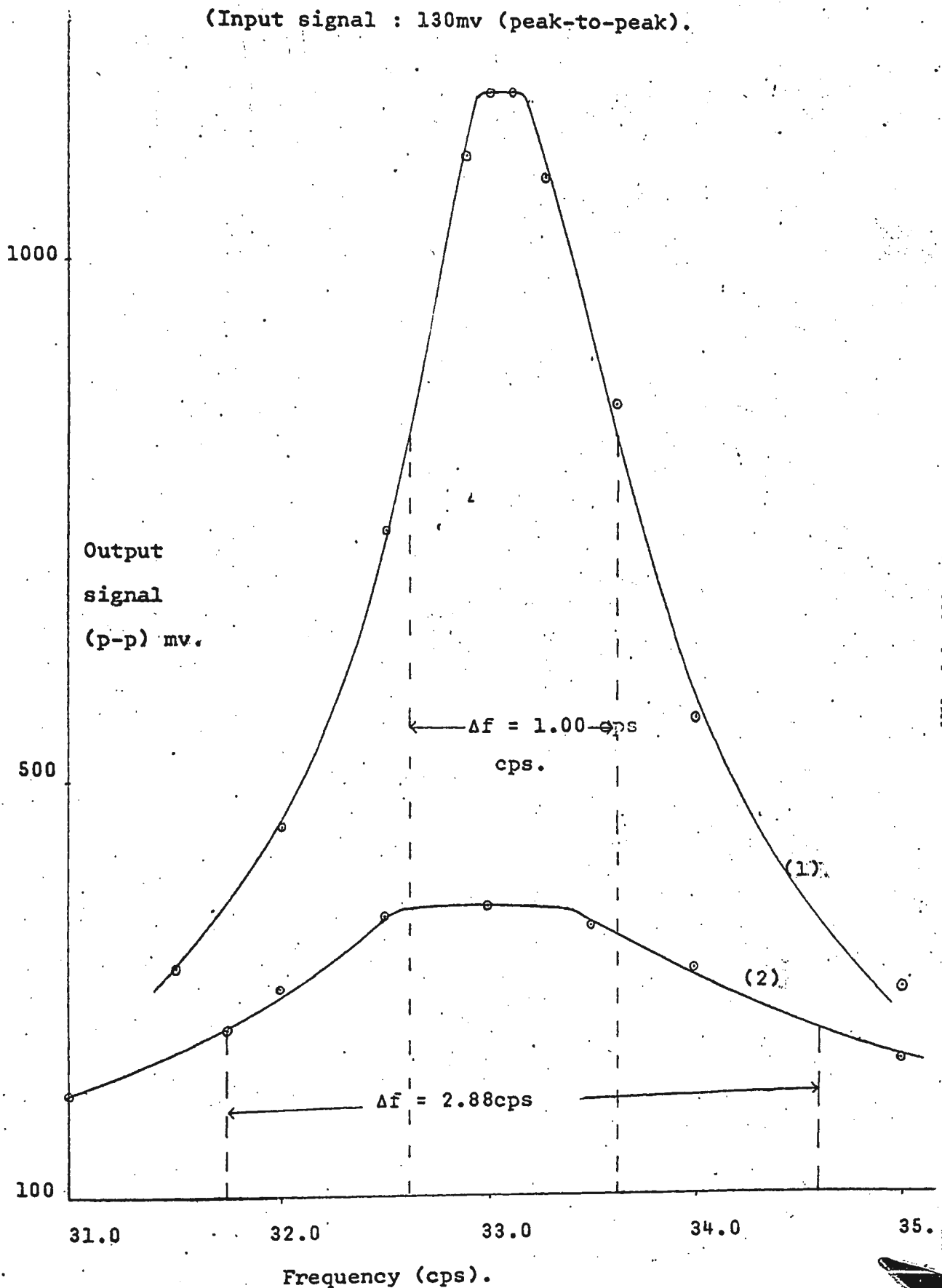


TABLE 3.3

DATA ON AMPLIFIERS IN THE BRIDGE OUPUT.

(The two amplifiers adapted from Stacey's (1959) design are used in cascade. The single Crocker (1966) amplifiers is an alternative unit. In all cases the tuning frequency is  $f = 33.0 - 33.5\text{cps}$ ).

	Amplifiers adapted from Stacey (1959).		Crocker's (1966)
	Amplifier 1	Amplifier 2	Amplifier
Input Impedance	920K $\Omega$	920 $\Omega$	45K $\Omega$
Output Impedance	300 $\Omega$	300 $\Omega$	5K $\Omega$
Gain	9.0	2.9	620
Bandwidth $\Delta f$ .	1.00cps.	2.88cps.	0.34cps
Tuning Frequency.	33.0cps	33.0cps	33.5cps
$\frac{A_1^*}{A_n^*}$	39.	12.5	

\*

where  $A_1$  is the amplitude of the fundamental mode

$A_n$  is the amplitude of the 2nd harmonic.

U. S. N. LIBRARY



Though the two amplifiers were used in cascade, thus having a gain of about 27 and a bandwidth less than 1.00cps, they do not have the gain, and consequently the sharp selectivity, of the amplifier designed by Crocker. Partly it was intentional to keep the selectivity below maximum sharpness, though this meant a reduction in gain, aim being to maintain maximum stability of the output of the amplifiers. This in turn was meant to ensure that the final "balanced" signal would not vary rapidly in amplitude - ideally it should not vary at all - as it did in the case of Crocker's amplifier.

This aim was only partially achieved, probably because the source of the instability is not only in the output section of the bridge circuit, but a large part of it is produced in the input to the Helmholtz coil; hence the double coil output would also exhibit continuous, small variations in magnitude if not frequency. As will be discussed later, this instability of the signal under near-balance conditions proved to be an effective limiting factor to the sensitivity of the double coil with the present auxiliary equipment. Since the unsteady behaviour of the balanced signal occurred only when the fundamental was almost balanced, leaving a prominent 2nd harmonic, it was decided to check the response of the tuned amplifiers at the frequency corresponding to the 2nd harmonic (66 cps.) It was observed that, though the amplifiers performed satisfactorily at the fundamental frequency, the magnitude of the output corresponding to the 2nd

U. S. N. LIBRARY

harmonic underwent a somewhat slow irregular variation with a time constant of roughly 6 seconds. The balanced signal from the coil, however, showed a more rapid variation with a time constant  $< 0.1$  second, again of irregular magnitude suggesting strongly that at least part of the cause of instability lies in the oscillator-power amplifier section of the input circuit. This will be discussed further in the next chapter.

## CHAPTER FOUR

### 'BALANCING' THE DOUBLE COIL.

#### 4. 1. Distributed Capacitance of Coils.

The following remarks, taken from Terman p.84 (1943), on the distributed capacitance of multilayer coils are appropriate to the ensuing discussion, since this factor was found to control the behaviour of the double coil - and thereby the "balanced achieved" - to a large extent.

"The voltage difference that exists between the different parts of the coil produces an electrostatic field in the air and in the dielectric near the coil. The effect of the resulting storage of electrostatic energy upon the behavior of the coil is to a good approximation equivalent to the effect produced by a small capacity shunted across the terminals of the coils. Such a hypothetical shunting capacity is termed the *distributed capacity* of the coil. Under practical conditions there are also capacities between the coil terminals and between lead wires which increase the total shunting capacity<sup>1</sup>.

"The distributed capacity is largely independent of the number of turns if there are a considerable number of turns and these are not very closely spaced.....

"Multilayer coils tend to have higher distributed capacity than do single-layer coils....

<sup>1</sup> "The effective distributed capacity will also depend to some extent upon the current distribution in the coil, and will, in general, be larger when the coil is shunted with a large external tuning capacity than when the coil is resonated with its self-capacity."

" Dielectric in the field of a coil, such as the form upon which the coil is wound, the insulation of the wire, etc., increases the distributed capacity. Metal objects such as a shield, metal panel, etc., near a coil increase the distributed capacity, particularly if the distance from the coil is of the same order of magnitude as the coil dimensions or less. ....

" The presence of the distributed capacity causes a partial resonance that modifies the apparent resistance and reactance of the coils as viewed from the terminals..."

#### 4. 2. Calculation of the Induced e.m.f. in the inner and the outer coil.

The induced emf is given by

$$e = - \frac{\partial \phi}{\partial t} \times 10^{-8} \text{ volts} \quad (4.1)$$

where  $\phi$  is the total flux linked with the coil at time  $t$ .

Then if a single circular turn of radius  $r$  lies in a uniform field  $H$  in air the maximum associated flux threading the turn is

$$\phi_o = \pi r^2 H \quad \text{maxwells} \quad (4.2)$$

$$\text{where } \phi = \phi_o \cos (wt) \quad (4.3)$$

in the case of the turn rotating in the field with uniform angular velocity  $w$ .

For a coil having  $n$  turns per cm., let

$W$  = width of the coil in cm.,

$dr$  = elemental thickness of winding at radius  $r$ , in cm.

and  $r_1$  and  $r_2$  = inner and outer radii of the coil, respectively, in cm.

Then for an elemental width  $dr$  cm. there will be  $n \cdot dr$  turns, and for each turn at constant radius (i.e. each turn in the same layer) there are  $n \cdot dr$  elemental turns in the same plane of the coil (i.e.  $n \cdot dr$  elemental "layers"). Hence there are  $nW$  turns in any one layer, and an elemental thickness of the coil will have  $nW \cdot n \cdot dr$  turns. Using (4.2) the maximum flux threading this elemental thickness is

$$d\phi_o = nW (n \cdot dr) \pi r^2 H_o \quad (4.4)$$

and therefore the maximum flux threading the entire coil is

$$\phi_o = \pi n^2 W H_o \int_{r_1}^{r_2} r^2 dr \quad (4.5)$$

Also, from (4.1) and (4.3) :

$$e = w \phi_o \sin (wt) \times 10^{-8} = 2\pi f \phi_o \sin (2\pi ft) \times 10^{-8} \text{ volts} \quad (4.6)$$

where  $f = 1/t$  is the frequency of the flux. Then the amplitude of the induced e.m.f. is

$$E_m = 2\pi f \phi_o \times 10^{-8} \text{ volts} \quad (4.7)$$

and, substituting (4.5) for  $\phi_o$ , we have

$$E_m = 2\pi^2 f n^2 W H_o \int_{r_1}^{r_2} r^2 dr \times 10^{-8} \text{ volts} \quad (4.8)$$

Similarly if  $H$  and  $|e|$  are the rms values of field and emf respectively:

$$\therefore |e| = 2\pi^2 f n^2 W H \int_{r_1}^{r_2} r^2 dr \times 10^{-8} \text{ volts rms} \quad (4.9)$$

If  $H = 0.5$  oe. rms (similar to field values commonly used with measurement of susceptibility of rocks):

$$\therefore |e| = \pi^2 f n^2 W \int_{r_1}^{r_2} r^2 dr \times 10^{-8} \text{ volts rms} \quad (4.10)$$

$$\text{and hence : } |e| = \frac{\pi^2 f n^2 W}{3} (r_2^3 - r_1^3) \times 10^{-8} \text{ volts rms} \quad (4.11)$$

For the present coil (see Tables 2.1 and 2.2)  $n = 22.15$ ,  
 $W = 7.90$  cms. ( $W$  is taken as the arithmetic mean of 7.70 and  
8.10 respectively. This is so because there is a slight de-  
pression in the central portion of the coil: see Fig. 2.5).

For the inner winding,

$$r_1 = 4.00 \text{ cm}; \quad r_2 = 13.0 \text{ cm}.$$

Then, using  $H = 0.5$  oe. rms and inserting the above values  
into (4.11), the rms voltage induced in the inner winding is

$$e_i = 27.6f \times 10^{-2} \text{ volts rms} \quad (4.12)$$

Similarly, for the outer winding, the above values of  
 $n$  and  $w$  apply, with

$$r_1 = 13.0 \text{ cm}; \quad r_2 = 16.0 \text{ cm}.$$

Therefore, the rms voltage induced in the outer winding is

$$e_o = 24.4 f \times 10^{-2} \text{ volts rms} \quad (4.13)$$

For a frequency  $f = 33$  cps.,

$$e_i \text{ (calculated)} = 9.1 \text{ volts rms}$$

$$e_o \text{ (calculated)} = 8.1 \text{ volts rms}.$$

while

$$e_i(\text{measured}) = 8.0 \text{ volts rms.}$$

$$e_o(\text{measured}) = 7.9 \text{ volts rms.}$$

The above calculated and measured values refer to the completed coil near balance. Though the coil was designed such that the calculated value of  $e_i$  equals  $e_o$ , the effect of distributed capacitance caused a change in the number of turns on the outer winding, causing the calculated value of  $e_o$  to deviate from that of  $e_i$ .

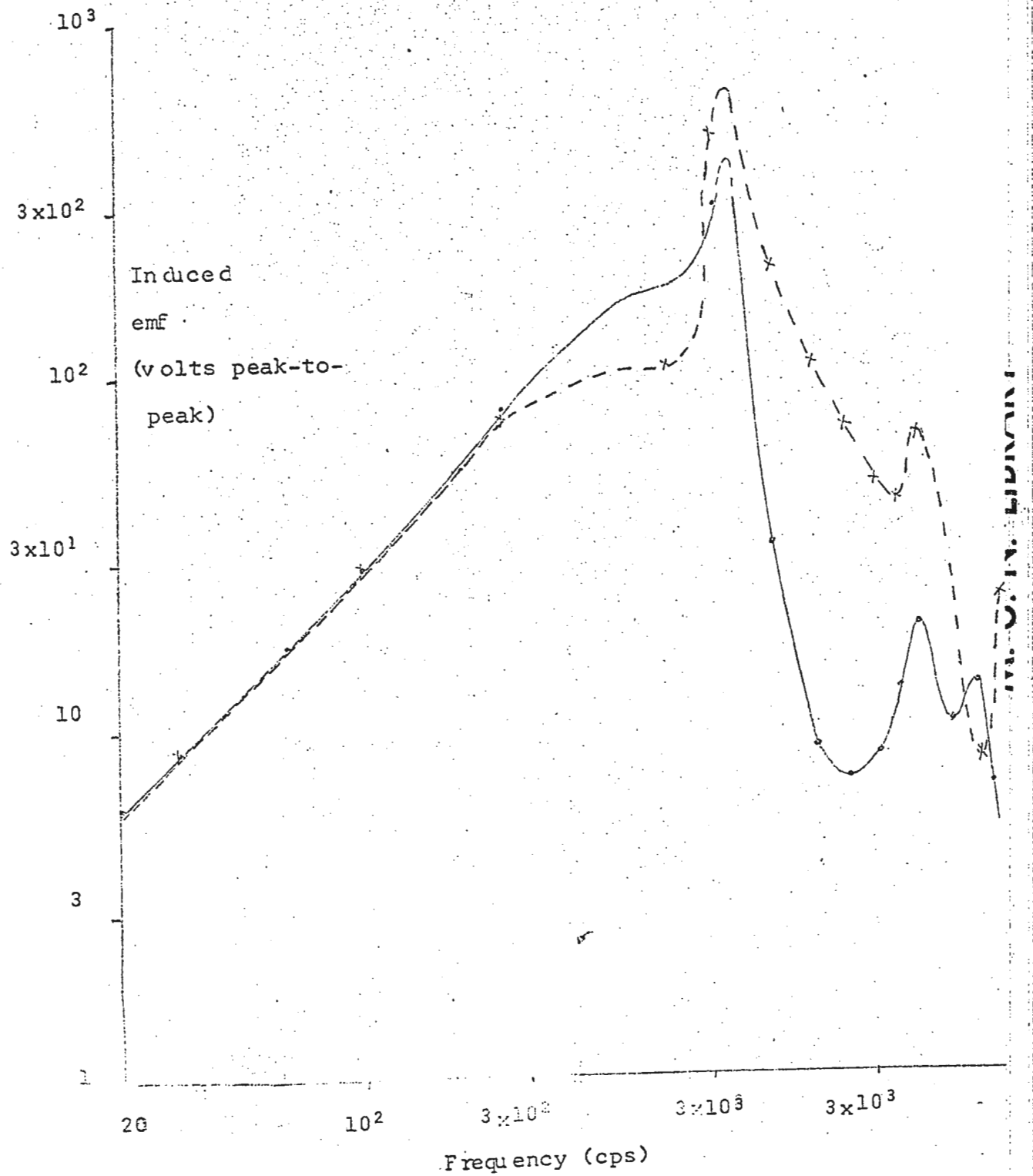
The calculated values of the induced emf show an excess for the inner winding not borne out by measurements made by a high-impedance voltmeter (in the present case both a V.T.V.M. and a transistor voltmeter were used). The discrepancy arises because the calculated values fail to take into account the distributed capacitance which is greater for the inner winding (see Section 4.4). At the same time, the fact that the calculated and measured values agree to within 14% shows that, as expected, the effect of the distributed capacitance is not prominent at low frequencies such as 33 cps. At higher frequencies (i.e., >250 cps.) the effect is very predominant and the measured voltages show much greater deviation from the theoretically calculated values. This will be discussed in the next section.



4. 3. Induced voltages of the inner and outer windings as a function of frequency.

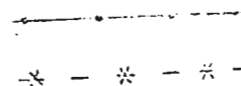
The induced voltages in the inner and the outer windings were measured as a function of frequency for a magnetizing field of 0.20 oe (rms). The theory predicts [ eqns (4.12) and (4.13) ] a linear increase in the induced voltages with frequency, but in case of both windings, the actual behaviour was linear only up to about 250 cps. (Fig. 4.1). Above this frequency the departure from linearity becomes observable and at higher frequencies the induced voltages in the two windings begin to differ markedly. The difference becomes increasingly large as the frequency increases, and close to 1100 cps. both windings have a resonance peak - a direct consequence of the distributed capacitance because each winding behaves as an L-C-R resonant circuit. Above the self-resonant frequency there is a sharp decrease in the voltage induced by a given alternating dipole, but both windings possess irregular secondary resonances. The observed decrease in the induced voltages is due to the fact that at frequencies greater than 1100 cps, the impedance offered by the coil as a whole is very much greater than the parallel impedance due to the intercapacitance between neighbouring turns and layers respectively. The current, taking the path of least impedance, therefore does not flow through the coil to build up the emf.

Fig. 4.1. Voltage induced in the double coil windings by an alternating field  $H = 0.56\text{oe.}$  (peak-to-peak) as a function of frequency.



Graph for inner winding:

Graph for outer winding:



Phase difference between the voltages induced in the inner and the outer coil windings.

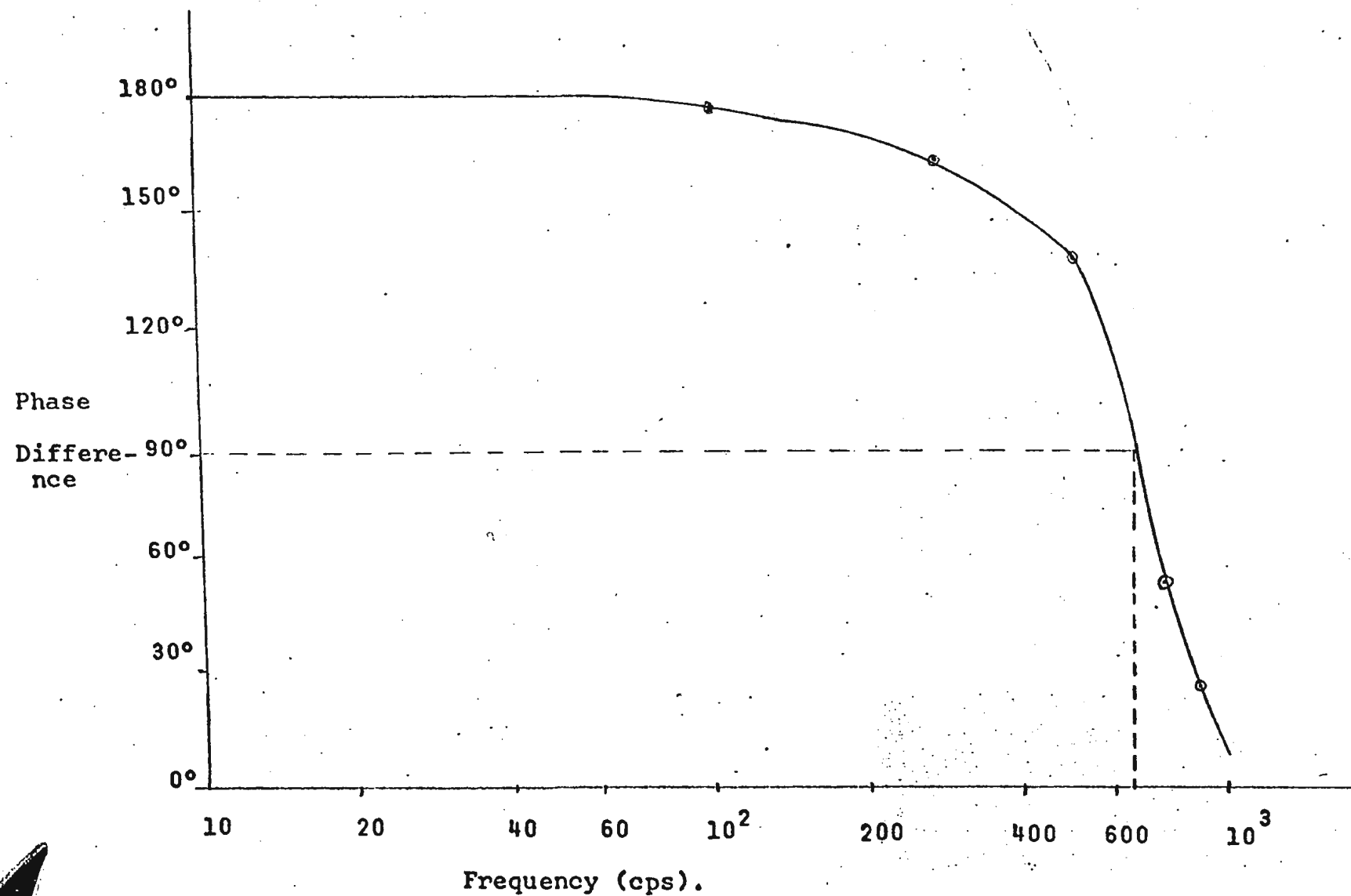
Separate phase measurements were carried out with an Analab Dual Trace Oscilloscope, Type 1120, for the emf's induced in the inner and outer coil windings by an alternating field of 0.25 oe. rms. The variation of the phase difference between the two windings is shown in Fig. 4.2 for the range of frequencies 10 to 1100 cps. For  $f < 50$  cps, there is no significant departure from  $180^\circ$  phase difference, while at 100 cps. the difference is about  $176^\circ$ . However, the phase difference changes sharply above 250 cps., dropping to  $90^\circ$  at 660 cps. and to  $9^\circ$  at 1000cps. Thus above 660 cps the two voltages are no longer acting in opposition, a result of the predominant differential effect of the distributed capacities upon the two coil windings.

Differential Voltage as a function of frequency.

The differential voltage as a function of frequency was studied up to 500 cps. It was found (Fig. 4.3) that the differential voltage increases as the square of the frequency.

Though, from equations (4.12) and (4.13), the differential voltage should be a linear function of frequency, the above observations up to 400 cps can be explained by the effect of the distributed capacitance, which is to make the resultant

Fig. 4.2. Phase difference between the voltages induced in the double coil windings by an alternating field, as a function of frequency (measured values)



The 4 separate curves were obtained after removal of a number of layers from the originally overwound outer winding, as indicated by the accompanying numbers. Extrapolation of the lowest curve (3/4 layers removed) to the origin indicates that a balance condition has been approximated at the fundamental frequency.

3.0

2.0

Resultant output

emf  
(volts peak-to-peak)

1.0

0.0

0.0

2.0

4.0

6.0

8.0

10.0

(Frequency,  $f$ )<sup>2</sup> x 10<sup>3</sup> (cps<sup>2</sup>)

-5 layers

-6

-7

-6

-7

3/4

Fig. 4.3. Resultant output voltage of double coil as a function of the square of frequency, for different numbers of layers in the outer winding

voltage proportional to the square of the frequency [ Harris (1957) p.664]. That this effect is present even at such low frequencies as 20 or 30 cps is due to the very large inductances (121 and 53 henries, respectively) of the inner and outer coil windings.

The above discussion indicates that the present double coil cannot be adapted easily to study the frequency variation of susceptibility, which was mentioned in the Introduction as a possible field of investigation.

Before concluding this section it is worthwhile comparing the present double coil with that used by Likhite and Radhakrishnamurthy (1965).

	Present author	Likhite and Radhakrishnamurthy
Inner radius of the inner winding ( $r_1$ )	4.00cms	1.5 cms.
Inner radius of the outer winding ( $cr_1$ )	13.0cms	3.0 cms.
Outer radius of the outer winding ( $cr_1$ )	16.0 cms.	not given
Parameter "a"	3.25	2.0
Thickness factor ( $\Delta b$ )	1.97	3.40
Coil Thickness ( $r_1 \Delta b$ )	7.86cms	5.1 cms.
Total No. of turns in the double coil ( $N_1 + N_2$ )	45,640	30,027
Total Resistance of double coil,	$3.8 \times 10^3$ ohms.	$5.9 \times 10^3$ ohms.

The voltages induced in each of the two windings of Likhite and Radhakrishnamurthy's double coil show similar trends with increasing frequency as the trends shown in Fig. 4.1, except that in the former case, where the inductance of the coil is much smaller than in the present case, the emf's induced by a given field at given frequency are also correspondingly smaller. Likhite and Radhakrishnamurthy's coil exhibits two resonance peaks and the difference between the voltages induced in the two windings again becomes very pronounced at the higher frequencies. However, a crucial difference between the two double coils is revealed by comparison of the actual values of the minimum frequencies at which these effects become significant, as well as the location of the resonance peaks. Whereas the author's coil has a self-resonance at 1,100 cps, and the voltages induced in the two windings are closely equal and opposite up to about 250 cps., Likhite and Radhakrishnamurthy report the first self-resonance peak at 4,000 cps and roughly equal and opposite induced voltages up to about 650 cps.

Likhite and Radhakrishnamurthy have not published any data regarding the variation of the differential voltage with frequency, but from the performance of their coil it is to be assumed that either they did not observe a significant variation, e.g. a variation proportional to the square of the frequency, as observed by the author, or that the out-of-balance emf had been



sufficiently reduced, for example by a phase-shifting device (it is customary to use a small capacitor in parallel with one of the windings), to allow measurements to be made in the chosen frequency range with the required approximation to perfect balance conditions. Likhite and Radhakrishnamurthy, measured the susceptibility of rocks in frequencies up to 1,500 cps and, with the aid of a coil of still smaller dimensions, later extended the frequency range to 2,000 cps.

Thus the use of a coil of small dimensions helped to render the effect of the distributed capacitance almost negligible, unlike in the case of the author's coil. This may suggest that for studies on the variation of susceptibility with frequency it is quite necessary to use coils of small, though optimum, dimensions. Likhite and Radhakrishnamurthy's coil design were very different from optimum design. Unfortunately, the minimum signal detectable with such a coil will also be less than for the present coil, whereas the small susceptibility differences that must be measured in a frequency-dependence study require a coil of very low minimum-signal and great sensitivity.

#### 4. 4. Procedures in Balancing the Double Coil.

In an ideal case, the differential voltage of the double coil can be reduced to zero simply by adjustment of the number of turns in the two windings. This is not possible in actual practice because of the different distributed capacitances

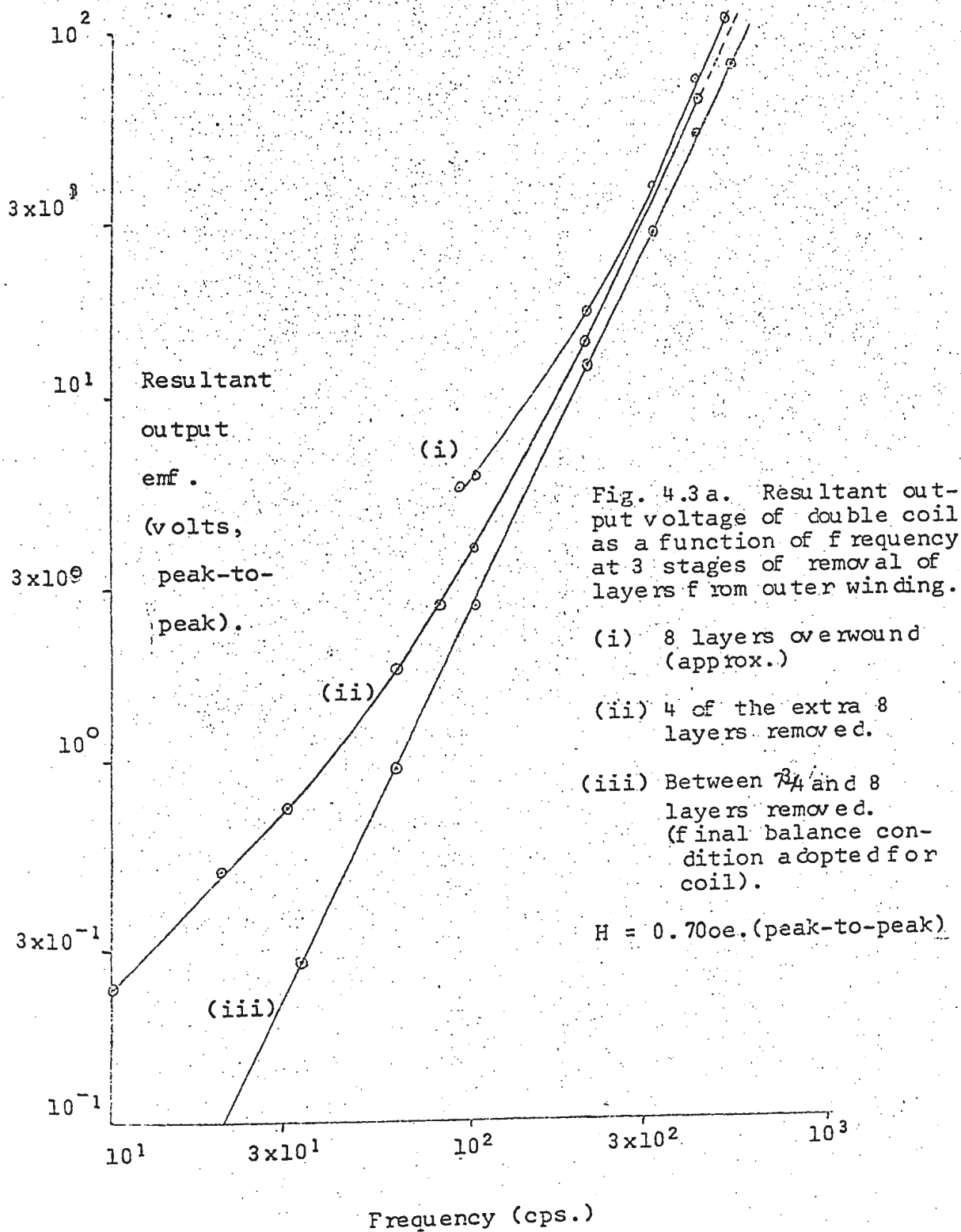
of the inner and the outer coil windings. While an adjustment in the relative number of turns in the two windings makes it easy to equalize the magnitude of the two induced emf's, it is also required that these voltages be out of phase by exactly  $180^\circ$ . When the coil is operated well below the lowest self-resonance frequency, (i.e. about 1,1000 cps in the present case - Fig. 4.1) final phase alignment is usually achieved with little difficulty with the aid of a small capacitor shunted across one of the coil windings.

Bishop (1965) made a detailed analysis of the behaviour of the coil at 60 cps., taking into account the inductance and distributed capacitance of each coil and the impedance of the measuring instrument (usually a vacuum-tube voltmeter). The self-inductances of the inner and outer coils are 121 and 53 henry, respectively, while the mutual inductance between them is 47h. These values were calculated from formulae given in Terman [ (1943), p.61 and p.73] and are quoted to 0.1% accuracy, assuming no error in measurements of dimensions and number of turns. With the actual estimated errors, these calculated values should be accurate to about 1%. The distributed capacitances were determined experimentally by Bishop and found to be  $554\mu\text{F}$  and  $350\mu\text{F}$  for the inner and outer coils respectively. His analysis showed that (as experimentally confirmed by the present author) the distributed capacitance effects at 60 cps are a small fraction of

those at higher frequencies (even those as low as several hundred cps), but are not negligible in the practical application, as they limit the extent to which balance is attainable by mere adjustment of the number of turns, even at frequencies as low as 30 cps. On the basis of his analysis, Bishop estimated that balancing of the fundamental mode would require an addition of 1200 turns, equivalent to about 8 layers, to the outer coil winding, bringing the total number of turns in that winding to 13,800

Accordingly, 1410 turns in eight complete layers were added to the second coil. Measurements of the induced voltages of the inner and the outer coil, their phase relationship and the differential voltage were carried out at a range of frequencies between 100 and 500 cps. while turns were systematically taken off. After 4 layers had been thus removed, the range of frequency measurements was changed to 10 - 100 cps. The differential output of the double coil depends on two factors: (1) inequality of the magnitude of the emf's induced in the inner and outer windings and (2) the phase difference between the two emf's. The former causes a linear variation of the differential output with frequency while the latter - due to the inequality of distributed capacitance of the two windings - varies theoretically with the square of the frequency. (Harris, p.664, 1957)

Fig. 4.3a (i) shows the case (for an excess of about



8 layers in the outer winding) when both the effects are present. At the higher frequencies factor (2) predominates, thus causing the resultant output to vary as the square of the frequency - the slope of the curve is about 2 for the frequency range of 250 - 500 cps. Towards the lower frequencies the curve tends to attain a gentler slope indicating the greater influence of factor (1) mentioned above. Unfortunately, no measurements were made at the very low-frequency end, but the trend nevertheless is evident. The behaviour outlined is to be expected, since the effect of the distributed capacitance becomes pronounced at the relatively higher frequencies.

Curve (4.3a (ii) shows the same variation after 4 layers had been removed from the outer winding. As the inequality between the magnitudes of the induced emfs in the two windings diminishes, the resultant output will show increasing dependence on the second (phase -) factor. Thus curve (ii) has a steeper slope than (i) at the lower frequencies.

The variation of the output for the final number of turns on the outer winding (after  $7\frac{3}{4}$  to 8 layers had been removed) is shown in curve 4.3a (iii). The magnitudes of the induced emf's have been almost equalized in the two windings, and hence the differential output is almost entirely due to the departure from  $180^\circ$  phase difference between the induced emf's. Since again the cause is the inequality between the distributed

capacitances in the two windings, one expects the resultant output emf. to be proportional to the square of the frequency. This is now approximately the case over the entire curve; i.e. when plotted on a log-log scale, curve (iii) is a straight line of slope 2.1 for the frequency range 20-500 cps.

The conclusion from the above set of measurements was that the number of turns on the outer winding before addition of the extra eight layers had been close to the correct value within a quarter-layer or so. The fact that removal of  $7\frac{1}{2}$ -8 layers from the outer winding brings the double coil close to balance condition is evident from inspection of Figs. 4.3b and 4.3c. In the latter case the out-of-balance emf has been plotted against  $f^2$  for  $f \leq 100$  cps and for various numbers of excess layers. The curves corresponding to an approach to balance conditions in the fundamental mode (i.e. mainly the 7 and  $7\frac{3}{4}$  curves) are not only straight lines in the lower range of frequencies, broadly conforming to proportionality of the emf. with  $f^2$ , but when extrapolated to zero frequency, they pass close to the origin: the curve for perfect balance (i.e. correct number of turns) should then pass exactly through the origin.

After  $7\frac{3}{4}$  layers had been removed once more, achievement of the required balance was, therefore, largely a matter of adjusting the phases of the two induced voltages in  $180^\circ$  opposition. In any case, at this stage adjustment of turns alone

revealed only a broad minimum the true balance being detectable only to the nearest 40-50 turns. Fig. 4.3b illustrates this in case of measurements carried out at 100 cps.

The adjustment of the phases is carried out by placing a capacitor in parallel with the winding having the smaller distributed capacity - usually the outer. The purpose is to equalize the self-capacities of the two coils. Previous workers, such as Bruckshaw and Robertson (1948) and Likhite and Radhakrishnamurthy (1965) achieved this with very small capacitances -  $1000\mu\text{F}$  or less - but when this was tried initially in the present case the reduction in the unbalanced emf was negligible. It was found instead that the achievement of good balance required capacitances of the order of  $0.08\mu\text{F}$ , or 80 times as large as those employed by the above-mentioned authors. A decade capacitor box was used in parallel with a General Radio Co. variable capacitor of 100-1100 $\mu\text{F}$  range, for fine adjustment.

While prior to phase adjustment the coil balance was relatively insensitive to changes in the number of turns, the out-of-balance voltage dropped to a sharp minimum for an optimum number of turns in the outer coil winding, after  $180^\circ$  phase adjustment has been achieved with the aid of a suitable capacitor connected in parallel with that winding. Thus the graph in Fig. 4.4 shows that, at this stage of the balancing procedure, the coil is easily balanced to the nearest 1-2 turns.

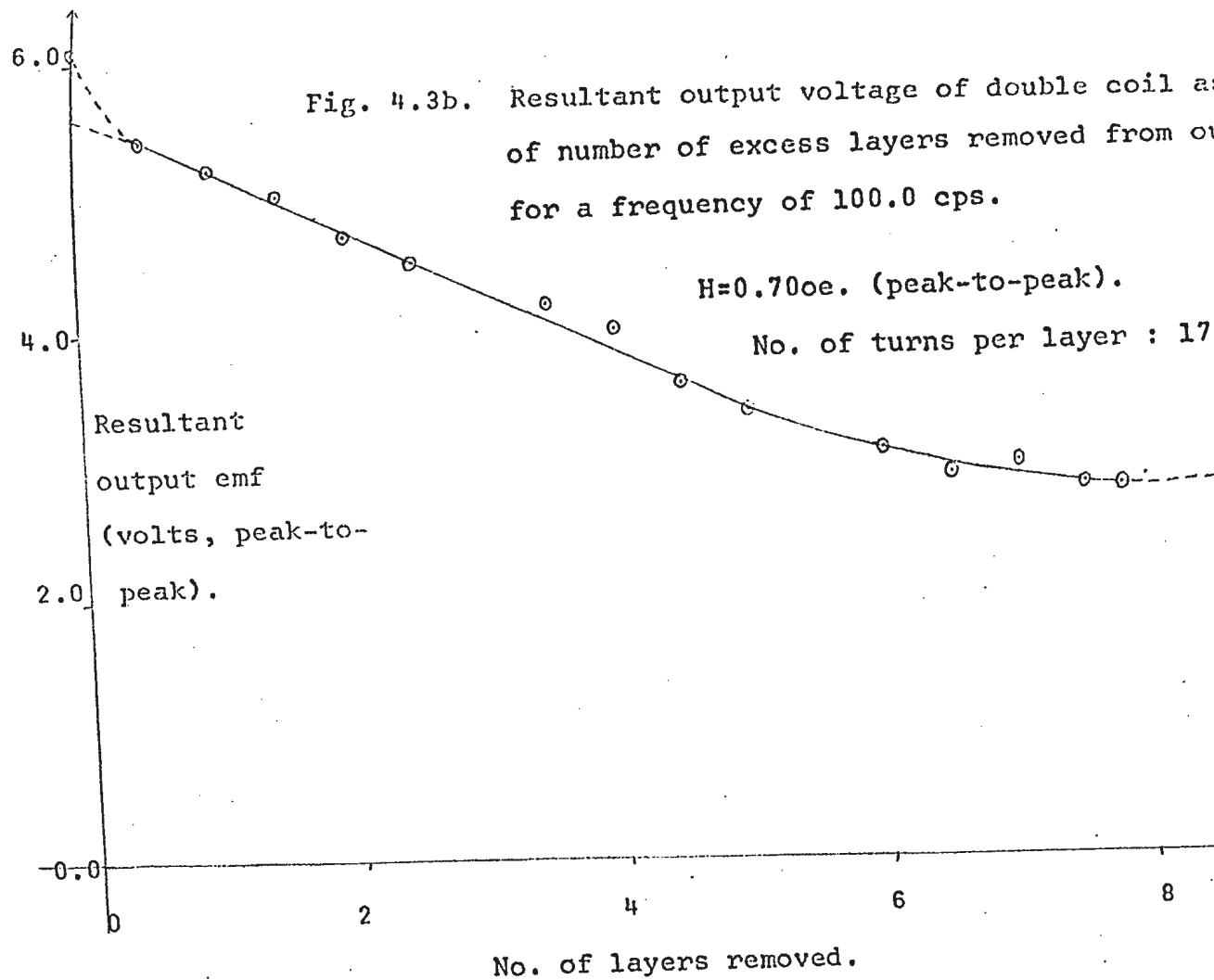
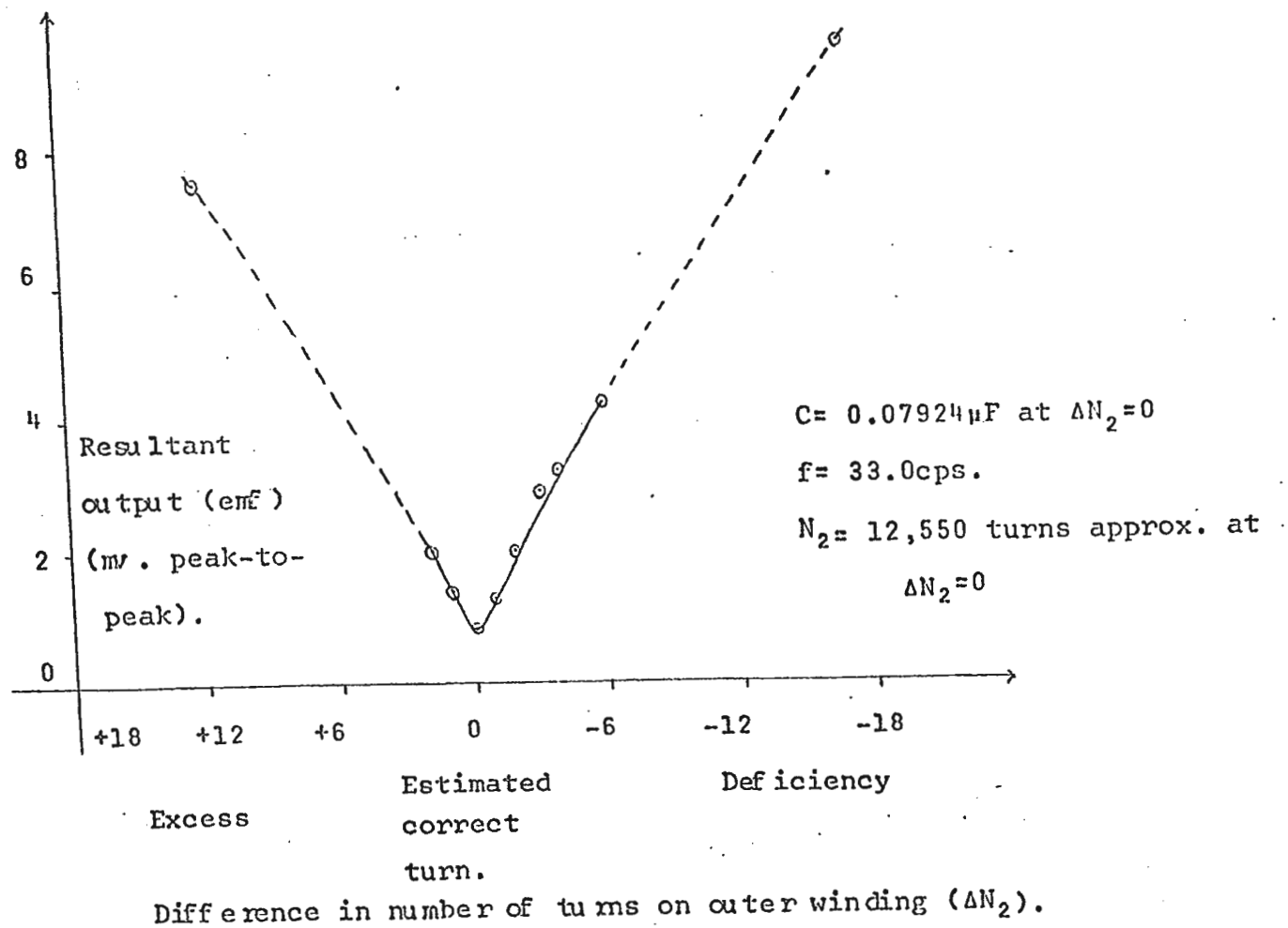




Fig. 4.4. Resultant output emf of the double coil as a function of the number of turns on the outer winding, after phase adjustment with a capacitor C across outer winding.



(For convenience of balancing and measurement, the number of turns on the outer coil was initially kept short of the estimated optimum value). In these measurements the amplifier designed by Crocker (1966) was used, but at a gain of unity, so that it acted only as a filter.

At optimum balance, and  $f = 33.0$  cps the residual emf was about 0.8 mv (peak-to-peak) and consisted predominantly of second harmonic. It was difficult to estimate the content of the out-of-balance emf in the fundamental mode, but as the emf induced by the same field in either winding alone was about 24 volts (peak-to-peak) the balance in the fundamental achieved at this stage can be said to be 1 part in at least  $3 \times 10^4$  of the emf. in either winding. Further balancing required additional filtering of harmonics, and in the final, operational stage (see Section 4.5) the balance in the fundamental is about 1 part in  $5 \times 10^6$ , while the ratio of total unbalanced emf (mainly harmonics) to the induced emf in either winding is about 1 part in  $8 \times 10^5$ . Further reduction of harmonics in the unbalanced output of the double coil can probably be achieved mainly through improvements in the input circuits, i.e. oscillator and input amplifier, and this will be discussed in section 4.5.

To achieve the final balance, the potentiometric arrangement described by Bruckshaw and Robertson (1948) was used (Fig. 4.5). Sixteen turns of the same wire (#AWG26) as in the

Wiring in present double coil

$W_1$ : 33,090 turns

$W_2$ :  $12,550 \pm 10$  turns

$W_3$ : 16 turns

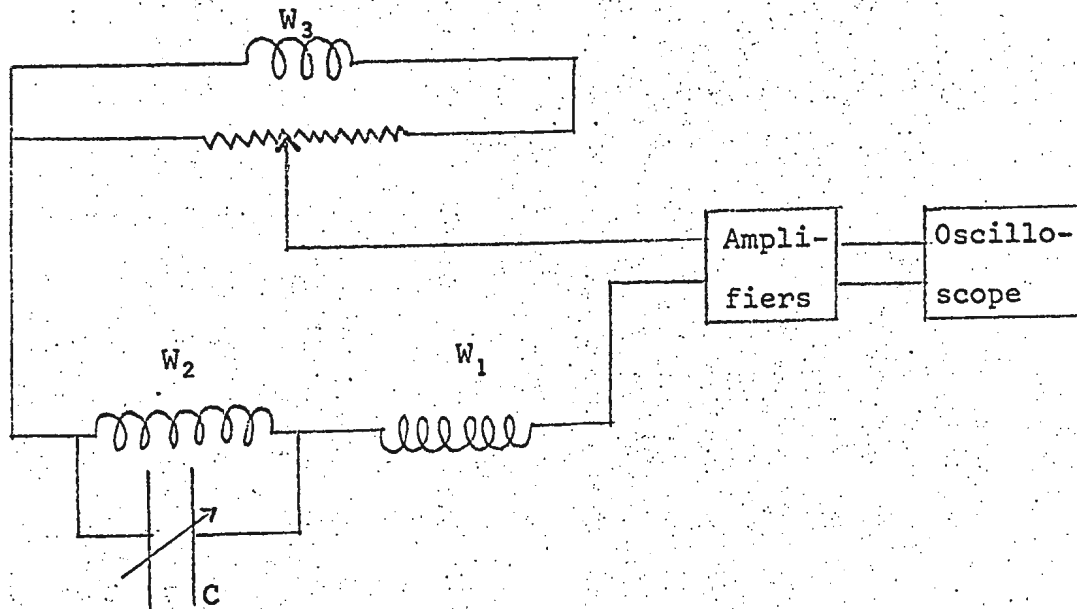


Fig. 4.5 Potentiometric arrangement for balancing of double coil (adapted from Bruckshaw and Robertson, 1948).

double coil proper were wound in the same sense as the outer winding so as to constitute a third winding ( $W_3$ ). The potentiometer was a Beckman "Helipot" of resistance  $10K\Omega$ , but an ordinary slide wire potentiometer of 10 meter length was alternatively used. The final balance is obtained by alternate adjustment of the tuning capacitance and the potentiometer tapping.

#### Choice of the operating frequency.

The large increase with frequency of the phase difference, and consequently of the differential voltage, made it necessary to operate the double coil at a low frequency (preferentially below 100 cps). On the other hand, ideally the signal corresponding to a given dipole moment on the coil axis is proportional to  $f$ , and hence operation at relatively high frequency would have been of advantage. An additional factor that must be considered, particularly when operating at low frequency, is the presence in the laboratory of stray fields of 60 cps and its harmonics and subharmonics. Hence it was desirable to operate the double coil at a frequency far removed from 60 cps., though also significantly different from 30 cps. This is all the more necessary since the tuned amplifiers cannot select very sharply (i.e.  $\Delta f < 1$ ) at the lower frequencies. Thus, for the present investigations a frequency of 33.0 cps was chosen.

#### 4. 5. Discussion of the 'Balance'.

During the balancing procedure described above it was observed that, as the out-of-balance emf. is reduced to the order of some tens of microvolts, the balance becomes unstable. As described in Section 3.5 this instability was manifested as an irregular change of the pattern on the oscilloscope screen in a time too short to permit accurate measurements to be made with the relatively less susceptible specimens. In practice this corresponds to a loss of sensitivity of the bridge.

Fig. 4.6a shows the best balance obtained in a magnetising field of 0.5 oe.(rms), using Helmholtz Coil A. The second harmonic predominates and, taking the amplitude of the 'fundamental' to correspond to about 10 mv. (peak-to-peak) on the oscilloscope screen, a balanced double coil output of approximately  $10\text{mv}/2000, = 5\mu\text{v}$ . is indicated, since a total amplification of 2000 was involved in this case. If this balance had remained steady it would have permitted though! (on a higher sensitivity - scale of the oscilloscope) easy measurement of volume susceptibility of about  $5 \times 10^{-5}$  cgs units when the specimen is placed on the bounding plane, and about  $3 \times 10^{-5}$  cgs units when placed at the coil center .

The calculated signal due to a specimen of the above susceptibility is about  $12\mu\text{v}$  and  $17\mu\text{v}$  (peak-to-peak) when it is placed at the bounding plane and the coil center, respectively.

Caption for figure 4.6.

Specimen No : VR 3(2) (sedimentary breccia from  
Virgin Rock shoal off Grand Banks of  
Newfoundland).

Position of specimen :- 0.63 cm. beyond a bounding plane.

Volume susceptibility :  $9.6 \times 10^{-4}$  c.g.s. units.

Voltage scale on CRO : 50 mV/cm.

Time Scale : 5 millisecc/cm.

Helmholtz coil used : A

Double trace indicates instability of the pattern, with  
time constant  $< \frac{1}{25}$  th sec.

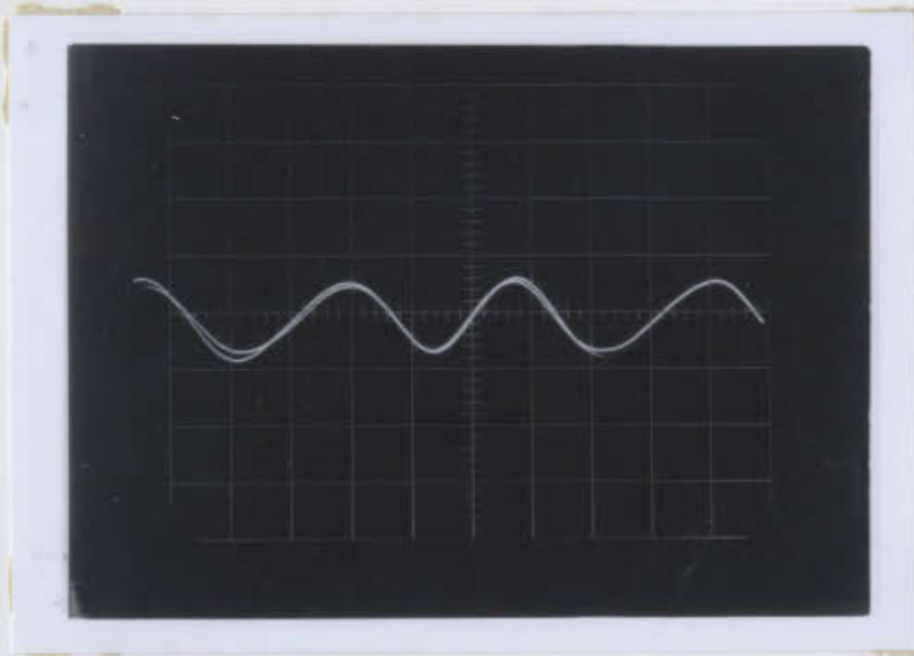


Fig. 4.6a

Bridge Output without specimen.

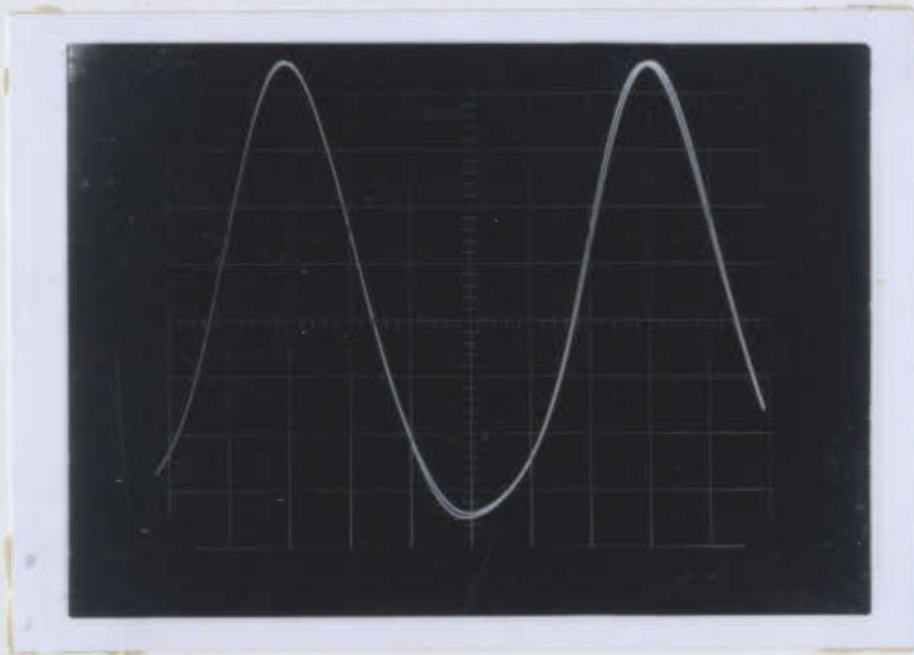


Fig. 4.6b

Bridge Output with specimen.

Because of the instability, however, a specimen of volume susceptibility  $8 \times 10^{-5}$  cgs units or so would have to be placed at the coil center to give a signal that could be measured with comparable accuracy. When specimen VR3(2), having a susceptibility of  $9.6 \times 10^{-4}$  cgs units, was placed centrally along the coil axis at the edge of the coil - which is 0.63 cm. beyond the bounding plane of the windings - the signal shown in Fig. 4.6b was obtained. This signal suffered some distortion due to the presence of the harmonics (mainly second harmonic). The signal of approximately 400 mv. (peak-to-peak) in this case corresponds to an unamplified output emf of about 200  $\mu$ v, which in turn corresponds to a susceptibility of  $9.5 \times 10^{-4}$  cgs units thus agreeing with the value  $9.6 \times 10^{-4}$  quoted above.

The effect of reduced harmonic distortion in the input current to the Helmholtz coils is brought out very sharply when one compares Fig. 4.6 (a,b) with Fig. 4.7 (a,b). The latter pair of oscillograms corresponds to the same specimen [VR3(2)] as in the former case, alternately magnetized in a field of the same amplitude and frequency but which is now produced by the second pair (B) of Helmholtz coils (see Section 3.3). In this case the current output of the power amplifier is reduced to approximately one-half of the current required to produce the same field with Helmholtz pair A. Thus the harmonic distortion in the input current also reduces in approximately the same



Caption for figure 4.7.

Specimen No : VR 3(2) (sedimentary breccia from  
Virgin Rock shoal off Grand Banks of  
Newfoundland).

Volume susceptibility :  $9.6 \times 10^{-4}$  c.g.s. units

Position of specimen : 0.63 cm. beyond a boundry plane.

Volume scale on CRO : 50mv/cm.

Time scale : 5 millisec/cm.

Helmholtz coil used : B.

Double trace indicates instability of the pattern, with  
time constant  $< \frac{1}{25}$  th sec.

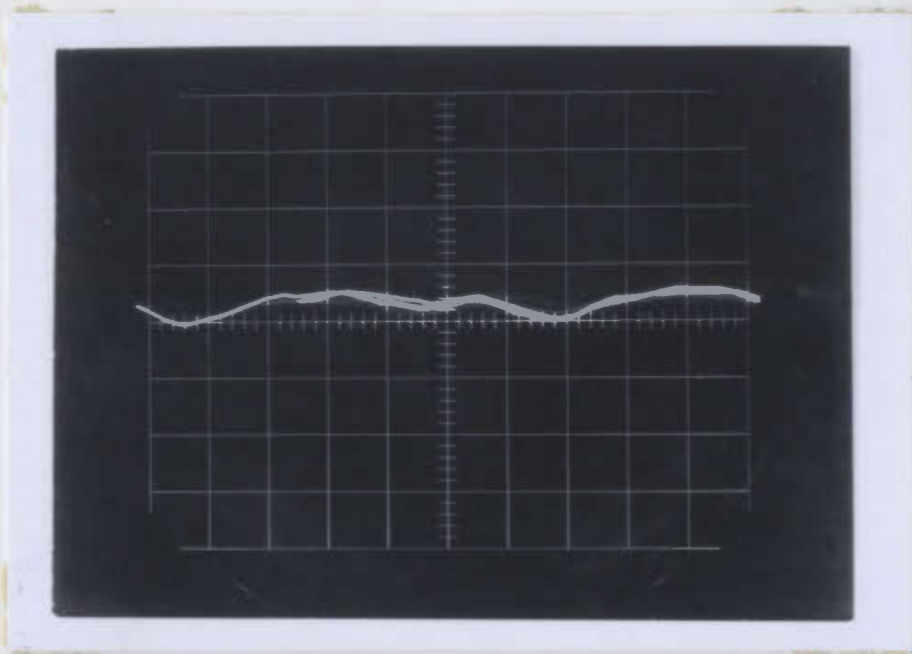


Fig. 4.7a

Bridge Output without specimen.

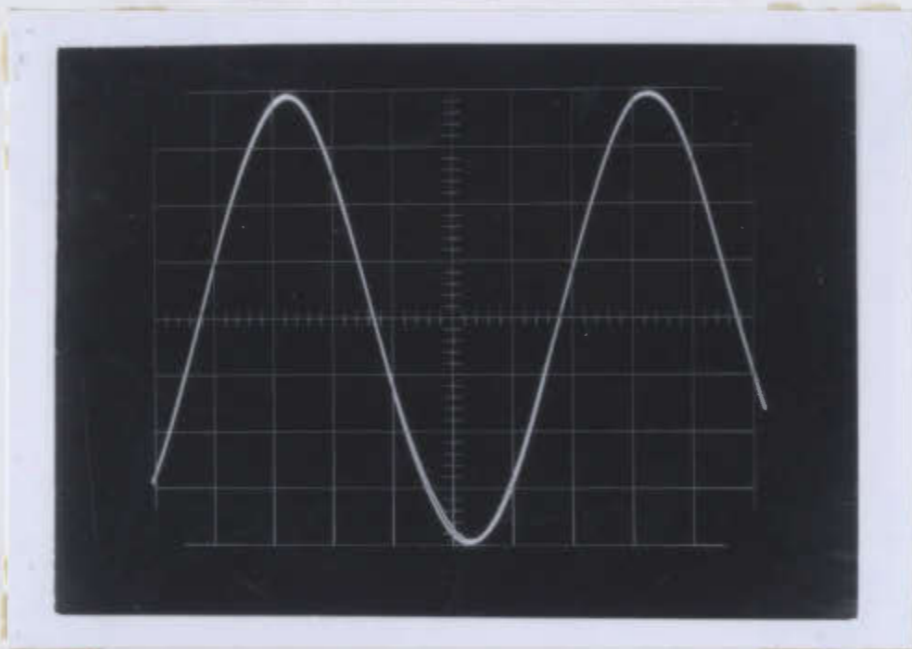


Fig. 4.7b

Bridge Output with specimen.

proportion. The specimen now produces a clean sinusoidal signal on a scale of 50 mv/cm.

Fig. 4.8a shows the same balance as in Fig. 4.7a but on a higher sensitivity scale (20mv/cm.) of the oscilloscope. The bridge output with a specimen of susceptibility of  $8.6 \times 10^{-5}$  cgs units placed at the center of the coil is shown in Fig. 4.8b.

Fig. 4.9 illustrates the signal due to a strong specimen (HH3B1) of susceptibility  $3.9 \times 10^{-3}$  cgs units on the oscilloscope scale of 500mv/cm. The nearly horizontal line represents the balanced output voltage for a magnetizing field of 0.5 oe.rms.

The maximum change in emf represented by the double trace on the screen (e.g. Fig. 4.8a) is about 10 mv in 0.04 sec., corresponding to a drift in double coil output of 5 $\mu$ v which is a significant fraction of the signal due to the specimen itself: this illustrates quantitatively to what extent the present instability imposes a limit upon the performance of the bridge. Therefore, though the accuracy of measurements obtainable with the second pair (B) of Helmholtz coils is definitely an improvement over that achieved with pair A, the lack of stability in the balance still proved to be a serious limiting factor to an increase in the practical sensitivity of the bridge; thus, for the time being, is limited to measurement of volume susceptibility  $K > 5 \times 10^{-5}$  cgs units.

Caption for figure 4.8.

Specimen No : HH 27 A) (Arkose from Henley Harbour,  
Labrador).

Volume susceptibility :  $8.6 \times 10^{-5}$  c.g.s. units

Position of specimen : at the coil center.

Voltage scale on CRO : 20mv/cm.

Time scale : 5 millisec/cm.

Helmholtz coil used : B

Double trace indicates instability of the pattern, with  
time constant  $< \frac{1}{25}$  th sec.

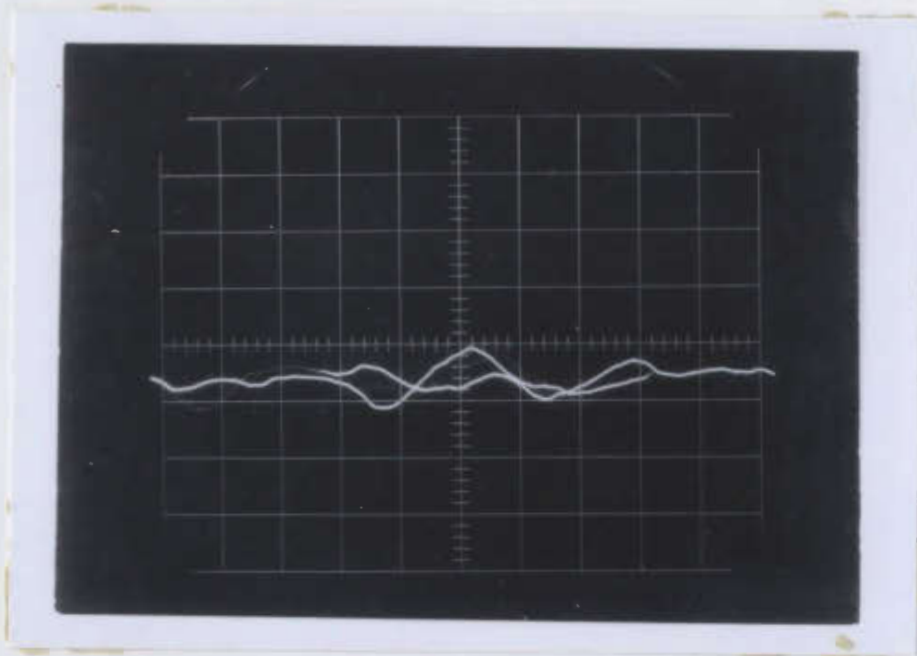


Fig. 4.8a

Bridge Output without specimen.

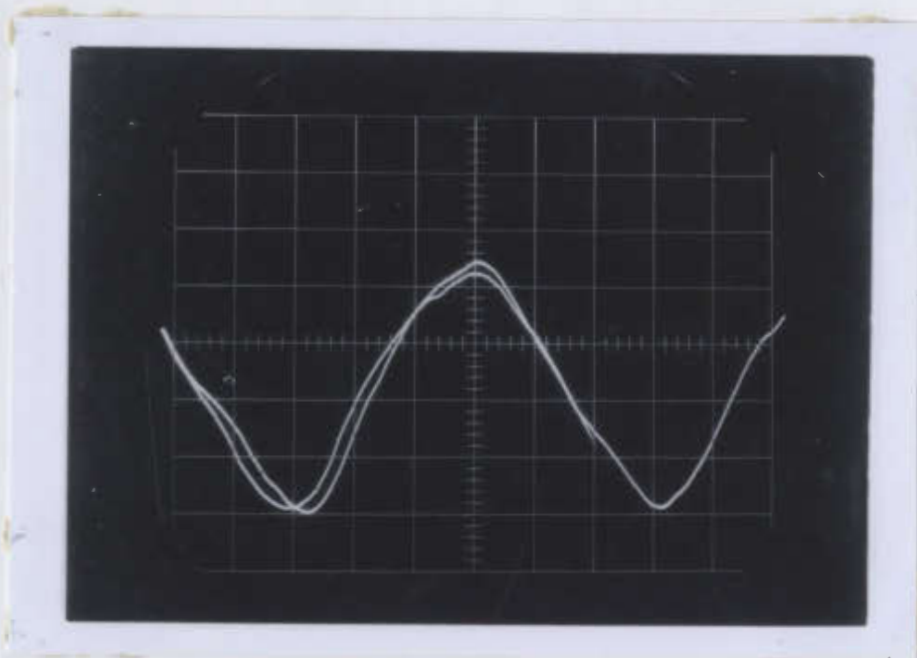


Fig. 4.8b

Bridge Output with specimen.

Caption for figure 4.9.

Specimen No : HH 3 B 1. (Basalt from Henley Harbour,  
Labrador).

Volume susceptibility :  $3.9 \times 10^{-3}$  c.g.s. units

Position of specimen : 0.63 cm. above the bounding  
plane.

Voltage scale on CRO : 500 mv/cm.

Time scale : 5 millisec/cm.

Helmholtz coil used : B.

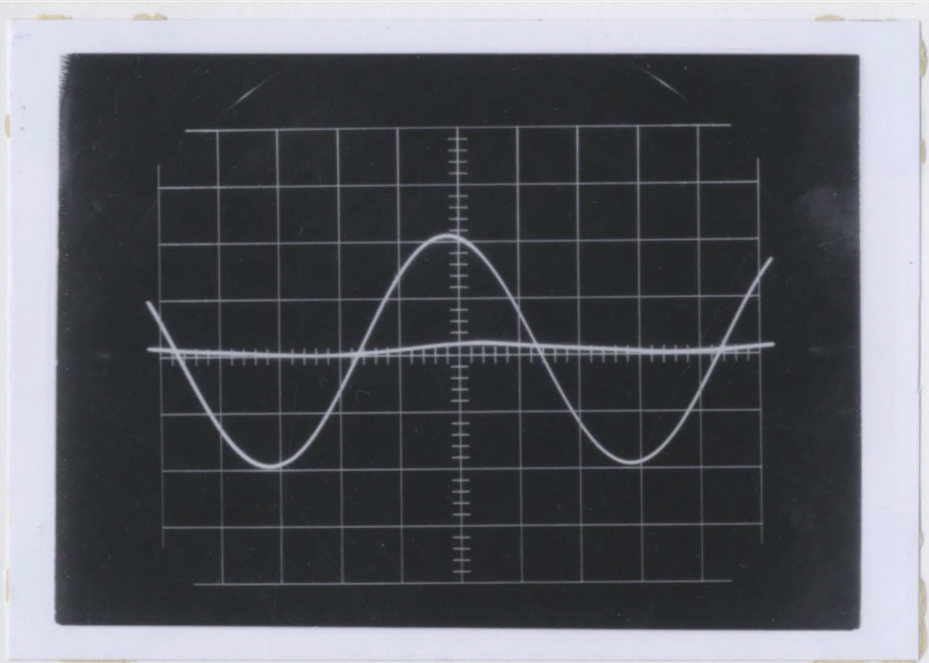


Fig. 4,9.

Bridge Output with and without specimen.

#### 4.6 Probable reasons for instability of the balance.

As mentioned earlier, one of the causes of instability lies in the unstable response of the tuned output amplifiers at frequencies near that of the 2nd harmonic, i.e. 66 cps. A close check of the output of the power amplifier showed that the input current, and hence the magnetizing field itself, was subject to short-period (1 sec. or so) irregular variations in amplitude, the maximum variation being about  $\pm 0.005$  oe. (rms). The balance was found to be very critically dependent upon both the magnitude and frequency of the magnetizing field, where any irregular variations in the field contributed towards an upset of the existing balance condition. The time-varying, out-of-balance emf. in the double coil output then has three possible main components:

(1) A change in the amplitude of this emf, due to changes in the amplitude of the magnetizing field (at constant frequency). It was observed that the value of the capacitance placed across the outer coil (for balancing the double coil) varied with the magnetizing field - probably due to a change in the current distribution in the coil (see Section 4.1). Thus at the balance condition the out-of-balance emf did not vary linearly with the magnetizing field because of non linear changes between the emfs induced in the two windings at different fields.

(2) A complicated change in the magnitude of the fundamental component of the out-of-balance emf, reflecting a frequency change in the field. This unbalance occurs because the phase



difference between the two coil windings (adjusted after tuning with a capacitor across the outer coil winding to compensate for the differences in distributed capacitance) is exactly  $180^\circ$  only at a fixed input frequency;

(3) A difference in the relative contribution of harmonics to the unbalanced emf, reflecting frequency changes mainly in the second harmonic of the coil input which in turn result in small phase changes in the double coil.

Initially, the oscillator and the power amplifier were connected directly to the mains, and fluctuations in the line voltages affected the coil input, and hence the balance. However, insertion of a voltage regulator between the mains and the oscillator did not lead to a significant improvement. Hence it is likely that the short-time variations in the output emf at balance were mainly due, either to frequency drift in the oscillator or to variations in the output signal from the power amplifier. Probably both causes contributed, as was indeed verified in the laboratory, though by qualitative tests only. The magnitude of the above drift in the double coil input emf is so small that the variations cannot be observed directly on the oscilloscope screen; however, as shown in Section 4.6, the corresponding drift in the output balance over time intervals of a few seconds or so correspond to changes in emf comparable to the small emf's in the signal itself (e.g.  $3\mu\text{v}$  for a specimen of susceptibility of  $1 \times 10^{-5}$  emu/cc when placed at the center.) As mentioned before,

this instability therefore sets a limit to the practical sensitivity obtainable at present, and this calls for improvement in the design of the input circuits in particular.

Slow Drift of the balance.

Besides the short-period instability, there is a slow drift in the balance. It was observed that the potentiometer reading at balance gradually decreased for the first half-hour after the equipment is switched on. Subsequently, only the short-time instability remained. This drift could be due to the fact that the oscillator requires at least thirty minutes warm-up time for maximum stability.

During the period when measurements have been made with the bridge - about 3 months - it was found necessary on four to five occasions to change the number of turns on the outer coil. Only a few turns-3 to 4 at most - had to be added and removed at a time and for this reason no permanent connection was made at the outer terminals of the second coil. There are two possible reasons for this: First, during the time when the "correct" number of turns was being established, the coil was kept under heavy pressure in a direction parallel to the axis, by means of wooden blocks clamped against the sides of the coil. This was done in order to prevent tensions set up in the winding sections of the newly-wound coil from causing deformation, but

before placing the permanent non-metallic (plastic) bolts across the bounding plates of the coil former at its perimeter, which would have made it awkward to add or remove turns from the outer layer. However, during the removal of the wooden pressure blocks and their replacement by the plastic bolts and nuts, the coil probably was deformed slightly; this, together with gradual "settling" of the wiring sections, would cause relative changes in the wiring cross-sections, sufficient to account for an "unbalancing" equivalent to a few turns in the outer winding.

The second reason probably lies in the fact that the coil has not so far been placed in a temperature-controlled environment. Thermo-stating of the coil may become necessary in the future, when improvements in the design are to be made to produce greater sensitivity.

CHAPTER FIVE  
CALIBRATION AND SUSCEPTIBILITY MEASUREMENTS.  
WITH ROCK SPECIMENS FROM LABRADOR.

5. 1 Method of Measurement.

With the aid of the variable capacitor across the outer winding, the bridge is balanced first without the specimen, and the potentiometer reading is noted. The specimen is then placed centrally along the axis of the double coil at the position where the measurement is desired. The bridge is balanced again and the potentiometer reading noted. The difference between the two readings is a measure of the susceptibility of the specimen. As an additional check against drift, the bridge is balanced once again without the specimen, and a mean of the two potentiometer readings without the specimen is used for the calculation of susceptibility. Generally the two null readings agreed to within  $\frac{1}{2}$  division on the potentiometer corresponding to about  $15\mu\text{v}$  (peak-to-peak) in the double coil output. In the calibration a mean of five repeat readings was taken for specimens of high susceptibility, while as many as ten readings were averaged for the weaker specimens. Errors of measurement will be discussed in Section 5.3.

5. 2 Calibration.

The bridge was calibrated with specimens whose

susceptibility had been determined previously with the astatic magnetometer recently set up in the Physics Department (Murthy, 1966). Five specimens, representing a susceptibility range of two orders of magnitude ( $10^{-4}$  to  $10^{-2}$  cgs units), were chosen for the calibration and their susceptibility determined by the following procedure, which is similar to that described by Blackett (1952): The direct currents in the three orthogonal pairs of Helmholtz coils are first adjusted for their usual function of providing a field-free space in the central region of the magnetometer. An additional current is then sent through the E-W pair of coils, whose axis is horizontal and makes an angle of  $89^\circ$  or so with the local magnetic declination. Any current through this pair other than that required for field-nulling produces a uniform, horizontal field component, which causes opposing torques to act upon the two magnets in the astatic system; these magnets may be closely approximated by dipoles aligned antiparallel to one another in a N-S direction. The net torque then tends to deflect the astatic system, which is suspended by a fine, elastic fibre, about its vertical axis. This effect is measured in terms of the deflection of a light spot on a scale. In an ideal astatic magnetometer (that is, one with infinite astaticism) a uniform field should not cause any deflection of the spot. However, as a consequence of finite astaticism, as in all astatic magnetometers, the moment vectors of the two magnets are not exactly equal and opposite, so that a net deflection in one sense or

another, and proportional to the magnitude of the normal field component, is observed in practice.

An excess torque is then applied to the upper magnet to restore the light spot to the null position it occupied when the astatic system was in field-free space. This torque is produced in a horizontal field having a nearly uniform vertical gradient in the region of the astatic system. This field in turn is produced by a small coil placed with its axis in the E-W direction and its center vertically above the astatic system at a distance much greater than that between the two magnets.

After the light spot has been exactly re-positioned by regulation of the current through the gradient coil, the test specimen is placed vertically below the astatic system, and sufficiently close to the lower magnet to allow accurate measurement of the induced magnetization. However, natural rock specimens with ferromagnetic constituents nearly always have observable remanent magnetization, and often (e.g. in many igneous rocks) the intensity of this remanent component will exceed the component induced in the same rock by fields of the order of the earth's field. To eliminate the effect of the remanent component in the susceptibility measurements, the direction of that component is first measured with the magnetometer. The specimen is then placed in the holder in such a position that the remanent vector lies as closely as possible in the plane of the magnetic meridian; i.e., ideally it should produce no deflection of the astatic system.

The light spot will be deflected after introduction of the specimen, however, because the horizontal component of magnetization induced in it by the E-W field exerts an excess torque upon the lower magnet. Correct alignment of the remanent vector is checked by rotating the specimen through  $180^\circ$  and noting any change in the final position of the spot; i.e. the same deflection from the null position (caused by the induced magnetization only) should be observed in the  $0^\circ$  and  $180^\circ$  positions. If this is not the case, the specimen position in the holder is adjusted until the spot remains unaffected upon a  $180^\circ$  rotation. The scale position of the light spot corresponding to the specimen position with J pointing north is then noted; this reading is called  $a_1$ . A second reading is taken with J pointing south and is called  $a_2$ . Ideally  $a_1 = a_2$ , but due to slight departure of the remanent moment from the north-south direction, or slight displacement of the specimen center from the vertical axis of the astatic system, that two readings may differ by a small amount. Hence the arithmetic mean of the two readings,  $a = (a_1 + a_2)/2$ , is taken.

The current in the E-W pair is then reduced once again to the value required for field nulling, and, simultaneously, the gradient field due to the gradient coil is reduced to zero. For these zero conditions the position (b) of the light spot is again noted. Then if the total deflection of the spot due to

the induced moment vector  $I$  is called  $i$ ,

$$i = |b-a| \quad (5.1),$$

where the sign of  $(b-a)$  depends on the direction of the applied field  $H$ . In order to reduce further the contribution of random errors, including the error due to misalignment of the remanent vector with the north-south direction, the above procedure is repeated twice and  $i$  is obtained as the average value of the three sets of readings ( $\therefore$  a total of 6 readings for  $a$  and 3 readings for  $b$ ). Knowing the reciprocal sensitivity  $H|i$  of the magnetometer, the distance  $Z_L$  between the specimen center and the center of the lower magnet, the separation  $L$  between the two magnets and the size of the specimen,  $I$  can then be determined. In the astatic magnetometer used, the constants were:  $L = 6.0\text{cm}$ ;  $H/i = 3.9 \times 10^{-7}$  oe/mm deflection at 1.80 meter distance from the astatic system to the scale: and the value of  $Z_L$  is chosen so that a suitable deflection is produced by a specimen of given intensity. The specimens were either cylinders of height = diameter = 2.22cm. or cubes of side length 2.00cms. Since the net field,  $H$ , produced by the E-W pair of Helmholtz coils is also known for a given current through the coils,  $k$  can be determined from the relationship

$$k = I/H \quad (5.2)$$

which holds in the case of initial susceptibility, as measured in fields of low magnitude as in the present case (see Section 1.2).



An example of a susceptibility determination by this method is given below for a specimen (no. HH1B3) of basalt from Henley Harbour on the coast of Labrador (Murthy, 1966). The first three readings are taken in the absence of the specimen:

(1) Relative spot reading on the scale when a field-free region surrounds the magnetometer system: 250.0mm.

(2) Reading when an additional current of  $^{200}_{\Lambda}$  ma. (corresponding to 0.050oe.) is passed through the E-W coils: 260.0mm.

(3) Reading after restoration of the original position of the astatic system in a gradient field: 250.0mm.

(4) Readings with the specimen placed in position at a distance  $Z_L = 4.50$  cms, and magnetizing and gradient fields as in step (3):

Remanent vector J pointing south:  $a_1 = 300.0\text{mm.}$

Remanent vector J pointing north:  $a_2 = 299.0\text{mm.}$

Mean:  $a = 299.5\text{mm.}$

(5) Reading in field-free space with a specimen in the same position as (4) :  $b = 251.0\text{mm.}$

(6) Introduce the magnetizing and gradient fields, as in step (4), Repeat (4) with:

Remanent vector J pointing north:  $a_1 = 300.5\text{mm}$ .

Remanent vector J pointing south:  $a_2 = 299.0\text{mm}$ .

Mean :  $a = 299.8\text{mm}$ .

(7) Repeat (5). Reading :  $b = 250.5\text{mm}$ .

(8) Repeat (6). Reading with

Remanent vector J pointing south:  $a_2 = 299.5\text{mm}$ .

Remanent vector J pointing north:  $a_1 = 300.5\text{mm}$ .

Mean :  $a = 300.0\text{mm}$ .

(9) Repeat (5). Reading :  $b = 252.0\text{mm}$

Mean zero reading[(4), (6) and (8)]:  $\bar{a} = 299.8\text{mm}$ .

Mean reading due to induced magnetization [ (5), (7) and (9) ]:

$\bar{b} = 251.1\text{mm}$ .

Mean deflection :  $|(b - a)| = \underline{48.7\text{mm}}$ .

From the known constants of the magnetometer, and for  $Z_L = 4.50\text{cms}$  with a cylindrical specimen, a maximum deflection of  $1.00\text{mm}$ . on the scale corresponds to an intensity of magnetization.

$$\underline{I^1 = 3.95 \times 10^{-6} \text{ emu/cc.}}$$

Therefore, for the observed deflection,

$$I = (48.7 \times 3.95 \times 10^{-6}) \text{ emu/cc.}$$

Since the magnetizing field is 0.050 oe. insertion of the values of H and I into (5.2) yields, finally,

$$\kappa = 3.85 \times 10^{-3} \text{ cgs units.}$$

As mentioned before, the plane of the E-W coils is about  $1^\circ$  out of meridian, so that in the entire procedure above, the net inducing field makes an angle of  $89^\circ$ , instead of an exact right angle with the magnetic moments of the magnets. Hence the magnitude of the torque exerted upon either magnet is  $1 - \cos 1^\circ$ , or about 0.02%, lower than that corresponding to a field normal to the magnets. This difference is quite negligible compared with the errors of the present measurements. (see Section 5.3).

The susceptibility of five other calibration specimens - NN2B1, TH4C3, HH3C2, HH1C1, LB2B2 - were determined in the manner described above.

Following the measurements with the astatic magnetometer the change in the potentiometer tapping required to re-balance the bridge upon introduction of each of the above six specimens was determined when they were placed

(1) at the bounding plane;

(2) at the center of the double coil.

The magnetizing field in the above determinations was 0.50 oe. (r.m.s.) at 33.0cps.

Tables 5.1a and 5.1b summarize the results of the above measurements. Figs. 5.1a and 5.1b show that the bridge measurements, as expressed in divisions,  $\Delta R$ , on the potentiometer required to restore balance after the specimen has been placed on the double coil axis, increase linearly with the volume susceptibility  $k$  which had been determined independently with the astatic magnetometer. On the relevant graph the calibration constant  $K/\Delta R$  may be read off at the  $k$  intercept of the extrapolated curve corresponding to 1 division on the potentiometer, but this is less accurate than taking the slope, which gives  $K/\Delta R$  with 2-3% error.

Since the specimens represent two orders of magnitude of  $k$ , the scale constants determined separately for each specimen in Tables 5.1a, b have different accuracy, and hence it would be incorrect to assign the same weight to each scale constant in the last column; nevertheless, for each of the two specimen positions, the arithmetic mean of the scale constant agreed to two significant figures to the respective value obtained from the slope of the graph. From the two graphs, the scale constants are:

- (1) Specimen at the bounding plane:  $K/\Delta R$   
 $= (1.41 \pm 0.04) \times 10^{-4}$  cgs units/division.
- (2) Specimen at the center of the coil:  $K/\Delta R$   
 $= (0.73 \pm 0.02) \times 10^{-4}$  cgs units/division.

Table 5.1 Calibration of the Susceptibility Bridge.

(a) Specimen placed 0.63cm. beyond the bounding plane of the double coil. (Fig. 5.1a).

Specimen No.	K (cgs units $\times 10^{-4}$ )	No. of potentiometer divisions $\Delta R$ (units)	'K' per division (K/ $\Delta R$ ) (cgs units $\times 10^{-4}$ )
NN2B1	259	189.0	1.37
TH4C3	101	69.0	1.46
HH1B3	38.7	28.5	1.36
HH1C1	42.8	32.0	1.34
HH3C2	23.7	16.5	1.44
LB2B2	4.3	2.5	1.3

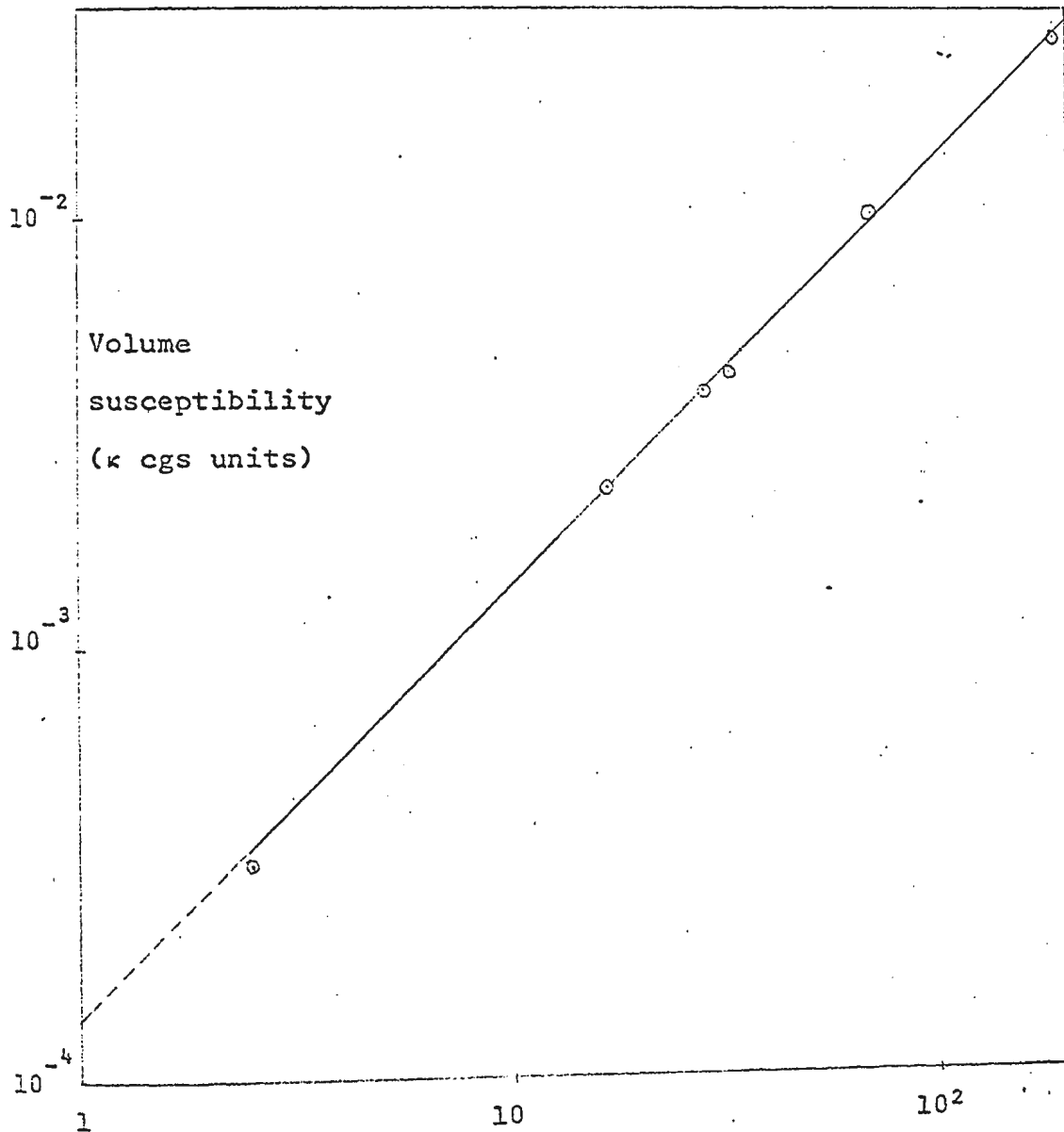
(b) Specimen at the center of the double coil (Fig. 5.1b).

Specimen No.	K (cgs units $\times 10^{-4}$ )	No. of potentiometer divisions $\Delta R$ (units)	'K' per division (K/ $\Delta R$ ) (cgs units $\times 10^{-4}$ )
NN2B1	259	357.0	0.73
TH4C3	101	134.0	0.75

Table 5.1 (Contd.)

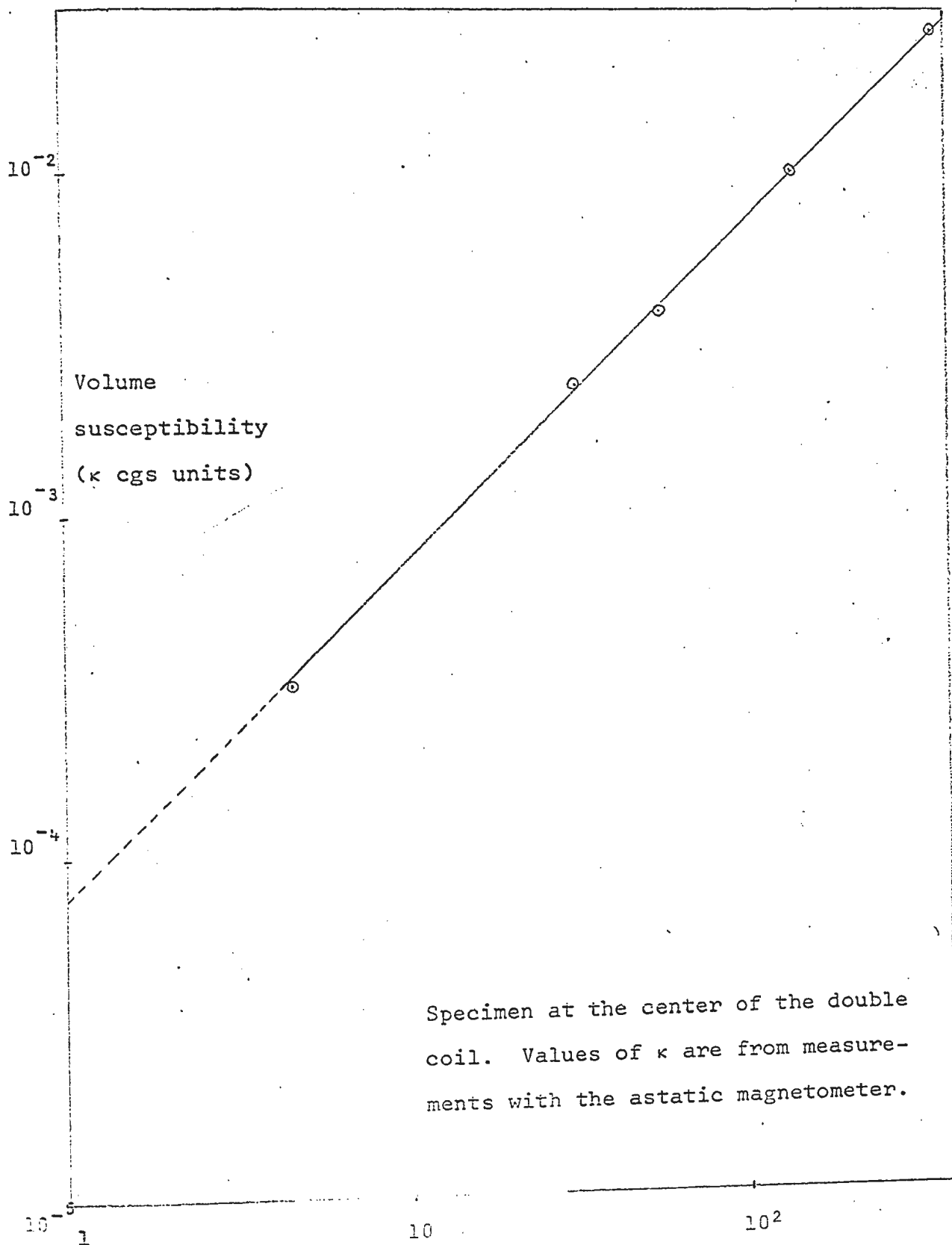
Specimen No.	K (cgs units $\times 10^{-4}$ )	No. of potentiometer divisions $\Delta R$ (units)	'K' per division ( $K/\Delta R$ ) (cgs units $\times 10^{-4}$ ).
HH1B3	38.7	55.5	0.70
HH3C2	23.7	31.0	0.76
LB2B2	4.3	4.5	0.71

Fig. 5.1.a Calibration of the Susceptibility Bridge.  
Specimen at 0.63 cm beyond the bounding plane  
of the double coil.



Values of  $\kappa$  are from measurements with the astatic magnetometer.

Fig. 5.1.b Calibration of the Susceptibility Bridge.





### 5. 3. Discussion of Errors.

The method of calibration employed is subject to two main sources of error: (1) error in the susceptibility determination using the astatic magnetometer, and (2) error in the a.c bridge measurement. The total error in (1) is composed of the error in the actual measurement as well as in the constants required for calculation of the intensity of magnetization. These constants (Section 5.2) are (i) the reciprocal sensitivity of the magnetometer, (ii)  $L$ , (iii)  $Z_L$ , and (iv) the volume of the specimen. The chief additional errors are: (v) wrong positioning, of the specimen in the holder, (vi) inhomogeneity in the magnetization of the specimen, and (vii) inaccurate knowledge of the value of the magnetizing field. As these sources include systematic as well as random components of error, it is difficult to estimate the total error in  $k$ .

Murthy (1966) discussed the measurement of remanent intensity,  $J$ , with the astatic magnetometer. The main components of this error are those listed above, except for error (vii) which does not enter the measurement of  $J$  as long as field-free space is approximately maintained. The main component in the expected error in  $J$  is then due to inaccurate knowledge of the magnitude, and mean position of the dipole moment of the specimen; this in turn involves the errors under (iv), (v) and (vi), above when the direction of magnetization is measured separately in the magnetometer. Both lateral and vertical mis-positioning in

the specimen holder is possible, but the vertical error tends to be the largest single component in the total error in  $J$ , as the deflection of the light spot is approximately proportional to  $(1/Z_L)^3$ . It is easy to mis-position vertically by  $\frac{1}{2}$  mm., and at  $Z_L = 4.5$  cm, this causes an error in deflection, and hence in  $J$ , of the order of 3%. On the other hand, the safe reading error of a single observation is well below 1% and the total observational error (apart from vertical mis-positioning and small systematic errors) can be virtually eliminated by a suitable measuring procedure.

In palaeomagnetism, large variations in  $J$  between different samples from the same rock formation are commonly found, and measurement of  $J$  with an error as high as 5% can often be considered satisfactory in palaeomagnetic studies. For this reason Murthy (1966) computed  $J$  from an approximate formula in which each magnet of the astatic system is assumed to be a point dipole at the magnet center; the approximate formula yields an error of about 1% for specimens placed 4.5 cm below the lower magnet (i.e.  $z_L = 4.5$  cm), and hence its use was justified in the case of most measurements, where  $z_L > 4.5$  cm. For very weakly magnetized specimens that had to be placed closer to the lower magnet, the error from this source increases, but so do a number of other errors.

In the present measurements (of  $I$ , rather than  $J$ ),

the calibration curves ought to yield the scale constant  $K/\Delta R$  as accurate as possible. Most of the measurements were made at  $z_L = 4.5\text{cm}$ , so that employment of the approximate formula would have introduced a systematic error of 1% into the values of  $I$  and  $K$ . This was avoided by use of a correction for the finite dimensions of the lower magnet. Otherwise, the same errors apply, except that the effect of the remanent component can be virtually eliminated by the procedure outlined in Section 5.2. Further, since  $K$  is required, the total error is increased by any significant error in the value of the magnetizing field  $H$ ; on the other hand, the error in  $K/\Delta R$  is less than that of  $I$  in a single measurement, because the curves (Figs. 5.1a,b) are each based upon five-six determinations of  $K$ .

The limitations of the bridge have already been discussed. However, the error in the scale constant is a calibration error and hence incorporates individual errors due to imbalance in the output signal, presence of harmonics, etc. For the present range of susceptibilities the estimated error in the scale constant,  $K/\Delta R$ , then combines errors due to causes (1) and (2), i.e. magnetometer and a.c bridge errors. This error can then be estimated from the uncertainty in the gradient of the calibration plot; the best fit appeared to be a straight line, with an estimated error of 3% in  $K/\Delta R$ .

Since the susceptibility is found by means of a measurement of the potentiometer balance with the calibrated bridge, the error in  $K$  itself essentially depends upon the error

in the final coil balance and in measurement of the potentiometer reading due to the specimen. It incorporates also errors due to mis-positioning of the specimen, and inaccurate knowledge of its volume. If the potentiometer reading is  $\Delta R$  (scale divisions), then we have

$$K = \frac{K}{\Delta R} \cdot \Delta R \quad (5.3)$$

The total error in K is then the sum of the error in the scale constant (~3%) and that in the determination of  $\Delta R$ : the latter tends to increase with decreasing K. Using a 10-meter wire potentiometer, where the reading accuracy is about  $\frac{1}{4}$  cm., the expected errors in the determination of K with the bridge are:

Volume Susceptibility K (cgs units)	Total Expected Error in Bridge Measurements.	
	Specimen at Bounding Plane	Specimen at Coil Center.
$1 \times 10^{-2}$	$4\frac{1}{2}\%$	4%
$1 \times 10^{-3}$	7%	6%
$1 \times 10^{-4}$	-	25%

In actual practice, the susceptibility is obtained as the mean of a number of repeat measurements, so that the standard

deviation of the mean of a measurement will be less than the errors quoted above. Once the balance is stabilized, it will be possible not only to extend the measurements to  $K = 5 \times 10^{-5}$  cgs units, but also to reduce the error in  $K$  by a large factor.

It is also possible to calibrate the bridge on the basis of the expected behaviour of the circuit components; i.e. the susceptibility corresponding to the amplitude of the output signal for a given location relative to the coil may be deduced from the known amplification and the theoretical signal output for a specimen of given susceptibility. However, this method involves errors arising from

- (1) Approximation of the specimen as an alternating point dipole;
- (2) Departure of the double coil from its theoretical design parameters. ;

Error (1) is due to the fact that, even in a uniformly magnetized specimen placed on the coil axis, the distribution of flux linkages with the coil is not quite the same as that computed from a theoretical model in which the total magnetic dipole moment is assumed to reside at the center. If one considers the rock to be composed of uniformly distributed elemental dipoles, the field at a point  $P$  due to an elemental dipole moment varies inversely as the cube of the perpendicular distance to  $P$ .

As a result the specimen is considered to be composed of two half sections, that half composed of the dipole elements whose distance to a given turn of wire is less than the average distance, will induce slightly more than half the total emf. :

In a double coil the total effect is more complicated, but the order of magnitude of the error can be estimated from the graph of Fig. 5.4. A specimen of height  $h$  with its axis lying on the coil axis, can then be divided into two semi-cylinders with their centers at  $x = \pm h/4$  from the specimen center; for a given distance  $x$  from the coil center, the error in the centered dipole assumption corresponds to the difference in  $F_1 - F_2$  (i.e. the difference in coil output) due to a dipole centered at  $x$ , on the one hand, and the combined effect of the two semi-cylinders (at  $x = \pm h/4$ ), on the other. The error changes sign at the bounding plane, and for cylinders with  $h = 2.2\text{cm}$ . (as in the present case) its magnitude is about 1% at the center and  $< 1\%$  at other points along the coil axis. For cubes of 2.0 cm. side length, the errors will be similar. Bruckshaw and Robertson (1948) estimated this error to be less than 0.5% for measurements made with their double coil.

The error under (2) is inevitable because of the virtual impossibility of winding large coils with dimensions exactly conforming to theory; this error has already been discussed in Section 2.3.

In Figs. 5.<sup>3</sup>/<sub>8</sub> and 5.<sup>4</sup>/<sub>8</sub>, the measured coil output as a function of distance  $x$  has been compared for two specimens with the theoretical output, assuming a coil of optimum proportions and a centered dipole. (Fig. 5.<sup>2</sup>/<sub>8</sub>). Choosing the same measured and theoretical output at the bounding plane, the experimental curve in each case falls slightly below the theoretical curve at large values of  $x$  and also near the coil center where the difference is about  $3\frac{1}{2}\%$ . These relatively small discrepancies probably can be explained by the errors discussed above: error (1) (dipole assumption) would result in a smaller measured than theoretical value near the coil center and this was actually found. (Figs. 5.<sup>3</sup>/<sub>8</sub> and 5.<sup>4</sup>/<sub>8</sub>). The remaining contribution to the observed discrepancy is probably due to the error under (2).

The above discrepancies, though small, are of sufficient magnitude to make it preferable to adopt the alternative calibration method, with specimens of known susceptibility. It should be noted that a third source of error in measurements with the bridge contributes to either method of calibration; namely a positioning error along the axis. It is estimated that the specimens were positioned axially with less than 1mm. error, resulting in maximum output error of 1%. An advantage of using a coil of large dimensions becomes apparent here, for this value is much less than the value of 2-3% quoted by Bruckshaw and Robertson (1948) for their (much smaller) double coil, and described as the largest single error in their measurements

Once the stability of the balance has been achieved

Fig. 5.<sup>2</sup>/<sub>4</sub>. Variation of theoretical output signal of the double coil with distance of an alternating point dipole from its center, when the dipole is in the coil axis.

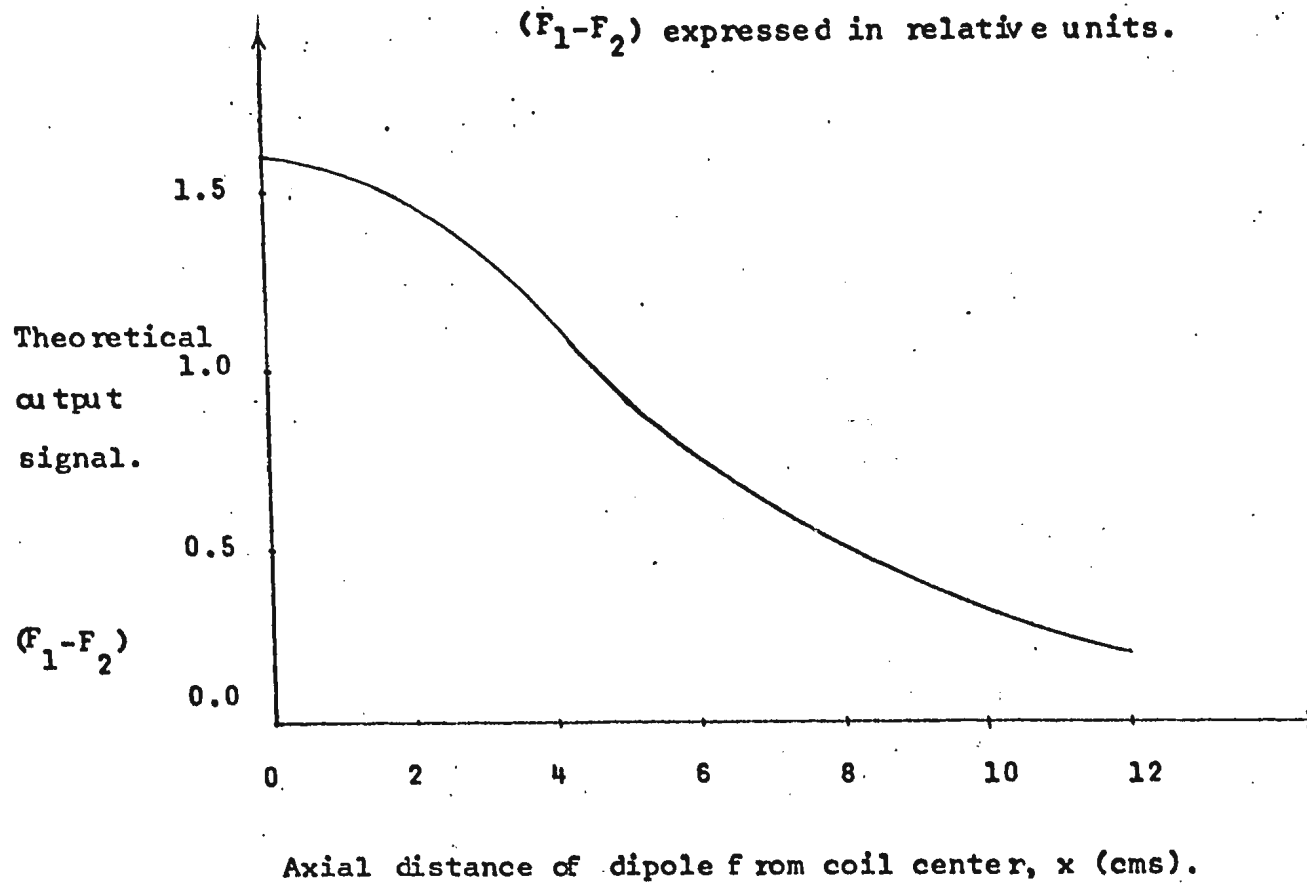




Fig. 5.3. Variation of output signal of the double coil with distance between the coil center, and the center of the specimen on its axis.

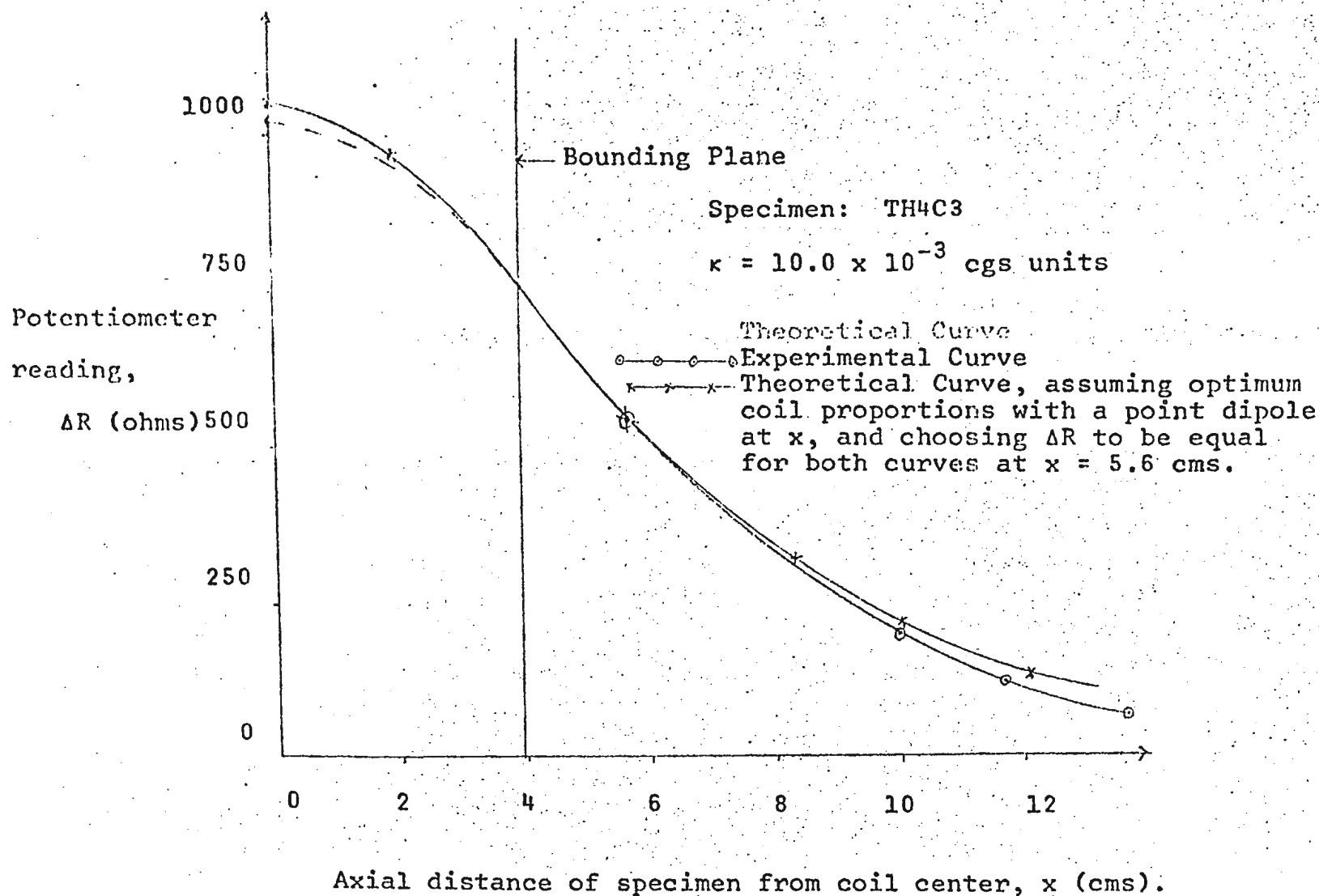
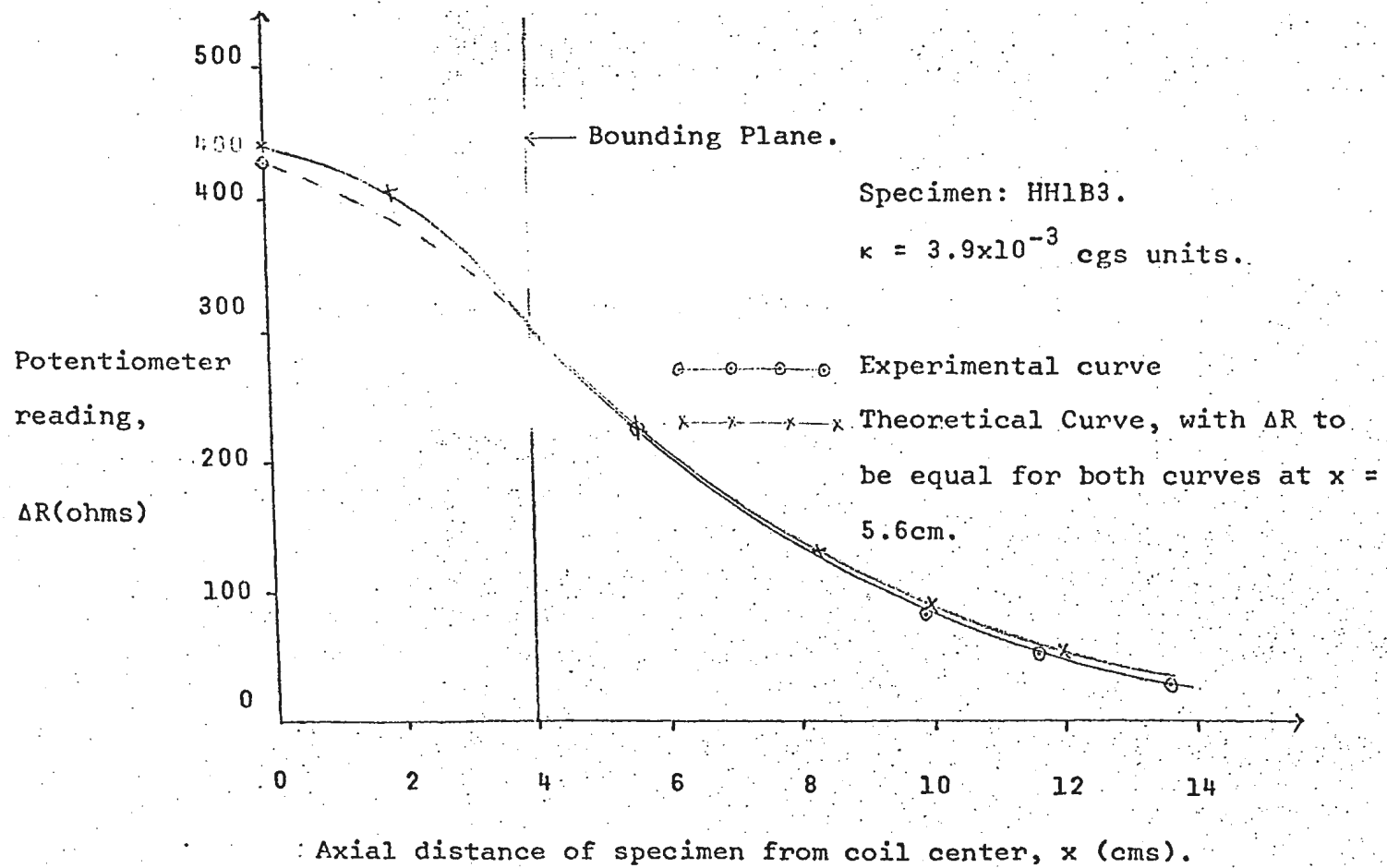


Fig. 5.6<sup>4</sup> Variation of output signal of the double coil with distance between the coil center, and the center of the specimen on its axis.



= 142 =

it would be preferable to use salts of iron, manganese, nickel or cobalt of known susceptibility for calibration purposes in the range below  $K = 1 \times 10^{-4}$  cgs units. In that range measurements with the astatic magnetometer become less accurate, while the choice of standard solutions is much more versatile. Moreover in a direct method of this kind the calibration error could be greatly reduced.

5.4. Determination of the susceptibility of rocks from  
Henley Harbour and Table Head, Labrador.

Cylindrical cores of height and diameter equal to 2.2cm. each were cut from seventeen samples collected from Henley Harbour and four samples from Table Head. (The collection was carried out by members of the Physics Department of Memorial University, during the summer of 1965 (Murthy, 1966). The specimens were positioned at the bounding plane and their susceptibility determined in an a.c magnetizing field at 0.50oe. (rms) at 33.0 cps. In these rocks the scatter between susceptibility values for specimens tends to be much less than the scatter between mean sample values. To show this, the values of K for specimens from three typical samples are compared with each other in Table 5.2, along with a comparison of the sample averages in Table 5.3.

Table 5.2a Volume Susceptibility of Specimens from  
"Typical" Basalt Samples from Henley Harbour  
and Table Head, Labrador.

Sample	Specimen	Mean Volume Susceptibility K (cgs units $\times 10^{-3}$ )
HH3	B1	2.1
	B2	1.9
	C1	2.0
	C2	2.2
	D1	2.4
	D2	1.9
HH8	A2	3.8
	B1	4.9
	B2	4.0
	C1	3.3
	C2	3.3
	C3	3.3
HH12	D2	3.3
	B2	3.1
	D1	2.9
	F1	3.2
	H2	2.6
	I2	3.1

Table 5.2 (Contd.)

Sample	Specimen	Mean Volume Susceptibility K (cgs units $\times 10^{-3}$ ).
--------	----------	--

TH2	A2	10.3
	B2	9.2
	C1	9.1
	D1	9.3

Table 5.2b Mean Susceptibility of the Samples.

Sample	No. of Specimens averaged.	Mean K (cgs units $\times 10^{-3}$ )	Standard deviation in K ( $\sigma$ ) (cgs units $\times 10^{-3}$ )
--------	-------------------------------	---	--

HH3	6	2.11	0.17
HH8	7	3.99	0.56
HH12	6	2.98	0.21
TH2	4	9.46	0.47

Table 5.3 Volume Susceptibility of Samples from Henley  
Harbour and Table Head, Labrador.

Sample No.	No. of Specimens averaged.	Mean volume of susceptibility, K (cgs units $\times 10^{-3}$ )
HH1	6	4.3
HH3	6	2.1
HH4	6	2.1
HH6	3	1.7
HH7	4	1.9
HH8	7	4.0
HH10	3	4.4
HH12	6	3.0
HH13	3	3.7
HH14	3	3.7
HH16	4	4.6
HH17	3	2.8
HH18	3	4.6
HH19	3	1.7
HH24	2	3.7
HH25	2	2.3
HH26	2	3.8

Table 5.3 (Contd.)

Sample No.	No. of Specimens averaged.	Mean volume of susceptibility, K (cgs units $\times 10^{-3}$ )
TH2	4	9.5
TH4	3	9.8
TH5	3	9.8
TH6	3	10.0
<hr/>		
Mean 'K' for basalts from		
Henley Harbour	:	$3.27 \times 10^{-3}$ cgs units
Standard deviation	:	$1.02 \times 10^{-3}$ cgs units
Mean 'K' for basalts from		
Table Head	:	$9.74 \times 10^{-3}$ cgs units
Standard deviation	:	$0.19 \times 10^{-3}$ cgs units

The standard deviation in the mean susceptibility of the four samples given in Table 5.2b indicate a larger error of measurement than mentioned earlier. This is because the standard deviation includes not only the error due to measurement outlined in Section 5.3 but also incorporates the inhomogeneous concentration of ferromagnetic minerals in a rock sample.

The latter effect can be much more pronounced when one considers the mean susceptibility of a geologic formation such as the basalt flows from Henley Harbour. This leads to a large value for the standard deviation as is actually the case for the Henley Harbour basalts.

#### 5.5 Measurement of susceptibility in low magnetizing fields.

It was mentioned in the Introduction that for geophysical purposes the susceptibility of rocks should be measured in magnetic fields of the same order as that of the earth. Partly for this reason, and more so due to the loss of instrumental sensitivity at very low fields measurements of susceptibility in fields considerably lower than that of the earth are not generally made. Nagata (1961), however, measured the susceptibility of some igneous rocks at fields as low as 0.1 oe., and, in some cases obtained a prominent decrease in susceptibility with decreasing field. Blackett (1952) measured the susceptibility of some metal cylinders in fields of 0.02 oe. With an astatic magnetometer. Nagata quotes (1961): "In spite of the experimental difficulties involved, a determination of the range of the initial susceptibility of rocks seems to require a more thorough investigation in the light of various elementary magnetization processes".

Measurements of susceptibility in magnetizing fields as low as 0.005 oe. were attempted, using the present double coil; this is an order of magnitude lower than the



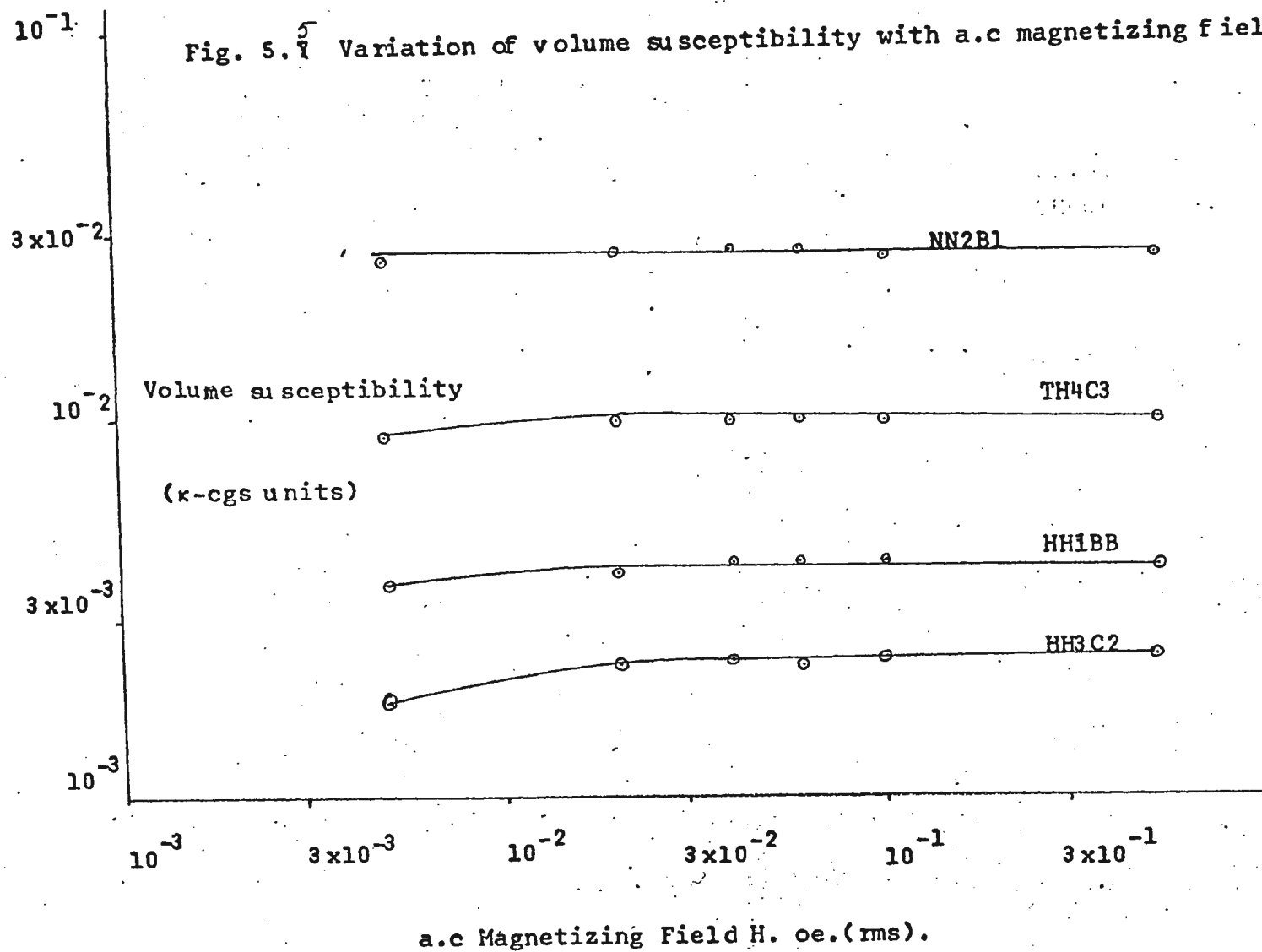
fields employed by Blackett or Nagata. The specimens chosen for calibration purposes were also used in the above set of observations. The aim was primarily to test whether or not the instrument allowed susceptibility measurements to be made at fields as low as 5 milli oersted. A decrease in susceptibility was observed in all cases(except one), when H was reduced below 0.020 oe.

At a magnetizing field of 5 milli oersted the specimens whose susceptibility is  $5 \times 10^{-3}$  cgs units can be measured with an error of 7-8%. For specimens such as LB2B2 ( $\kappa = 3.2 \times 10^{-4}$ ) the error is about 20%. The above low field measurements were made on the sensitivity scale of 2mv/cm on the oscilloscope.

However, when the specimen is measured at different fields some of the errors( such as the error due to mis-positioning) are then the same in all cases, and since the  $\kappa$ - values of the four relatively strong specimens in Fig. 5.5 decrease by much as 20% when the field is reduced from the higher values to 0.005oe., these decreases may be regarded as significant (except possibly in the case of NN2B1).

An oscillogram (Fig. 5.6) displays the differential voltage for a sedimentary rock specimen (HH29A1, with  $\kappa = 2.5 \times 10^{-4}$  cgs units) in a magnetizing field of 0.025oe. rms., when placed 0.60 cm. beyond the bounding plane. This

Fig. 5.5 Variation of volume susceptibility with a.c magnetizing field.



Specimen: HH29A1.

Rock Type: Arkose

$\kappa = 2.5 \times 10^{-4}$  cgs units.

Position: 0.63 cm. beyond  
bounding plane.

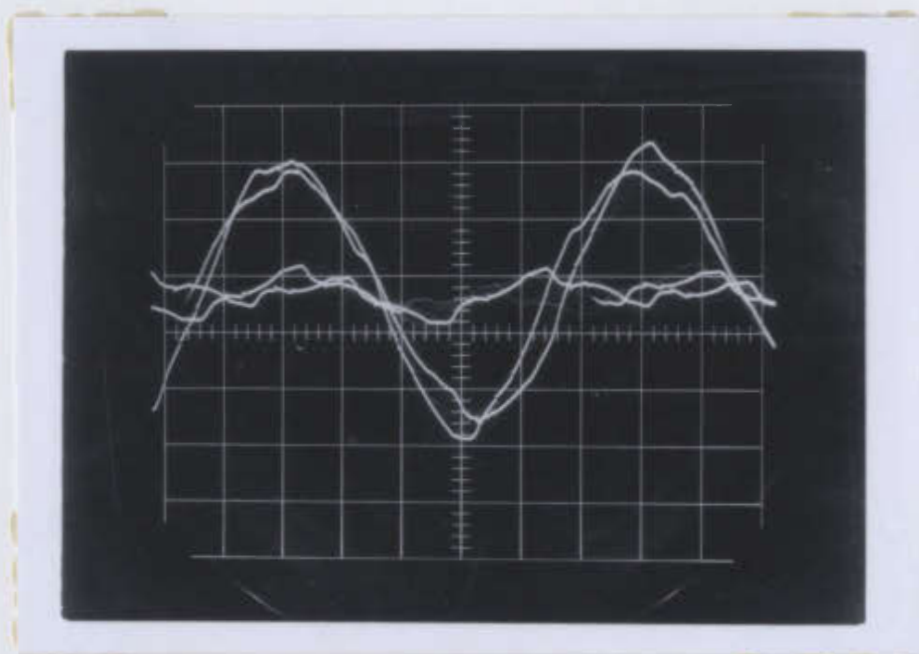
Helmholtz Coil: B

CRO scale: 10mv/cm.

H = 0.025oe. rms.

Time between double  
exposures : 0.020 sec.

Fig. 5.8 Bridge output with and without specimen in a weak field.



oscillogram shows the instability of the out-of-balance emf., which was discussed in Section 4.5. Since the exposure time and the sweep frequency were 0.040 sec. and 50/sec. respectively, the balanced bridge output is displayed as a double exposure with an interval of 0.020 sec. between the two traces. Since the CRO scale constant was 10mv/cm, the instability corresponds to a typical change of 3-5 millivolts on the screen during that time, or a change in the double coil output of 1-2 $\mu$ v. A double exposure with an instability of similar magnitude is displayed after the specimen has been placed in position.

Another point of interest is that a decrease in the magnetizing field is not accompanied by a proportionate reduction in sensitivity. Thus, the measurement of specimen HH3C2 ( $K=2 \times 10^{-3}$  cgs units) in a field of the order of 0.005oe. rms (fig. 5.5) implies that a specimen with  $K=2 \times 10^{-5}$  cgs units should be theoretically measurable at a field  $H=0.5$ oe. rms., but we have seen that this susceptibility is too low to be measured with the present sensitivity of the bridge. From the discussion in Section 4.5., it is clear that the relative increase in sensitivity at lower fields results from a decrease in the harmonics content in the double coil input accompanied by a reduction in the instability of the output signal. Both effects are due to reduced output of the power amplifier.

Since the Helmholtz Coil axis was vertical the magnetizing field for all measurements was superposed on the local vertical component of the earth's field ( $H_z=0.47\text{oe.}$ ). Thus the measurements carried out at low fields essentially measure the average slope of a small hysteresis loop at a point on the magnetization curve of the specimen corresponding to  $H=0.47\text{oe.}$

To perform the above measurements in a zero d.c field (in other words at  $H=0$  in Fig. 1.1), the double coil, Helmholtz coils and specimen should be placed inside a suitable arrangement for field nulling, e.g. one or more pairs of d.c Helmholtz coils of rather large dimensions. In that case the magnetization curve of a specimen would be a small loop about the point 0 in Fig. 1.1, provided the specimen is initially in a demagnetized state, so that one could state conclusively that the average slope of the small hysteresis loop corresponds to the initial reversible susceptibility.

However, rocks used in rock magnetism studies are generally not found in a demagnetized state but have a permanent magnetization. In that case, the above-mentioned hysteresis loop is not at the point 0 but at E. There appears to be no a priori justification in assuming that the slopes of the hysteresis loops at 0 and E will be equal, even if the a.c magnetizing field is the same in the two cases. Hence, unless it is proved experimentally or otherwise that the reversible susceptibility is independent of the state of magnetization, one cannot

conclude that the reversible susceptibility measured at E (corresponding to a rock specimen having a significantly directed remanent magnetization) is identical with the initial susceptibility, however low the a.c magnetizing field may be.

As far as the author is aware the above question has not been discussed exhaustively by previous workers. However, the effect of viscous and remanent magnetization on the differential susceptibility measured in a d.c. field has been discussed by Vincenz (1965) on the basis of Néel's - (1950) theory of the viscosity field. Néel considered the behaviour of massive ferromagnetics in the Rayleigh region (i.e. the low-field region in which the intensity of magnetization  $J$ , obeys Rayleigh's Law:

$$J = AH + BH^2 \quad (5.4.)$$

where H is the magnetizing field and A and B are constants), which he interpreted in terms of thermal fluctuations causing the domain walls to overcome the potential barriers to their motion. For magnetite dispersed in a non-magnetic matrix, Vincenz showed that in a d.c field of 0.5 oe. the differential susceptibility differs by only a few per cent from the reversible susceptibility in a weak low-frequency, alternating field when the time interval between measurement and application of the d.c field is one minute or less.

However, the term "Rayleigh region" implies that the ferromagnetic substance is initially in a demagnetized state. As mentioned earlier this is not the case for natural rocks which often have a stable remanence,  $J_r$  (TRM, IRM or CRM) associated with high coercivity,  $H_c$ —two or three orders of magnitude larger than the Earth's field are not uncommon.

In such rocks,  $J_r$  and  $H_c$  correspond to points on a hysteresis loop that has been taken to high fields or even to saturation; or in the actual mechanism of TRM, they correspond to rocks that have been "saturated" in the Earth's field as they cooled through the Curie points of their ferromagnetic constituents. Thus, for rocks containing a magnetically "hard" constituent, the susceptibility measured in a weak a.c. field should correspond to the mean slope of a small subsidiary loop close to point E in Fig. 1.1 rather than in the Rayleigh region, which is the region near point O considered in the discussion by Nagata (1963) and Vincenz (1965). The question is then whether the subsidiary loops traced at points E and O in a low a.c. field are different from one another. This question may be posed in another way: 'will the presence of a stable remanent magnetization in the rock have a significant effect upon the reversible susceptibility measured in a weak, alternating field?'

The author has discovered only one direct comment on this point in the literature: this is a statement by Mooney (1952)

affirming that the remanent magnetization of a natural rock has no effect on the a.c field susceptibility measurement. While Mooney's statement is made without elaboration or citation of evidence, theoretical considerations would make it appear plausible, since it can be argued that the domains in the high-coercivity region of the spectrum are not significantly affected by the weak a.c magnetization process. In that case, the relevant magnetization curve for the low-coercivity (i.e. reversible) component is not the full hysteresis loop of Fig. 1.1 but a Rayleigh-type loop occupying a small region near point O. Results of repeat susceptibility measurements made with the present a.c bridge have an indirect bearing upon this question: two specimens (HH3B1 and TH4C3) had each acquired a viscous component in the laboratory between the first measurement of their susceptibility and several measurements in the course of 4-5 weeks. While in both specimens the acquisition of the VRM results in a roughly threefold increase in the observed remanence, no change within experimental error was found in either value of susceptibility. However this experimental error is sufficiently large to prevent the detection of a change in susceptibility smaller than  $8 \times 10^{-5}$  cgs units. Hence no generalization will be attempted here: this becomes possible only when tests have been made with equipment capable of measuring considerable smaller differences of susceptibility.



CHAPTER SIX.

SUMMARY AND CONCLUSIONS

1. An a.c bridge for the measurement of the magnetic susceptibility of rocks in weak fields has been constructed and calibrated. The sensing unit is a double coil with two windings connected in series opposition and of such proportions that the net e.m.f. induced by the alternating field from a pair of Helmholtz coils co-axial with the double coil will be zero. The magnetization induced by the alternating field in a rock specimen on the axis of this system results in a slight distortion of the field threading the turns of the double coil, and this causes a net emf whose amplitude is a measure of the magnetic susceptibility. With suitable amplification of this signal it is theoretically possible to measure volume susceptibilities lower than  $10^{-6}$  cgs units in fields as low as that of the earth.

The bridge method was adapted from the original design by Bruckshaw and Robertson (1948), while the proportions of the double coil were chosen on the basis of a treatment by Hall (1963) aimed at maximizing its sensitivity. The actual design is one of almost optimum proportions for the case when the specimen is placed on the coil axis at one of its bounding planes. The coil dimensions are larger than is usual; in such

coils (thickness: 7.86cms; outer radius of outer winding: 16.0 cms; inner radius of the inner winding: 4.0 cms; number of turns  $N_1 = 33,090$ ,  $N_2 = 12,550 \pm 10$ , for the inner and outer winding, respectively), because of the use of relatively thick wire (A.W.G no.26). This led to a low combined resistance for the two windings ( $3.8K\Omega$ ) and a low Johnson noise level ( $e_n = 7.0 \times 10^{-9}$  volts rms for a bandwidth of 1cps). Because of the approach to optimum proportions, the signal-to-noise ratio  $e/e_n$  is also relatively high. The signal-to-noise ratio for a specimen of  $\kappa = 1 \times 10^{-5}$  placed 4.0 cms from one of the bounding planes is 95.

2. The presence of distributed capacitance effects - which are proportional to the square of frequency - limit the operating frequency  $f$  of the double coil to low values. In the present investigation a value of  $f = 33.0$  cps was used. Frequencies close to 60cps or its subharmonics were avoided in order to reduce the effect of external noise. Initial balancing of the double coil was carried out by adjusting the number of turns of the outer winding. The correct number of turns could thus be determined to within 40-50 turns. Placing a  $0.079\mu F$  capacitor across the outer coil brought the induced voltages in the two windings very close to  $180^\circ$  opposition and made the balancing possible to within one turn. The final balance is achieved by putting a third winding of 16 turns

over the outer winding; the emf induced in this winding is then balanced against the differential output of the double coil, using a potentiometric arrangement. The fundamental mode could thus be reduced to the order <sup>of</sup> a few tens of microvolts (peak-to-peak) when the induced emf in each winding was about 25 volts (peak-to-peak). Further reduction in the fundamental could not be achieved due to short-period (<1sec) amplitude instability of the unbalanced signal, consisting of the fundamental and harmonics (mainly second harmonic). A qualitative study of the causes of the instability showed that it arises partly from fluctuations in the signal from the oscillator and power amplifier that provide the input signal for the Helmholtz coils, though part of the instability can also be traced to the output amplifiers.

3. The calibration of the susceptibility bridge was carried <sup>out</sup> with 6 specimens whose susceptibility was determined independently using an astatic magnetometer. The following calibration values were obtained for two positions of the center of the specimen on the double coil axis:

$$\frac{\kappa}{\Delta R} = (1.41 \pm 0.04) \times 10^{-4} \text{ cgs units per potentiometer division}$$

when the specimen is kept at a distance of 0.63cm. beyond the bounding plane of the windings.

$$\frac{\kappa}{\Delta R} = (0.73 \pm 0.02) \times 10^{-4} \text{ cgs units per potentiometer division}$$

when the specimen is kept at the coil center.

On a 10-meter wire potentiometer the value of  $\Delta R$  corresponds to 1 division = 1.0cm.

With these scale constants it was possible to measure the susceptibility of a wide variety of igneous rocks and some of the more strongly magnetic sedimentary rocks. The error in the calibration arises from two causes:

1) Error in the measurement of susceptibility by the astatic magnetometer;

2) Error in the bridge measurements. The latter error incorporates errors in the zero balance of the bridge, in the positioning of the specimen and in the potentiometer readings. For specimens  $\kappa = 1 \times 10^{-3}$  cgs units, the error of a single measurement is about 5%, though it reaches 25% or so for  $\kappa = 8 \times 10^{-5}$  cgs units. In practice one can reduce these errors somewhat by carrying out a number of repeat observations.

4. The present double coil was used to determine the volume susceptibility of samples from basalts flows at Henley Harbour and Table Head on the south coast of Labrador. Measurements were made with 67 specimens cut from 17 of the Henley

Harbour samples and 13 specimens from 4 Table Head samples. The mean susceptibility was  $(3.27 \pm 1.02) \times 10^{-3}$  and  $(9.74 \pm 0.19) \times 10^{-3}$  cgs units for the Henley Harbour and Table Head basalts respectively, where the quoted standard deviations are based on sample averages and may be taken as a measure of the inhomogeneity in the distribution of the chief ferromagnetic constituents in the rock. Specimens from a sample, however, show a much greater agreement in the value of susceptibility. On the other hand, measurement of remanent magnetization of these rocks (Murthy, 1966) showed that the specimens from the same sample sometimes had as much or more scatter than the samples from either of the two collection sites.

5. It was found that with the present bridge circuit, the sensitivity per unit field increased as the field was reduced. Because of this it was possible to measure rocks with susceptibility as low as  $5 \times 10^{-4}$  cgs units in a field of 0.005 oe. rms. Four specimens were measured in fields ranging from 0.5 to 0.005 oe. rms, and in all cases, the value of  $\kappa$  measured at  $H = 0.005$  oe. was from 3 to 20 percent lower than that observed in the same specimen at fields between 0.02 and 0.50 oe. In three out of the four specimens the drop in  $\kappa$  as the field was lowered exceeded the experimental error.

6. The variation of the output signal (and hence the variation of sensitivity) as a function of the specimen-position

was determined experimentally for given specimens placed along the axis of the double coil and at different distances from its center.

The results were compared with the theoretically calculated variation/ A small discrepancy is observed and could be due to

- (1) Error in positioning the specimen;
- (2) deviations of the actual coil proportions from the theoretical design, because of insertion of insulating material and distortion of the coil former;
- and (3) Error in the assumption that the specimen acts as an alternating point dipole.

Suggestions for further work.

To enable the present susceptibility bridge to measure volume susceptibilities of the order of  $5 \times 10^{-7}$  cgs units or even less, further work is necessary in two aspects.

1. The instability of the out-of-balance emf proved the chief limiting factor in the achievement of higher sensitivity. Since it has been shown that both the oscillator and the power amplifier in the input section, as well as the tuned output amplifiers are mainly responsible for the instability,

these units have to be redesigned for extremely stable operation at frequencies up to 100cps. A single-frequency ( $< 100$  cps) generator with very high stability both in voltage amplitude and frequency is necessary. Further a power amplifier should be designed for the above frequency range with an output of about 60 watts so that it can be used at very low levels of amplification to give the desired current output to the Helmholtz coils. This will considerably reduce the harmonic content in the fundamental mode.

2. For measurement of susceptibility of the order of  $5 \times 10^{-7}$  cgs units, a very high gain (about  $10^5$ ) selective amplifier is required. It's bandwidth should be approximately 1cps and must be stable at the high levels of amplification. This amplifier would replace the present cascade arrangement with two amplifiers.

3. In addition to the above changes certain modifications in the pre-amplifier, as suggested by Brophy (1955), will be necessary before signals corresponding to  $\kappa = 5 \times 10^{-7}$  cgs units can be detected. These modifications are made at the input stages of the pre-amplifier and reduce the internally generated noise level by approximately an order of magnitude when its bandwidth is about 50 cps.

4. As already mentioned further increase in sensitivity can be obtained with an increase in the size of the specimens.

5. Following the above stated improvements the coil should be able to measure the volume susceptibility of relatively weak sedimentary rocks.

6. The measurement of susceptibility of rocks should be extended to higher temperatures.

7. It is possible to use this double coil to determine the frequency dependence of susceptibility in a range from 1 to 250 cps, where theoretically a decrease in  $\kappa$  of nearly 10% should occur. (Vincenz; 1965).

8. Measurement in d.c-field-free space could be carried out to determine:

- (a) The variation of  $\kappa$  with H in very low a.c fields.
- (b) The effect of small superimposed time-dependent d.c fields on  $\kappa$ .
- (c) The effect of remanent magnetization on the value of  $\kappa$ .



# APPENDIX I

## Resistance of a Double Coil when the Insulation is taken into Account.

Let the total resistance  $R_T^1$  of the double-coil be given by

$$R_T^1 = \frac{\rho \bar{L} N}{A} \quad (i)$$

where  $\rho$  is the resistivity, in ohm-cm;  $\bar{L}$  is the average length of a turn in cm,  $N = N_2 + N_1$  is the total number of turns of insulated wire.

$A$  is the cross-section of the conducting (or metal) section of the wire in  $\text{cm}^2$ .

$$\text{Then, } L_{\max} = 2\pi cr_1 \quad (ii)$$

$$\text{and } L_{\min.} = 2\pi r_1$$

where  $L_{\max.}$  and  $L_{\min.}$  are the respective lengths of a turn in the outermost and innermost layers.

$$\text{Therefore, } \bar{L} = \frac{2\pi r_1 (c+1)}{2} = \pi r_1 (c+1) \quad (iii)$$

Also, the total number of turns is given by

$$N = N_1 + N_2 = n_1 (A_{w1} + A_{w2}) = \frac{A_{w1} + A_{w2}}{d_1^2} \quad (iv)$$

APPENDIX I (Contd.)

Resistance of a Double Coil when the Insulation is taken into Account.

where  $n_1$  is the number of turns of insulated wire per unit cross-sectional area;  $d_1$  is the diameter of an insulated turn (i.e. conducting section plus insulating layer); and  $A_{w1}$  and  $A_{w2}$  are the cross sectional areas of the inner and outer windings, respectively.

$$\text{But } A_{w1} = (c-a)r_1 (\Delta b) r_1 = (c-a) \Delta b r_1^2 \quad (v)$$

$$\text{and } A_{w2} = (a-l) r_1 (\Delta b) r_1 = (a-l) \Delta b r_1^2$$

Hence, substitution of equations (v) into (iv) yields

$$N = \frac{C-l}{d_1^2} r_1^2 \Delta b \quad (vi)$$

$$\text{Also, } A = \frac{\pi d^2}{4} \quad (vii)$$

where  $d$  is the diameter of the conducting section of the wire.

Inserting, (iii), (vi) and (vii) into (i), and simplifying one obtains,

$$R_T^1 = \frac{4\pi r_1^3 (\Delta b) u^2}{d_1^2 d^2} \quad (viii)$$

APPENDIX I (Contd.)

Resistance of a Double Coil when the Insulation is taken into Account.

which reduces to equation (2,22) when the insulation thickness is negligible, i.e.,  $d_1 = d$ .

REFERENCES

- BALSLEY, J.R. and BUDDINGTON, A.F.; Econ. Geology, vol. 53, p.777-805, (1958)
- BARKHAUSEN, H.; Phys. Z., vol. 20, p.401, (1919)
- BISHOP, R.B.; B.Sc. (Hons) Thesis, Memorial University of Newfoundland, (1965)
- BITTER, F.; Phys. Rev., vol. 38, p.1903, (1931)
- BLACKETT, P.M.S.; Phil. Trans. Roy. Soc. London, ser.A, vol. 245, p.303-370, (1952).
- BRUCKSHAW, J. McG. and ROBERTSON, E.I.; Jour. Sci. Instrum., vol. 25, p.444-446, (1948)
- BROPHY, J.J.; Rev. of Sci. Instrum., vol. 26, No.11, p.1076, (1955).
- CHEVALLIER, R.; Ann. Phys., vol. 4, p.5, (1925).
- COLLINSON, D.W. and CREER, K.M.; "Measurements in Palaeomagnetism", Methods and Techniques in Geophysics, vol. 1, ed. by S. K. Runcorn, Inter-science Pub., London-New York, p.158-210, (1960).
- CROCKER, R.; B.Sc. (Hons) Thesis, Memorial University of Newfoundland, (Unpublished) (1966).
- CURIE, P. and CHENEVESEU, C.; Journ. Phys. Radium, No. 4, p.769, (1903).
- FULLER, M.D.; A.C Bridge Methods for the Measurement of Susceptibility Anisotropy; Gulf Research Laboratory Report.
- GIRDLER, R.; J. Geophys. Res., vol.v, No. 1, p.34-44, (1961).
- GOTTSCHALK, V.H.; Physics, vol. 6, p.27, (1935)

- GRAHAM, J.W.; Preliminary Account of a Refined Technique for Magnetic Susceptibility Anisotropy Measurements of Rocks, South West Center for Advanced Study Report, Dallas, (1964).
- GRANT, F.S. and WEST, G.F.; "Interpretation Theory in Applied Geophysics"; McGraw Hill, Inc. p.355-381, (1965).
- GRENET, G.; Ann. de Phys. Ser. 10., vol. 13, p.309, (1930).
- GUOY, L.G.; C.R Acad. Sci., Paris, 109, 935, (1889).
- HALL, D.H.; Gph. vol. 28 No. 5, p.767-777, (1963).
- HARRIS, F.K.; "Electrical Measurements", p.664, John Wiley and Sons. Inc. (1957)
- HEISENBERG, W.; Z. Physik. vol. 49, p.619, (1928).
- HUGHES, D.E.; Phil. Mag., Series 5, vol. 8, p.50-56, (1879).
- JOHNSON, E.A.; Rev. of Sci. Instrum., vol. 9, p.263-266, (1938).
- KELVIN, LORD; Brit. Assoc. Rep. (1890).
- KING, R.F. and REES, A.I.; J. Geophys. Res. vol. 67, No. 4, p.1565-1572, (1962)
- LIKHITE, S.D. and RADHAKRISHNAMURTHY, C.; Pre-print - to be published in Bull. Natl. Geophys. Res., Hyderabad, (1965).
- MOONEY, H.M.; Gph. vol. 27, p.531-543, No. 3, (1952).
- MOONEY, H.M.; and BLEIFUSS, R.; Gph. vol. 18, p.383-393, (1953).
- MURTHY, G.S., M.Sc. Thesis, Memorial Univ. of Newfoundland, (Unpublished), (1966)
- NAGATA, T.; "Rock Magnetism", rev. ed., Maruzen, Tokyo, (1961).

- NAGATA, T.; Bull. Earthquake Res. Inst., vol. 18, p.102 (1940).
- NÉEL, L.; J. Phys. Rad., vol. 11, p.49, (1950).
- SLICHTER, L.B.; Magnetic Properties of Rocks, p.293-297 in F. Birch (ed.), "Handbook of Physical Constants", Geol. Soc. America Spec. Paper 36, (1942).
- STACEY, F.D.; J. Geophys. Res. vol. 65, No. 8, p.2429-2442, (1960).
- STACEY, F.D.; Jour. of Sci. Instrum., vol. 36, No. p.355-359, (1959).
- STONE, D.B.; Geophys. Jour. Roy. Astron. Soc., 7, p.375-390, (1962).
- STSCHODRO, N.; Gerl. Beitr. Geophys., vol. 17, p.148, (1927).
- TERMAN, E.T.; "Radio Engineer's Handbook", p.84, McGraw Hill, Inc. (1943).
- UYEDA et. al.; J. Geophys. Res., vol. 68, No. 1, p.279-291, (1963).
- VINCENZ, S.A.; J. Geophys. Res., vol.70, No.6, p.1371-1377, (1965).
- WEISS, P.; J. Phys., vol. 6, p.661, (1907).

### ACKNOWLEDGEMENTS.

The author wishes to acknowledge with thanks the assistance received from the following members of the Physics faculty and staff at Memorial University of Newfoundland:

Dr. E. R. Deutsch under whose supervision the present investigations were carried out and who painstakingly guided the author throughout the course of the present work;

Dr. S. W. Breckon - Head of the Department, who offered generous use of facilities and equipment;

Professor P. D. P. Smith who offered valuable suggestions on aspects of the instrumentation and who also made equipment available;

Mr. A. Walsh, Scientific Assistant, who built the support of the double coil and took the photographs of the double coil and the tuned amplifiers;

Mr. G. W. Pearce, graduate student in Geophysics who gave much of his time particularly in helping with the photographs of the oscillograms and in demagnetizing some of the specimens;

Mr. G. S. Murthy, graduate student in geophysics (now at University of Alberta) who offered considerable help

in the use of the astatic magnetometer and made available the rock specimens from Labrador;

Mr. S. K. Tak, graduate student in geophysics who drew the diagrams and helped in several other ways towards completion of the thesis;

and Mr. R. Crocker, Honours student in Physics (now at University of Alberta) who designed and constructed one of the three tuned amplifiers in the present investigations.

The author also wishes to express his gratitude to Memorial University of Newfoundland for the grant of a Graduate Fellowship during the period 1964-1966 and to the National Research Council of Canada for providing financial assistance during the Summers of 1965 and 1966 under Grant A-1946 (to Dr. E. R. Deutsch).

Finally, the author wishes to thank Mrs. H. R. Peters for typing the thesis.







